

BIOLOGICAL AND CHEMOENZYMATIC SYNTHESIS OF ANTICOAGULANT
HEPARAN SULFATE

Michael Bernard Duncan, II

A dissertation submitted to the faculty of the University of North Carolina at Chapel Hill in partial fulfillment of the requirements for the degree of Doctor of Philosophy in the School of Pharmacy (Medicinal Chemistry and Natural Products)

Chapel Hill
2006

Approved by
Advisor: Jian Liu
Reader: Kenneth Bastow
Reader: Moo Cho
Reader: Michael Jarstfer
Reader: Lee Pedersen

ABSTRACT

MICHAEL DUNCAN: Biological and Chemoenzymatic Synthesis of Anticoagulant Heparan Sulfate
(Under the direction of Jian Liu)

Heparan sulfate (HS) is a linear, heterogeneously sulfated polysaccharide that is ubiquitous to most mammalian tissues. The roles played by HS on the cell surface and in the extracellular matrix (ECM) are diverse in function. A number of HS/protein interactions have been studied and have led to a more detailed understanding of signal transduction pathways, enzyme activation, and ligand presentation. Accumulating evidence has supported the role of the fine structure of HS in high-affinity interactions with serine protease inhibitors, growth factors, and microbial coat proteins. These findings have led to a great deal of interest in understanding how specific HS structures are generated and the mechanisms that regulate HS biosynthesis.

Complex HS sequences are generated by a number of biosynthetic enzyme families, including the *N*-deacetylase *N*-sulfotransferases, epimerase, 2-*O*-, 6-*O*-, and 3-*O*-sulfotransferases. Herein, studies are presented that explore the functions of *N*-deacetylase *N*-sulfotransferase and the 3-*O*-sulfotransferases. In addition, we report a chemoenzymatic approach to synthesizing anticoagulant heparin, a structural analogue of HS. The anticoagulant effects of heparin, derived from natural sources, have been exploited in the clinic for over seventy years. A synthetic approach to heparin production could provide the anticoagulant with reduced side effects. It would also allow for the investigation of other

therapeutic benefits of heparin and HS. In conclusion, the work presented herein provides detail into the biosynthetic machinery and biological properties of HS, as well as strategies to control the assembly of heparin and HS polysaccharides.

DEDICATIONS

To my wife, Gina Lynn, your love and support has been essential to the completion of this body of work

To my parents, and my sister, Michael, Gloria, and Monique, thank you for your love and such broad shoulders to stand on.

To my grandmothers, Berniece and Cleo, thank you for setting a wonderful example of what it means to persevere and to excel

To my family-in law, Geno, Lynne, Mary Ruth, and Brittany, thank you for your love and tremendous support.

ACKNOWLEDGEMENTS

I am indebted to many for their contributions and assistance in helping me put forth the work, time, and focus necessary to complete this work. I am extremely grateful to my advisor, Jian Liu, for his guidance and consistent support throughout the completion of this work. I wish to thank the David and Lucille Packard Foundation for funding and support. Finally, I would like to thank my labmates past and present Jinghua Chen, Miao Chen, Ron Copeland, Suzanne Edavettal, Courtney Jones, Rempeng Liu, Tanya Scalert, Danyin Song, and Ding Xu, for their technical expertise, helpful discussions, and support throughout my graduate studies.

TABLE OF CONTENTS

LIST OF TABLES.....	xi
LIST OF FIGURES.....	xii
LIST OF ABBREVIATIONS.....	xiv

Chapter

I. INTRODUCTION

Heparan Sulfate Structure, Biosynthesis, and Biological Functions.....	1
Physio-chemical properties of HS and heparin.....	1
Important HS Protein Interactions.....	4
Growth Factors.....	4
Antithrombin.....	6
Thrombin.....	8
Chemokines.....	10
Herpes Simplex Virus 1 glycoprotein D.....	12
HS Biosynthetic Pathway.....	15
Core proteins.....	15
Step One: GAG Linkage Region Synthesis.....	15
Xylosyltransferase.....	16
Galactosyltransferase.....	17
Glucuronyltransferase.....	17

Step Two: Heparosan Polymerization.....	18
HS copolymerase.....	18
Step Three: Polysaccharide Chain Modification.....	19
<i>N</i> -Deacetylase <i>N</i> -Sulfotransferase.....	19
Epimerase.....	22
2- <i>O</i> -sulfotransferase.....	22
6- <i>O</i> -Sulfotransferase.....	23
3- <i>O</i> -Sulfotransferase.....	24
Physiologic and Pathophysiologic Roles of HS.....	30
Cardiovascular biology.....	30
Heparanase in cancer.....	31
Microbial attachment and cellular entry.....	32
Chemoenzymatic Synthesis of Heparin and HS Analogues.....	33
Enzymatic and chemoenzymatic synthesis of heparin.....	33
Statement of Problem.....	41
II. METHODS.....	43
General Procedures.....	43
Mammalian cell culture.....	43
Preparation of chemically competent origamiB cells expressing groES/EL.....	43
Agarose gel electrophoresis.....	44
Concanavalin A (Con A) Sepharose Aging.....	45
Polysaccharide Preparation.....	45

Heparosan isolation.....	45
Preparation of [³⁵ S]HS.....	46
Preparation of [³ H, ³⁵ S] HS.....	47
[³⁵ S]PAPS Preparation.....	47
Protein Expression and Purification.....	48
Preparation of NDase expression plasmid.....	48
Expression of <i>N</i> -sulfotransferase (NST).....	49
Preparation of C ₅ -epimerase bacterial expression plasmid and protein.....	49
Preparation of 2OST and 6OST1 bacterial expression plasmid and protein.....	50
Preparation of 3OST1 bacterial expression plasmid and protein expression.....	51
Preparation of AST IV bacterial expression plasmid and protein expression.....	51
Enzymatic Activity Assay.....	51
<i>N</i> -deacetylation of heparosan by NDase.....	51
Radioactive sulfotransferase assay.....	52
Polysaccharide digestion by heparin lyases.....	53
Preparation of 3OST5 Stable Expression Cells (3OST5/CHO).....	53
RT-PCR and Northern blot analysis.....	53
HS Polysaccharide Structural Analysis.....	54
Degradation of <i>N</i> -deacetylated heparosan by nitrous acid....	54
Determination of the distribution of <i>N</i> -sulfated glucosamine residue in HS.....	55
Reverse phase ion pairing HPLC (RPIP-HPLC)	

	of non-sulfated disaccharides.....	55
	RPIP-HPLC of sulfated disaccharides.....	55
	HS/Protein Interactions Biochemical Assays.....	56
	AT affinity fractionation.....	56
	Determination of the binding affinity by affinity co-electrophoresis.....	56
	Assay for the AT-mediated deactivation of factor Xa by HS.....	57
	The binding of the cells to fluorescently labeled AT.....	58
	Chemoenzymatic Synthesis of Heparin Analogues.....	58
	Preparation of immobilized HS sulfotransferases.....	58
	Measurement of enzymatic activities of immobilized proteins.....	59
	2OST modification of <i>N</i> -sulfo K5 polysaccharides.....	60
III.	Biosynthesis of Anticoagulant Heparan Sulfate by 3OST Isoform 5.....	62
	AT- and gD- binding to HS.....	62
	Determination of the expression of 3OST5 in 3OST5/CHO cells.....	64
	3OST5/CHO generates multiple 3- <i>O</i> -sulfated Disaccharides.....	66
	Effects of 3OST5 overexpression on HS structure.....	68
	Binding affinity of HS from 3OST5/CHO with AT.....	70
	3OST5 modified HS promotes AT mediated deactivation of factor Xa.....	70
	Comparing the cell surface antithrombin-binding	

	sites between 3OST5/CHO cells and CHO-K1 cells.....	73
	Conclusions.....	75
IV.	Localization and Characterization of the N-Deacetylase Domain of NDST2.....	78
	Expression and characterization of ND domain fusion protein.....	78
	Structural characterization of NDase-treated heparosan.....	82
	Distribution of N-deacetylated glucosamine residues in NDase treated heparosan.....	84
	Conclusions.....	86
V.	Chemoenzymatic Synthesis of Anticoagulant Heparin Analogues.....	87
	Expression and characterization of the HS biosynthetic enzymes.....	87
	Chemical deacetylation and <i>N</i> -sulfonation.....	88
	Size distribution and chemical degradation of the N-sulfo K5 polysaccharide.....	89
	Epimerization of capsular K5 polysaccharide.....	91
	Epimerase coupled 2- <i>O</i> -sulfonation.....	91
	6- <i>O</i> -sulfonation of K5PNS2S.....	95
	3- <i>O</i> -sulfonation and anticoagulant activity of K5Hp analogues.....	98
	Conclusions.....	99
VI.	Conclusions.....	101
	APPENDIX 1. Curriculum Vitae.....	103
	REFERENCES.....	107

LIST OF TABLES

Table

1. Core Proteins and their biological location.....	15
2. Summary of the products and biological functions of 3OST modified HS.....	25
3. Analysis of the sulfotransferase activity of selected 3OST1 and 3OST3 mutants.....	30
4. Summary of the substrates used in radioactive sulfotransferases reaction.....	53
5. Relative percentages of oligosaccharides resulted from nitrous acid degraded HS from 3OST5/CHO and from wild-type CHO.....	68
6. Disaccharide composition of heparin analogues.....	98

LIST OF FIGURES

Figure

1. Disaccharide repeating units of heparan sulfate and heparin.....	2
2. Structure of heparin oligosaccharides.....	3
3. Two binding modes of the FGF:FGFR:heparin interaction.....	5
4. The allosteric activation of AT by the high affinity HS derived pentasaccharide.....	7
5. The high affinity AT binding HS pentasaccharide.....	8
6. Crystal structure of heparin bound to thrombin.....	9
7. Entry of HSV-1 into Chinese Hamster Ovary (CHO-K1) cells and transfected CHO-K1 cells.....	13
8. The structure of gD-binding octasaccharide purified from a HS derived library.....	14
9. The proteoglycan tetrasaccharide linkage region.....	16
10. The heparin binding cleft of NST.....	21
11. Substrate specificities of 3OSTs.....	25
12. A charged surface diagram of the proposed heparan binding cleft of the sulfotransferase domains of NST1 and 3OST1.....	27
13. The structure of the tetrasaccharide substrate.....	28
14. Stereo diagrams of the binding of 3OST3 and tetrasaccharide.....	29
15. The synthetic route to anticoagulant heparan sulfate.....	36
16. Enzymatic synthesis of the HS derived AT binding pentasaccharide.....	38
17. A schematic of the synthesis of sulfated polysaccharides and the PAPS regeneration system.....	40

18. Completely desulfated re-N-sulfated heparin (CDSNSHp).....	60
19. 3OST5 modified HS binds to both AT and gD.....	63
20. Northern blot and RT-PCR of 3OST5/CHO.....	65
21. RPIP-HPLC chromatograms of the disaccharide analysis of HS.....	67
22. 3OST5/CHO N-sulfo domains do not vary from wild CHO.....	69
23. Determination of K_d by affinity co-electrophoresis.....	71
24. The inhibition of factor Xa activity by HS.....	72
25. Binding of fluorescently labeled AT to 3OST5/CHO and wild-type CHO cells.....	74
26. Determination of the activity of <i>N</i> -deacetylase activity.....	80
27. Determination of K_m of NDase towards heparosan.....	81
28. Disaccharide analysis of NDase-treated heparosan.....	83
29. Oligosaccharide profile of high pH nitrous treated NDase-treated heparosan.....	85
30. Expression of HS biosynthetic enzymes.....	88
31. Structural analysis of N-sulfo K5 polysaccharide.....	89
32. Size distribution of K5PNS.....	90
33. Epimerase generates IdoA residues.....	92
34. Epimerase accelerates 2-O-sulfotransfer.....	93
35. Coupled epimerization and 2-O-sulfonation enhances the IdoA content.....	94
36. RPIP-HPLC chromatograms of the disaccharide analysis of EPI/2OST modified polysaccharides.....	96
37. RPIP-HPLC chromatograms of the disaccharide analysis of EPI/2OST and 6OST modified polysaccharides.....	97
38. AT binding of heparin analogues.....	99

LIST OF ABBREVIATIONS

AnMan	Anhydrous mannitol
AST IV	Rat arylsulfotransferase IV
AT	Antithrombin
DEAE	diethylaminoethyl sephacel
DNA	Deoxyribonucleic acid
EPI	Epimerase
FGF	Fibroblast growth factor
FGFR	Fibroblast growth factor receptor
GAG	Glycosaminoglycan
gB, gC, gD...	HSV glycoprotein B, C, D...
GlcA	Glucuronic acid
GlcNAc	<i>N</i> -acetyl glucosamine
GlcNH ₂	<i>N</i> -unsubstituted glucosamine
HIT	Heparin induced thrombocytopenia
HPLC	High pressure liquid chromatography
HS	Heparan sulfate
HSPG	Heparan sulfate proteoglycan
IdoA	Iduronic acid
IL8	Interleukin 8
IPTG	Isopropyl- β -D-thiogalactopyranoside
K5Hp	K5 derived Heparin analogue
K5P	K5 Capsular polysaccharide

LMWH	Low molecular weight heparin
MBP	Maltose binding protein
NDase	<i>N</i> -deacetylase
NDST	Heparan sulfate <i>N</i> -deacetylase/ <i>N</i> -sulfotransferase
NMR	Nuclear magnetic resonance
NST	<i>N</i> -sulfotransferase
NTA	Nickel-nitrilotriacetic acid
OD ₆₀₀	Optical density at 600 nanometer wavelength
oriB _{groES/EL}	OrigamiB cells over-expressing groEL and groES
PAP	3',5' Diphosphoadenosine
PAPS	3'- phosphoadenosine 5'- phosphosulfate
PCR	Polymerase chain reaction
PNPS	para-Nitrophenol sulfate
PNP	para-Nitrophenol
PF4	Platelet factor 4
RPIP	Reverse phase ion pairing
RT-PCR	Reverse transcriptase polymerase chain reaction
SOC	Super optimal broth with catabolite repression
TBA	Tetrabutylammonium
TEA	Triethylammonium
UV	Ultra-violet light
ΔUA	4,5-unsaturated uronic acid
2OST	Heparan sulfate 2- <i>O</i> -sulfotransferase

3OST	Heparan sulfat 3- <i>O</i> -sulfotransferase
6OST	Heparan sulfat 6- <i>O</i> -sulfotransferase

CHAPTER I. INTRODUCTION

Heparan Sulfate Structure, Biosynthesis, and Biological Functions

Heparan sulfate proteoglycans (HSPGs) consist of a core protein with one or more covalently attached glycosaminoglycan (GAG) chains. These molecules are present on the cell surface and within extracellular matrices (ECM) including basement membranes. Traditionally, proteoglycans were thought to maintain the structural integrity of the ECM. However, over the past several decades it has been realized that these molecules play a variety of roles in both normal and pathophysiologic processes (Bernfield et al., 1999; Sasisekharan et al., 2002; Zak et al., 2002). Some broadly defined functions of heparan sulfate (HS) include promoting ligand receptor interactions (Park et al., 2000b), attachment and entry receptor roles in microbial pathogenesis (Liu and Thorp, 2002; Wadstrom and Ljungh, 1999), and producing chemotactic gradients via interactions with chemokines and cytokines (Gotte, 2003). The polysaccharide unit of HSPGs is composed of 50 to 200 disaccharide units containing glucuronic acid (GlcA) β 1,4 linked to *N*-acetylated glucosamine (GlcNAc). This polysaccharide backbone undergoes extensive sulfonation reactions forming a mature HS chain (Esko and Selleck, 2002).

Physio-chemical properties of HS and heparin- As depicted in Figure 1, uronic acid may be sulfated at the C2 position while glucosamine may carry sulfonyl groups at the C6, C3 or N2 position. The N2 position of glucosamine may also be unsubstituted, existing as

primary amine. Additional structural diversity of HS is achieved through epimerization of GlcA to iduronic acid (IdoA) residues. Heparin is a structural analogue of HS. The primary differences between heparin and HS are that heparin contains more IdoA residues and it is more highly sulfated. Also, heparin is produced exclusively by connective tissue mast cells while HS is produced by most metazoan cell types.

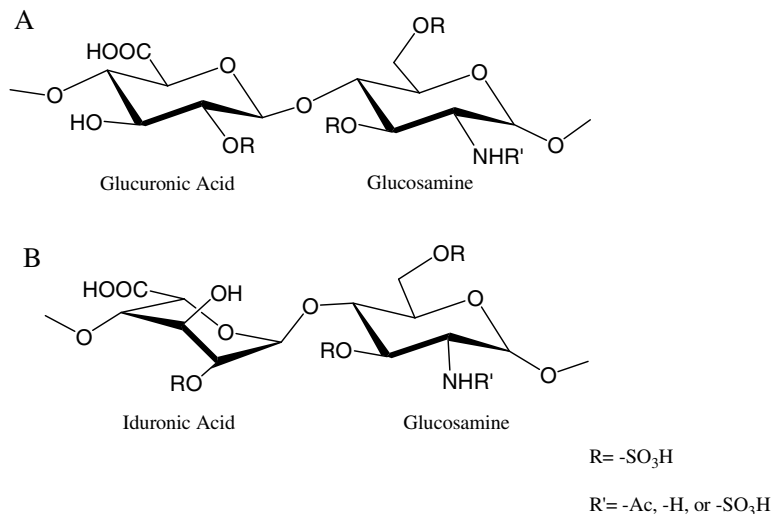
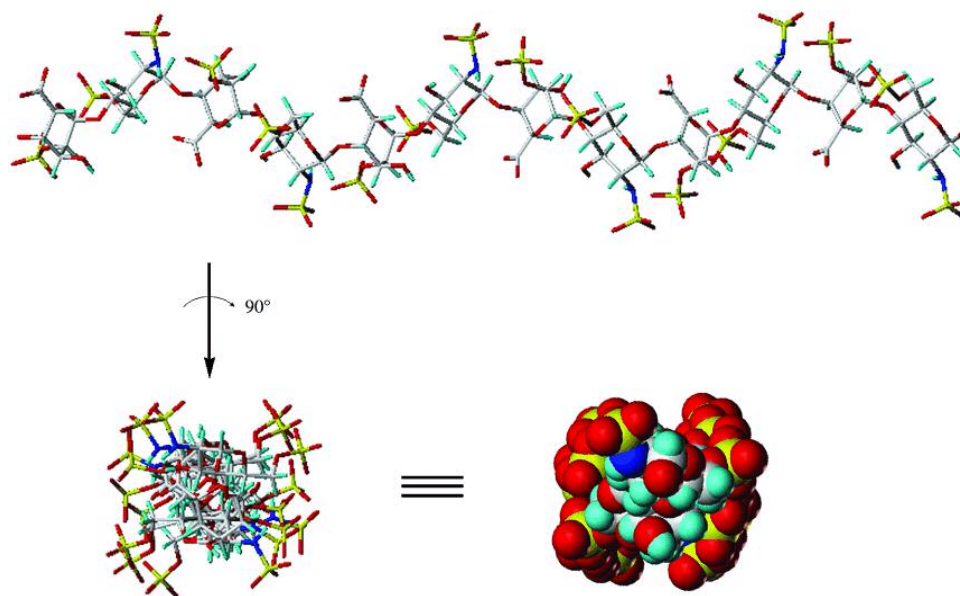


Figure 1. Disaccharide repeating units of heparan sulfate and heparin. Sulfonation (R = -SO₃) at Carbon 6 (known as 6-*O*-sulfo glucosamine) of glucosamine is common. Sulfonation at Carbon-2 of iduronic acid (known as 2-*O*-sulfo iduronic acid) is common. Sulfonation at Carbon-3 of glucosamine (known as 3-*O*-sulfo glucosamine) is rare. Both *N*-acetyl (R' = acetyl, GlcNAc) and *N*-sulfo glucosamine (R' = -SO₃, GlcNS) are common. *N*-unsubstituted glucosamine (R' = -H, GlcNH₂) is a low abundance component.

NMR and molecular modeling studies of heparin summarized in Figure 2A, reveal that it is a helical molecule in which its various sulfuryl groups project in an outward fashion (Mulloy et al., 1993). There appears to be little to no tertiary structure in heparin which allows the sulfo and carboxylate groups to display in relatively defined patterns. In a recent study on the dynamics of heparin oligosaccharides, it was determined that the flexibility of the saccharide molecule is reduced as the sulfuryl group content of the molecule increases (Angulo et al., 2005). This should have important implications for the way in which heparin binds to its various target proteins. Additionally, modifications of the heparin backbone also

dictate the conformation of individual monosaccharide units. For example, IdoA displays low energy equilibrium between two conformations, skew boat (2S_0) and chair (1C_4) [for reviews on HS and heparin structure see (Capila and Linhardt, 2002; Gama and Hsieh-Wilson, 2005; Noti and Seeberger, 2005)].

A.



B.

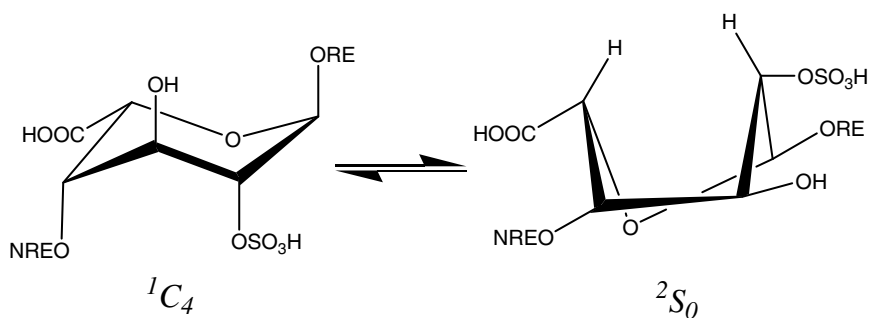


Figure 2. Structure of heparin oligosaccharides. (A) The NMR and molecular modeling of a heparin based oligosaccharide reveals that the molecule has a helical structure in which the sulfate groups are pointing outward in a recurring pattern. (B) The iduronic acid residue of HS is in equilibrium between a chair and skew boat conformation. The Reducing End (RE) and Nonreducing End (NRE) are indicated. Figure adapted from (Capila and Linhardt, 2002).

Both conformations of the uronic acid residue have been observed in co-crystal and NMR based structural analysis of heparin/protein interactions (Faham et al., 1996; Hricovini et al., 2001; Moon et al., 2004). These results suggest that the HS binding domain of a target protein can accommodate either conformation of the uronic residue.

Important HS Protein Interactions

Growth Factors- Growth factors are a large family of cytokines involved in regulating cell growth, proliferation, and differentiation (for a review see (Dailey et al., 2005)). There are 22 forms of fibroblast growth factors (FGFs) and 5 FGF receptors (FGFRs). The FGFRs are receptor tyrosine kinases and are responsible, in part, for initiating cell signaling cascades. It has been established that both FGF and FGFRs bind to heparin, and cell based studies have demonstrated that the interaction between these molecules is essential for FGF mediated cell signaling (Rapraeger et al., 1991; Yayon et al., 1991).

Two crystal structures of the FGF, heparin, and FGFR ternary complex have been solved (Pellegrini et al., 2000; Schlessinger et al., 2000). Figure 3 displays an overview of the two structures. In the 2:2:2 complex referred to as the “two end model”, two heparin molecules make extensive contacts with one FGF (green) and one FGFR molecule (orange). Each heparin molecule also makes additional contact with the second FGFR. In the second structure an “asymmetric” 2:2:1 stoichiometry was observed. Here a single heparin molecule makes contact with two FGF molecules and only one FGFR. The stark differences between the structures could reflect unique binding modes between different FGFs and FGFRs since different subtypes of each were used. Given the task to assess which structure is

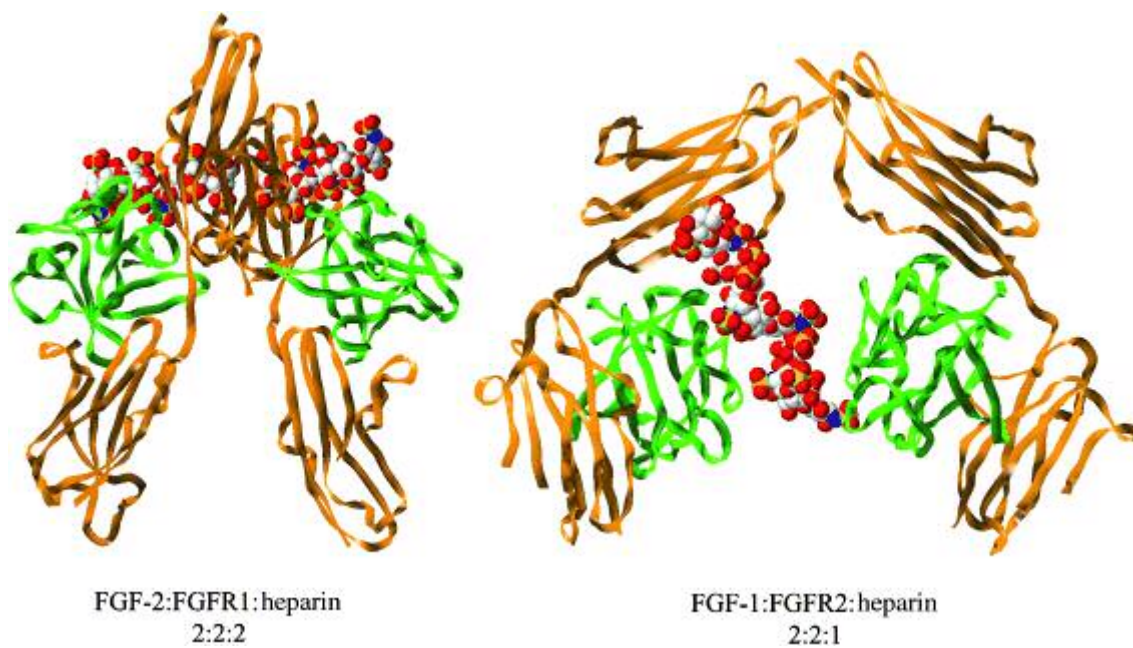


Figure 3. Two binding modes of the FGF:FGFR:heparin interaction. Two crystal structures of FGF and FGR in a complex with HS have been resolved. The FGF molecule is pictured in green, FGFR in orange, and heparin in white (carbon atom), blue (nitrogen atom), yellow (sulfur), and oxygen (red).

biologically relevant, it would appear that the two end model would put the two FGFR molecules in close proximity which could promote receptor dimerization. It is well established that the FGF mediated signaling cascades that are initiated by receptor tyrosine kinases undergo *trans* autophosphorylation, thus two FGFR that are adjacent to one another may reflect a more relevant structure (Mohammadi et al., 2005a; Mohammadi et al., 2005b).

Antithrombin- Antithrombin (AT) is a serine protease inhibitor that plays an essential role in regulation of the blood coagulation cascade. This glycoprotein inhibits the activity of several late stage serine proteases of the cascade including factor Xa and thrombin. The mechanism of inhibition involves the allosteric activation of AT. As shown in Figure 4, the active form of AT presents an amino acid P1 loop that serves as a substrate for the serine protease. When the loop is cleaved, AT undergoes a dramatic conformational change that leaves the serine protease covalently attached to AT as an acyl-enzyme intermediate and rendered inactive. AT activation proceeds through binding the cofactors heparin or HS.

The role of heparin and endothelial HS in the acceleration of AT activity has been studied extensively (Desai et al., 1998; Jin et al., 1997; Rosenberg et al., 1980; Rosenberg et al., 1997). HS increases the affinity of antithrombin (AT) for factor Xa and thrombin by approximately 1,000-fold, which in turn inhibits proteolytic activity and prevents formation of a blood clot. Antithrombin binding HS and heparin contain a structurally defined antithrombin-binding site; a pentasaccharide with the structure –GlcNS(or Ac)6S-GlcUA-GlcNS3S±6S-IdoUA2S-GlcNS6S- shown in Figure 5 (Atha et al., 1985). Within the HS binding site, the 3-*O*-sulfated glucosamine residue (GlcNS3S±6S) is essential for binding to AT. This single modification enhances binding affinity (K_d) by 10,000 fold. Crystal

structures of AT in complex with the HS pentasaccharide reveal that hydrogen bonds are made with the carboxylate groups of hexuronic acid and the 6-*O*- and 3-*O*- sulfo groups of glucosamine. Interestingly, the AT molecule does not make contact with 2-*O*-sulfo groups of iduronic acid. This finding is further supported by an analysis of AT binding of HS devoid of 2-*O*-sulfation (Zhang et al., 2001b). In the absence of 2-*O*-sulfation, the binding affinity of anticoagulant HS for AT shows a slight increase.

The physiologic importance of HS mediated activation of AT is underscored by the severe thrombotic phenotypes observed in patients that carry genetic mutations of AT that affect HS binding (Boyer et al., 1986; Koide et al., 1984; van Boven and Lane, 1997). The endogenous AT binding pentasaccharide is an essential component of clinically used anticoagulant Low Molecular Weight Heparin (LWMH) and is the structural the basis for the FDA approved drug Arixtra.

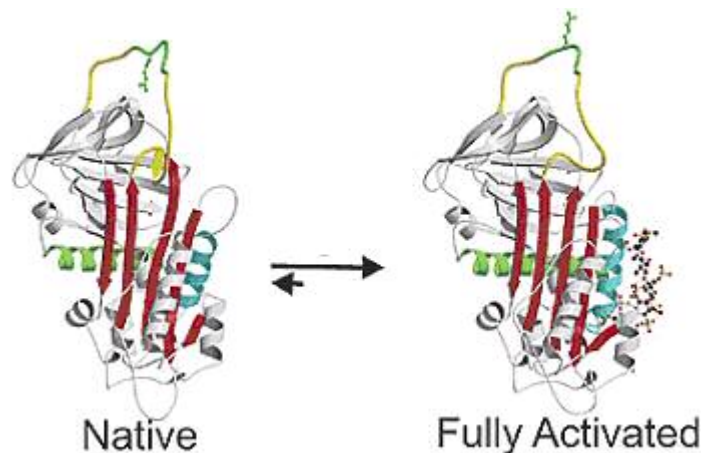


Figure 4. The allosteric activation of AT by the high affinity HS derived pentasaccharide. The AT binding pentasaccharide induces a conformational change in the protein that exposes its reactive loop which exposes an arginine residue. This loop serves as a suicide substrate for the serine proteases factor Xa and thrombin. Figure modified from (Johnson and Huntington, 2003)

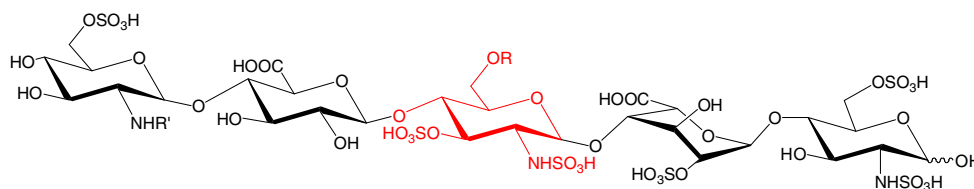
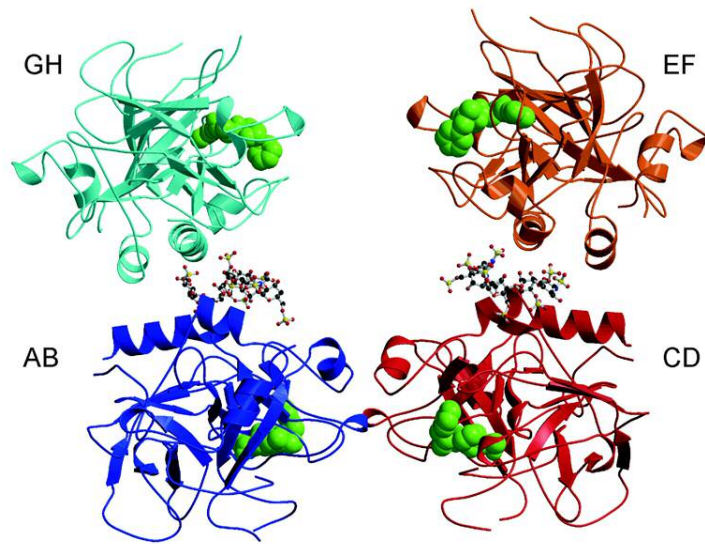


Figure 5. The high affinity AT-binding HS pentasaccharide. The R' represents sulfuryl (-OSO₃H) or acetyl (-COCH₃) groups and R represents hydrogen (-H) or a sulfuryl group. The essential 3-O-sulfated glucosamine residue is highlighted in red.

Thrombin- Thrombin, one of the late stage serine proteases of the blood coagulation cascade, plays essential regulatory roles in the balance between procoagulant and anticoagulant states. The molecular targets of thrombin are manifold in function (Huntington, 2005). Fibrinogen is the precursor of the blood clot constituent fibrin. Protein C, an anticoagulant factor, is activated by thrombin and forms a complex with additional factors to inhibit activation of thrombin and factor X, another member of the blood coagulation cascade. Additionally, thrombin serves a role in the positive regulatory feedback loop of the coagulation cascade. Thrombin can activate the early serine proteases Factors XII, VIII, and V, leading to subsequent activation of prothrombin to thrombin. The mechanisms which dictate recognition of various substrates in part is dependent upon cofactor binding. One such cofactor is heparin. Crystallographic studies have shown that two cationic patches (exosites I and II) exist on the surface of thrombin that could serve as a heparin binding domain. Site directed mutagenesis (Gan et al., 1994; Sheehan and Sadler, 1994; Ye et al., 1994) and a co-crystal structure of thrombin bound to a highly sulfated hexasaccharide fragment reveals that heparin binds to exosite II (Carter et al., 2005). The interaction appears to be nonspecific in nature since heparin was observed to bind thrombin in at least two distinct orientations as shown in Figure 6A.

A



B

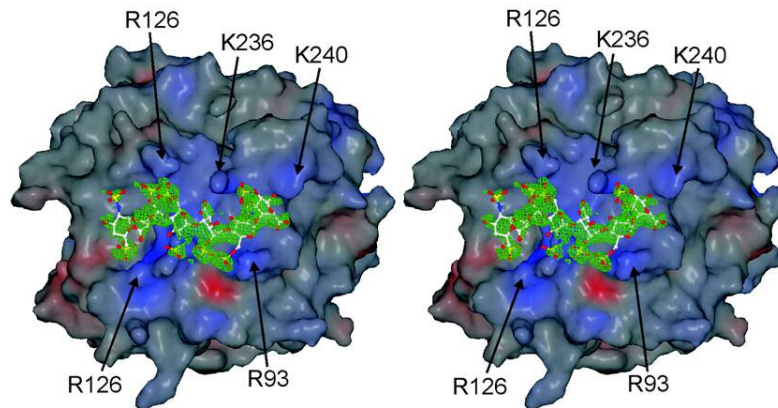


Figure 6. Crystal structure of heparin bound to thrombin. In (A) two distinct binding modes of a heparin hexasaccharide bridge two molecules of thrombin together; molecule AB with GH and CD with EF. A stereoview of the electrostatic potential diagram (B) depicts the heparin binding pocket of thrombin that is lined with basic arginine and lysine amino acid residues. This figure was adapted from (Carter et al., 2005).

Heparin binding is highly dependent on salt bridge formation between the negatively charged sulfuryl groups of the oligosaccharide and positively charged residues of basic amino acids of the protein some of which are depicted in Figure 6B. Based on the co-crystal structure and mutagenesis studies, the authors outline several amino acid residues that are critical for binding. Arg93 interacts with a 6-*O*-sulfuryl group via a salt bridge. Lys236 makes ionic contacts with the carboxylate and 2-*O*-sulfuryl groups of IdoA . Lys240 forms a salt bridge with a 6-*O*-sulfuryl group or an *N*-sulfuryl group depending on the orientation of the heparin molecule. Arg101 can make ionic and/or hydrogen bonds with a 6-*O*-sulfuryl group or an *N*-sulfuryl group depending on the mode of heparin binding.

AT-mediated deactivation of thrombin is dependent on HS and heparin acting as a bridge between the protease and inhibitor. One limitation of using the pentasaccharide-based Arixtra anticoagulant is that it is insufficiently long enough to form this bridge. Understanding the manner in which thrombin and heparin interacts should provide a great deal of insight on how to build anticoagulant heparin analogues that may be more effective in preventing and treating thrombotic events.

Chemokines- Virtually all chemokines bind to HSPGs, forming an interaction that is critical for the function of these small protein signaling molecules (Handel et al., 2005). Chemokines associate with cell surface HSPGs in order to generate concentration gradients on endothelial cells (Kuschert et al., 1999). This is an essential process in the immune response because it directs leukocytes to their site of action. HSPGs also enhance the half-life of chemokines by protecting them from protease digestion (Sadir et al., 2004). Indeed, the expression of HSPG biosynthetic enzymes and HSPG synthesis is enhanced in concert

with the immunologic response (Carter et al., 2003). HSPGs may also promote oligomerization which can provide high local concentrations of the chemokine to promote signaling via their cognate chemokine receptor(s) (Hoogewerf et al., 1997).

Several reports that characterize heparan sulfate that binds to chemokines have led to a proposed oligosaccharide structural motif essential for inducing chemokine dimerization (Stringer et al., 2002). In the HS structure, two *N*-sulfated domains (a hexasaccharide or greater) are bridged by a nonsulfated spacer region. The lack of sulfation of the linker group could provide flexibility in the HS molecule allowing it to wrap around two chemokine molecules. Structural analysis of the binding site of macrophage inflammatory protein-1 α (MIP-1 α) on heparan sulfate reveals that the nonsulfated linker region is protected from enzymatic cleavage, supporting this model (Stringer et al., 2002). Additionally, the types of *O*-sulfation and the size of the *N*-sulfo domains of chemokine binding HS vary. Several examples of this binding mode have been reported (Spillmann et al., 1998; Stringer et al., 2002; Stringer and Gallagher, 1997).

Platelet factor 4 (PF4) is the most highly abundant chemokine secreted by platelets. It is a CXC type chemokine and plays roles in a variety of physiologic processes. For example, this molecule is involved in the inhibition of angiogenesis, neutrophil adhesion, and the promotion of anticoagulant activity by protein C (Slungaard, 2005). PF4 binds to heparin and HSPGs and this complex is associated with thrombocytopenia, a troubling side effect of heparin treatment. Heparin Induced Thrombocytopenia (HIT) is a severe immunologic response initiated by antibodies formed against the heparin PF4 complex (Arepally and Cines, 2002). A structural analysis of HS that binds to PF4 by Gallagher and coworkers reveals that PF4 binds to a sequence of the HS polysaccharide that is enriched with iduronic

acid and 2-*O*-sulfation (Stringer and Gallagher, 1997). The saccharide structure is composed of three motifs; two tetradecasaccharide *N*-sulfo domains that carry the 2-*O*-sulfo iduronic acid residues, and a single *N*-acetylated domain of 16 saccharide units in length. Linhardt and co-workers demonstrated that a highly sulfated dodecasaccharide binds to PF4 and triggers structural changes (Mikhailov et al., 1999).

Interleukin 8 (IL-8) is a 72 amino acid CXC chemokine produced by a wide variety of cell types including macrophages and monocytes. It is a critical component in the acute inflammatory response, functioning as a chemotactic factor in neutrophil migration (Middleton et al., 1997). Studies have demonstrated that the interaction between IL8 and HSPGs (as well as chondroitin sulfate proteoglycans) is essential to its localization in lung tissues (Frevert et al., 2003). Structural analyses reveal that the IL-8 binding site on HSPGs is composed of two hexasaccharide *N*-sulfo domains that contain 2-*O*- and 6-*O*-sulfated iduronic acid and glucosamine units, respectively (Spillmann et al., 1998).

Differences in the unique structural requirements by chemokines for their HS binding sites underscore the importance of the mechanisms by which HS biosynthetic machinery control HS sequence.

Herpes Simplex Virus 1 glycoprotein D- Herpes simplex virus 1 (HSV1) is a member of the large *Herpesviridae* family of DNA viruses. The pathology associated with HSV1 infection includes formation of lesions typically in or near the mouth, cornea, and less frequently on genital tissues (Corey and Spear, 1986). The HSV1 virion is encased in a lipid envelope that contains at least 12 glycoproteins (Shukla and Spear, 2001). Several of these glycoproteins have been shown to mediate two essential processes in viral pathogenesis

(Spear, 2004). The attachment of the virion to the host cell surface proceeds through glycoproteins gB and gC, which are known to bind to cell surface HSPGs. Viral entry into a host cell is dependent upon the interactions between another envelope glycoprotein, gD, and its receptor on the host cell surface. In 1999, it was shown that cell surface HSPGs carrying specific 3-*O*-sulfated polysaccharide structures could serve as entry receptors for HSV1 through their interactions with gD (Shukla et al., 1999). An example of the viral entry assay is shown in Figure 7. The Herpes Virus Entry Mediator (HVEM) of the Tumor Necrosis Factor α (TNF α) receptor superfamily as well as nectin 1 and 2 of the immunoglobulin receptor superfamily and 3-*O*-HS can also function as HSV1 entry receptors (Spear et al., 2000). Notably, the 3-*O*-HS polysaccharide entry receptor has a similar binding affinity for

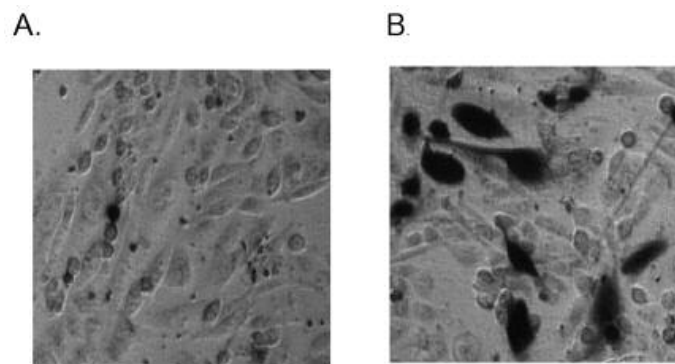


Figure 7. Entry of HSV-1 into Chinese hamster ovary (CHO-K1) cells and transfected CHO-K1 cells. CHO-K1 cells were transfected with control plasmid (A) or with pcDNA3.1-3OST5 (B). At 36 h after transfection, the cells were exposed to KOS-gL86 at 100 plaque-forming units/cell. Six hours later, the cells were washed, fixed, and incubated with X-gal to identify infected cells (*dark cells*). Figure from (Xia et al., 2002)

gD as do the HSV1 protein entry receptors. These initial findings led to the structural characterization of a gD-binding HS octasaccharide that carries the essential 3-*O*-sulfate group depicted in Figure 8A (Liu et al., 2002). The 3-*O*-sulfuryl group occurs within a highly sulfated domain on a rarely observed *N*-unsubstituted glucosamine residue.

A gD crystal structure and extensive mutagenesis studies have established that the heparan sulfate binding domain is located in the *N*-terminal ectodomain of this transmembrane

protein (Carfi et al., 2001; Yoon and Spear, 2004; Yoon et al., 2003). The HVEM and nectin 2 receptors are also sensitive to mutations in the N-terminal ectodomain of gD (Yoon et al., 2003). A strategy to blockade this region in the ectodomain of gD may prove useful in inhibiting viral entry via these two unique receptors. One such strategy is to use HS analogues to block viral entry. The gD-binding octasaccharide characterized by Liu and co-workers binds with low micromolar affinity (Liu et al., 2002) and structural analogues are being synthesized and tested in cell based assays as an HSV1 entry inhibitor.

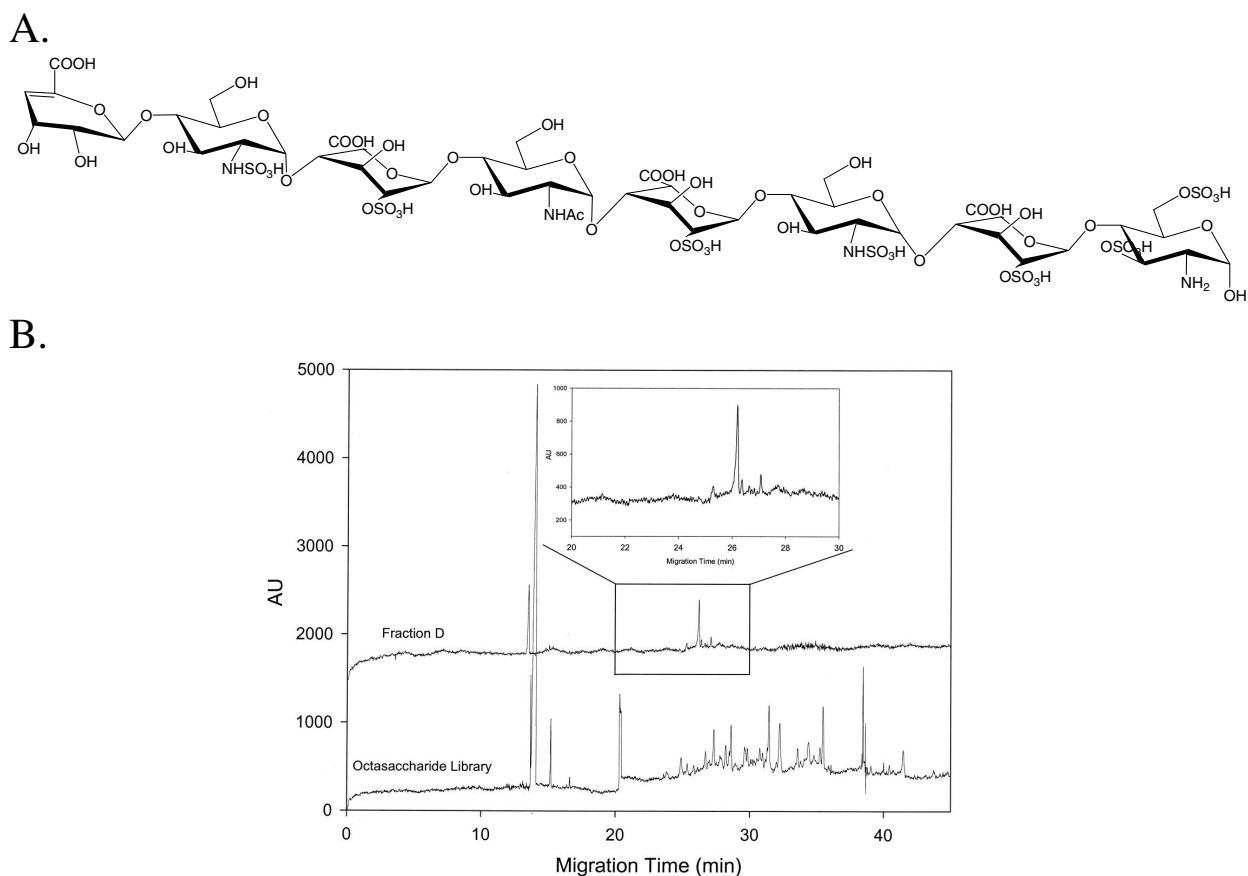


Figure 8. The structure of gD-binding octasaccharide purified from a HS derived library. (A) This molecule contains the three functional groups at the N position including the sulfonyl, acetyl, and primary amine. The octasaccharide was purified from a 3-O-sulfonated oligosaccharide HS library. As shown in (B) the purity of the octasaccharide was >80% based on analysis by capillary electrophoresis (adapted from (Liu et al., 2002)).

HS Biosynthetic Pathway

Core proteins- A variety of core proteins, which carry covalently linked GAGs and present them in their biological context have been identified (Hacker et al., 2005; Iozzo, 2005). These core proteins can be categorized into two groups. Soluble core proteins are secreted into the extracellular matrix, while cell surface core proteins are integrated into cell membranes¹. A list of core proteins and their cellular locale is presented in Table I. Once the core protein has been synthesized, it undergoes a variety of post-translational modifications, including GAG assembly that may be classified into three steps; linkage region synthesis, chain polymerization, and chain modification (Esko and Selleck, 2002).

Table 1. Core Proteins and their biological location

Core Protein (# of isoforms)	Location
Syndecan ^a	Cell surface
Glypican ^b	Cell surface
Perlecan ^c	ECM, basement membranes
Serglycin ^d	Mast Cells
Aggrin	ECM, Basement Membranes
Collagen XVIII	ECM Basement Membranes

- a. Expressed as type I membrane proteins that may be cleaved by extracellular proteases
- b. Expressed as Glycosylphosphatidylinositol anchored proteins and may be cleaved by GPIases.
- c. A modular protein that has at least 5 functional domains.
- d. The core protein of heparin. The protein component is cleaved before a mature heparin molecule is formed

Step One: GAG Linkage Region Synthesis

The GAG linkage region of CS and HS proteoglycans consists of the tetrasaccharide GlcA β 1,3Gal β 1,3Gal β 1,4Xyl β that is *O*-linked to serine residues (Figure 9) of the core

¹Cell surface HSPGs may also be released into the extracellular matrix. See Table I for details.

protein. The glycosyltransferases that synthesize this oligosaccharide are ubiquitously expressed in eukaryotic cells (Sugahara and Kitagawa, 2002). The formation of the linkage region is essential for GAG assembly and may dictate the type of GAG that will be extended.

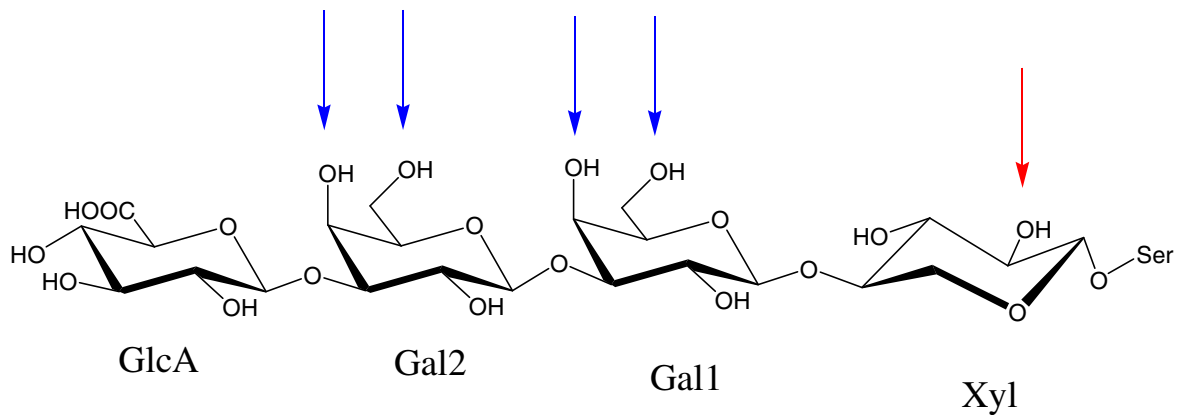


Figure 9. The proteoglycan tetrasaccharide linkage region. The tetrasaccharide is composed of glucuronic acid β 1,3 linked to galactose β 1,3 linked to galactose β 1,4 linked to xylose β linked to a serine residue of the core protein. The blue arrows indicate potential sulfation sites while the red arrow indicates the potential position for phosphorylation.

Xylosyltransferase- Two isoforms of human xylosyltransferase with 55% identity to one another have been cloned from JAR choriocarcinoma cells (Gotting et al., 2000). Enzymatic activity for XylT-I has been verified. With UDP-xylose as a sugar donor, XylT-I glycosylates serine residues contained in the Ser-Gly X (where X can be any amino acid residue) peptide consensus sequence (Brinkmann et al., 1997). Studies of a XylT-I negative CHO cell line indicate that this enzyme performs the rate limiting step in HS and CS/dermatin sulfate (DS) proteoglycan GAG linker region synthesis (Esko et al., 1985). Core protein xylosylation has been reported to take place in the pre-Golgi complex (Kearns et al., 1993). Studies have also shown that XylT-I is primarily secreted into the extracellular matrix (Gotting et al., 1999). The release of XylT-I from the Golgi complex and its relevance in an extracellular context have yet to be determined.

Galactosyltransferase- The galactosyltransferase I transfers galactose to *O*-linked xylosylproteins (Okajima et al., 1999) generating a $\beta 1 \rightarrow 4$ linkage while galactosyltransferase II preferentially catalyzes the formation of Gal $\beta 1 \rightarrow 3$ Gal linkages (Bai et al., 2001). Both of these enzymes belong to the six member $\beta 1,3$ -Galactosyltransferase family and are type II membrane bound proteins localized to the medial Golgi complex. GalTII is the only member of this family that recognizes terminal galactose residues. siRNA silencing experiments in cell culture demonstrate that it is an essential component of the GAG biosynthetic pathway (Bai et al., 2001).

Glucuronyltransferase- In the final step of GAG linkage region biosynthesis the Glucuronyltransferase I catalyzes formation of the $\beta 1 \rightarrow 3$ linkage between GlcA and Gal $\beta 1,4$ Gal $\beta 1,4$ Xyl $\beta 1$ -*O*-Ser (Kitagawa et al., 1998). The resultant tetrasaccharide serves as a substrate for both *N*-acetylglucosaminyltransferase as well as *N*-acetyl galactosaminyltransferase. Modification by GlcNAcT initiates HS polysaccharide synthesis while GalNAcT initiates the synthesis of CS and DS polysaccharides. Studies have demonstrated that the substrate selectivity of these enzymes may be dictated by regio-selective phosphorylation of the xylose residue (2-*O*-phosphoryl xylose) and/or sulfonation at the 4- and 6-hydroxyl position of the internal and/or external galactose residues of the GAG linkage region (Gulberti et al., 2005). Sulfonation of the tetrasaccharide linker increases catalytic efficiency of GlcATI, suggesting that this modification may promote GAG polysaccharide elaboration. Structural analysis of GAGs isolated from syndecan 1 of cultured NMuMG (normal murine mammary gland) cells revealed that sulfated galactose residues contained in the linker tetrasaccharide were only observed in CS and DS GAGs

whereas C2 phosphorylation of xylose is found in both HS and CS linkage regions (Ueno et al., 2001).

Step Two: Heparosan Polymerization

HS biosynthesis involves the extension of a linear polysaccharide backbone followed by various modification steps. The HS polysaccharide consists of up to 200 repeating disaccharide units of D-glucuronic acid $\beta 1 \rightarrow 4$ linked to *N*-acetylglucosamine $\alpha 1 \rightarrow 4$.

HS copolymerase- Repeating units of glucuronic acid $\beta 1 \rightarrow 4$ linked to acetylated glucosamine are extended from the linker tetrasaccharide by the bifunctional HS copolymerase. This enzyme is formed by peptides encoded by two genes, EXT1 and EXT2. EXT1 and 2 are type II membrane proteins that share 35% homology and possess glycosyltransferase activity (Lind et al., 1993; Wei et al., 2000). The catalytic efficiency of the individual proteins are low, however their activity increases substantially when they form a hetero-oligomeric structure that localizes it to the Golgi (Kobayashi et al., 2000; McCormick et al., 2000).

In vitro studies utilizing synthetic and affinity purified substrates containing the tetrasaccharide linkage region demonstrated that the EXT1/2 complex preferentially transfers GlcNAc and GlcUA to aglycons² that possess hydrophobic moieties (Kim et al., 2003). This work also demonstrated that the GlcNAcT believed to initiate HS polymerization may be dispensable since EXT1/2 can utilize GlcUA $\beta 1,3$ -Gal $\beta 1,3$ -Gal $\beta 1,4$ -Xyl $\beta 1$ -O-Ser-Gly-Trp-Pro-Asp-Gly as a substrate. However the HS EXT1/2 could not distinguish between full length

² Aglycon refers to an acceptor molecule of a glycosylation reaction.

glypican, a known HS proteoglycan, and α -thrombomodulin, a part-time³ proteoglycan. These findings may underscore the role of phosphorylated xylose and sulfonated galactose residues of the tetrasaccharide linkage region. Mutations in either EXT 1 or 2 genes can lead to loss of HS production. The hereditary bone disorder multiple exostoses linked to mutations in the EXT genes emphasizes the role these enzymes and HS in development (Zak et al., 2002).

Step Three: Polysaccharide Chain Modification

The functionality of the HS polysaccharide chain manifests through epimerization of D-glucuronic acid to L-iduronic acid and various sulfation reactions. The classes of enzymes that catalyze these reactions are C₅ epimerase (EPI), the bifunctional *N*-deacetylase/*N*-sulfotransferase (NDST), as well as the 2-*O*- 6-*O*-, and 3-*O*- sulfotransferases (2OST, 6OST, 3OST respectively). All of the sulfotransferases in the HS biosynthetic pathway utilize the sulfate donor 3'-phosphoadenosine 5'-phosphosulfate (PAPS) as a cofactor (Sugahara and Kitagawa, 2002).

N-Deacetylase *N*-Sulfotransferase- The *N*-deacetylase *N*-sulfotransferase is a bifunctional enzyme with two distinct catalytic activities. One involves removal of the acetyl group of glucosamine while the other catalyzes the transfer of a sulfonyl group from the cofactor PAPS to an *N*-unsubstituted glucosamine unit. The functional link between these two activities is obvious since most subsequent modification reactions require *N*-sulfonation.

³ Part time proteoglycan refers to those glycoproteins that have been isolated with and without GAG chains. Indeed some of these glycoproteins may only carry the GAG tetrasaccharide linkage region.

There are four distinct isoforms of the NDST gene (1 through 4) that possess unique tissue distribution patterns (Aikawa et al., 2001). Isoforms 1 and 2 both display wide and overlapping tissue distribution while isoform 3 is restricted to adult mouse brain, heart, muscle, and kidney. Isoform 4 is expressed in low levels of the brain and throughout embryonic development. Esko and coworkers have reported translational control of the NDSTs through the structured 5'-untranslated region and internal ribosome entry sites (Grobe and Esko, 2002). These finding suggests that while mRNA of isoforms 1 and 2 are ubiquitous to most tissues, translational regulation of this class of enzymes may be one mechanism to control HS synthesis.

The bifunctional activity of NDST has been demonstrated in several studies. Wei and Swiedler carried out a functional analysis of the cysteine residues of NDST (Wei and Swiedler, 1999). They concluded that the *N*-deacetylase activity of NDST prefers a reducing environment and is dependent on a cysteine residue at position 586 (rat liver NDST), while the *N*-sulfotransferase activity prefers a non reducing environment and is sensitive to most cysteine to alanine mutations of the full length protein. Also, studies have shown that optimal *N*-deacetylase activity occurs at pH 6.5, while optimal *N*-sulfotransferase activity occurs at pH 7.5. The *N*-sulfotransferase domain had been localized to the C-terminal domain. Indeed a crystal structure of this domain has been attained as well as a molecular description of substrate binding and the catalytic mechanism (Kakuta et al., 1999).

Figure 10 (A) shows that the overall shape of NST is roughly spherical with a large open hydrophilic cleft. Through molecular modeling and mutagenesis studies this open cleft was determined to be the substrate binding domain (Kakuta et al., 2003). Through sequence alignment with other sulfotransferases the PAPS binding domain was determined to be

internal to the polysaccharide binding site, placing the sulfuryl group of PAPS in close proximity to its acceptor site at the N2 position of glucosamine. The position of a glutamate residue relative to the bridging oxygen of the 5' phosphoryl group and its close proximity to the *N* position of glucosamine in the modeled hexasaccharide (Figure 10B) make it a



Figure 10. The heparin binding cleft of NST. Panel A shows the overall fold of the NST domain. Panel B shows a HS hexasaccharide that has been modeled into the proposed HS binding cleft. Residue E642 is in close proximity to the N2 acceptor site and a modeled sulfuryl moiety of PAPS.

candidate to serve as a catalytic base. The glutamate residue should enhance the nucleophilicity of the amino group, promoting a S_N2 type reaction mechanism.

The characterization of HS from mutant cell lines and knockout mice suggests that the type of functional unit at the *N* position (-Ac, -H, or -SO₃H) of glucosamine dictates the amount of adjacent *O*-sulfo groups (Bame and Esko, 1989; Holmborn et al., 2004; Ledin et al., 2004). Subsequently, it is sulfation patterning that determines the specificity of

interactions between HS and a target protein. Some HS/protein interactions are found to occur in highly sulfated domains of HS while others can occur in more variably sulfated domains (Chen and Liu, 2005; Liu et al., 2002; Pye et al., 1998; Stringer et al., 2002). This makes the NDST enzyme class a critical component in the biosynthetic pathway of multifunctional HS and heparin. Indeed, NDST knockout mice reveal that NDST 1 is essential for development (Fan et al., 2000) while NDST2 is essential only for mast cell production (Forsberg et al., 1999; Lyon et al., 2000).

Epimerase- Epimerase epimerizes the C5 carboxylate group of D-glucuronic acid converting it to L-iduronic acid. The IdoA epimer is a flexible conformer of the uronic acid residue since it is in equilibrium between a chair and skew boat conformation. This flexibility has been suggested to provide additional structural diversity in the HS polysaccharide for target protein binding. *In vitro*, the epimerization reaction is reversible (Hagner-McWhirter et al., 2000), however in cell culture, the reaction appears to be irreversible (Hagner-McWhirter et al., 2004). Targeted disruption of the C5-epimerase results in an embryonic lethal phenotype in mice (Li et al., 2003). The morphology of the HS $\text{Epi}^{-/-}$ embryo is strikingly distinct from the wild type. Some key differences include renal agenesis, immature lungs, and severe skeletal defects. These embryos also express HS that carries substantially fewer sulfate groups than the wild type. The HS $\text{EPI}^{-/-}$ phenotype demonstrates the manifold and essential roles of structurally diverse HS in development.

2-O-sulfotransferase- The 2-O-sulfotransferase catalyzes sulfo-transfer from PAPS to the 2-O- position of an uronic acid unit (Kobayashi et al., 1996). Characterization of HS isolated

from natural sources and *in vitro* sulfotransferase assays confirm that iduronic acid is the preferred acceptor over glucuronic acid (Rong et al., 2001). Notably, 2OST is the only HS sulfotransferase that exists as a single isoform. A gene trap mutation for 2OST results in renal agenesis and a neonatal lethal phenotype in mice (Bullock et al., 1998). Esko and coworkers have demonstrated an interaction between 2OST and epimerase *in vivo* (Pinhal et al., 2001). This finding highlights a potential mechanism whereby 2OST is able to locate its preferred substrate (IdoA) via a physical linkage with the enzyme that generates it.

6-O-Sulfotransferase- There are three members of the HS 6-*O*-sulfotransferase family. Isoform 1 appears to be strongly expressed in the liver, isoform 2 in brain, and isoform 3 appears to be broadly expressed in most mouse tissue types (Habuchi et al., 2000). Two splice variants of the human 6OST2 have unique expression patterns (Habuchi et al., 2003). The original 6OST2 appears to be restricted to brain tissues while the second 6OST2 variant is expressed in additional tissues including ovary, kidney, and pancreas. The role of the 6OST1 gene in zebrafish has been studied using morpholino antisense oligonucleotides (Bink et al., 2003). The loss of function phenotype displayed significantly reduced levels of 6-*O*-sulfation, but not 2-*O*-sulfation in its heparan sulfate chains. The 6OST knockdown showed developmental deficiencies in the white matter of axon bundles, high levels of myosinD expression, and severe muscle degeneration. The substrate specificity of the 6OSTs has been characterized and does not appear to vary among the different isoforms (Smeds et al., 2003). It is notable that 6OST can act on both *N*-acetylated and *N*-sulfonated glucosamine residues. The enzyme prefers *N*-sulfonated glucosamine that is at the reducing end of IdoA over *N*-sulfonated glucosamine at the reducing end of GlcA.

3-O-Sulfotransferase- The 3-*O*-sulfotransferases catalyzes sulfuryl transfer to the 3-hydroxyl position of various glucosamine residues. This modification is rare in heparan sulfate isolated from natural sources. The first 3OST to be identified was initially purified from L-cell conditioned media and later cloned (Liu et al., 1996; Shworak et al., 1997). It was determined that this enzyme makes the essential modification in the biosynthesis of anticoagulant heparin and heparan sulfate. Subsequently, additional members of the 3OST family have been cloned and characterized (Shworak et al., 1999; Xia et al., 2002; Xu et al., 2005). The expression pattern for this family of enzymes is quite diverse. The unique structures generated in AT- and gD- binding HS are largely due to the substrate selectivity of HS 3-*O*-sulfotransferases. Studies have shown that different members of the 3OST family can transfer a sulfuryl group to the 3-OH position of several glucosamine residues modified to a different extent as shown in Figure 11 (Liu and Rosenberg, 2002).

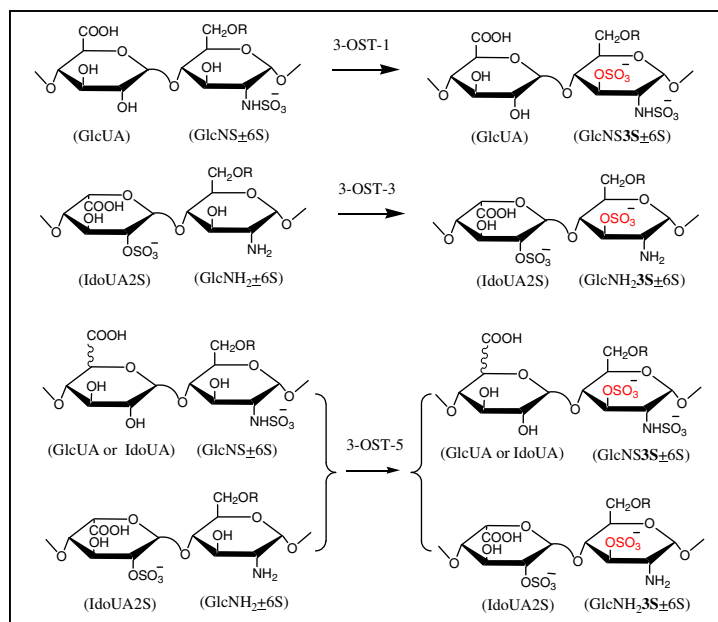


Figure 11. Substrate specificities of 3-OSTs. 3OST1 transfers a sulfuryl group to the *N*-sulfo glucosamine (GlcNS \pm 6S) residue that is linked to the nonsulfated glucuronic acid residue at the nonreducing end (GlcUA). 3OST3 transfers a sulfuryl group to the *N*-unsubstituted glucosamine (GlcNH $_2$ \pm 6S) residue that is linked to a 2-*O*-sulfo iduronic acid (IdoUA2S) residue at the nonreducing end. 3OST5 transfers a sulfuryl group to the glucosamine (GlcNS \pm 6S or GlcNH $_2$ \pm 6S) residue that is linked to either nonsulfated or sulfated iduronic (IdoA \pm 2S) and GlcUA residue. It appears the 3OST3 and 3OST6 have similar substrate specificity.

Traditionally, this substrate selectivity has been described at the disaccharide level and correlates strongly with the biological function of the modified HS chain, as shown in Table II. The disaccharide, GlcUA-AnMan3S \pm 6S, observed in chemically depolymerized 3OST1 and 5 modified HS is characteristic of anticoagulant HS while IdoUA2S-AnMan3S \pm 6S, produced by isoforms 3OST2 through 6 is observed in gD-binding HS.

Table 2. Summary of the products and biological functions of 3-OST- modified HS

Isoforms	Characteristic disaccharides prepared from enzyme modified has	Biological functions of the enzyme modified HS
3OST1	GlcUA-AnMan3S \pm 6S ^b	AT-binding HS
3OST2	GlcUA2S-AnMan3S and IdoUA2S-AnMan3S	Unknown ^c
3OST3A	IdoUA2S-AnMan3S \pm 6S	Entry receptor for HSV1 ^d
3OST3B	IdoUA2S-AnMan3S \pm 6S	Entry receptor for HSV1
3OST4 ^c	IdoUA2S-AnMan3S \pm 6S	Unknown ^c
3OST5	GlcUA-AnMan3S \pm 6S, IdoUA-AnMan3S \pm 6S and IdoUA2S-AnMan3S \pm 6S	AT-binding HS and Entry receptor for HSV
3OST6	IdoUA2S-AnMan3S \pm 6S	Entry receptor for HSV1

- a. The disaccharides were prepared by subjecting the enzyme-modified HS to the degradations of nitrous acid (AnMan represents 2,5-anhydromannitol; GlcUA and IdoA represent glucuronic and iduronic acid, respectively). AnMan is a product of nitrous acid degradation.
- b. The 3-*O*-sulfo group is bolded and underlined to emphasize the modification by 3-OSTs.
- c. A recent review by Shukla and Spear indicated that 3OST2 and 3OST4 generate entry receptors for HSV (Shukla and Spear, 2001).
- d. HSV represents herpes simplex virus type 1.
- e. The substrate specificity of 3OST4 was reported by Wu and colleagues (Wu et al., 2004).

Subsequent studies show that 3OST5 modified HS binds to antithrombin and to Herpes Simplex Virus glycoprotein D. It has also been demonstrated that this enzyme generates a wide range of 3-*O*-sulfated disaccharides, including IdoUA2S-AnMan3S±6S, GlcUA-AnMan3S±6S as well as IdoUA-AnMan3S±6S (Chen et al., 2003). In an additional study on the substrate specificity of this enzyme, Mochizuki et al. (Mochizuki et al., 2003) isolated a unique tetrasulfated disaccharide, ΔUA2S-GlcNS3S6S, from heparin modified by 3OST5. From these studies, 3OST5 appears to have a broad substrate specificity, which explains the fact that the products resulted from 3OST5 modification have multiple biological functions, including anticoagulant activity. Indeed, using purified recombinant 3OST5 expressed in insect cells, we demonstrated that 3OST5 modified HS binds to antithrombin, and the percentage of AT-binding HS is comparable to that of the HS modified by purified 3OST1 (Chen et al., 2003). These results demonstrate that 3OST5 is capable of generating AT-binding HS *in vitro*. However, the role of 3OST5 in synthesizing antithrombin-binding HS *in vivo* and the activity of 3OST5 modified HS in the deactivation of AT-mediated factor Xa remains to be investigated.

The crystal structures of PAP in complex with 3OST1 (Edavettal et al., 2004) and a ternary complex of 3OST3, PAP, and the HS tetrasaccharide UA2S-GlcNS6S-IdoUA2S-GlcNS6S (Moon et al., 2004) have been resolved. In comparing the structure of the previously crystallized *N*-sulfotransferase (NST) (Kakuta et al., 1999) with 3OST1, it appears

that they share a similar overall structural fold (Figure 12). However, in comparing the electrostatic potential diagram of the two enzymes as shown in Figure 10, it is evident that the proposed HS binding cleft of the 3OSTs contains more positively charged amino acid residues than that of NST (Edavettal et al., 2004). This observation fits well with our understanding of the differences in substrate preference between these two sulfotransferases since *N*-sulfonation of the glucosamine residue in HS is precursory to *O*-sulfation. The NST enzyme recognizes the unmodified structure, heparosan $(-\text{GlcUA-GlcNAc-})_n$ (Kusche-Gullberg and Kjellen, 2003), while the 3OSTs require more highly sulfated and negatively charged forms of HS (Liu et al., 1999). It is proposed that the positively charged cleft in the 3OSTs can provide more electrostatic contacts for the sulfated substrates of these enzymes.

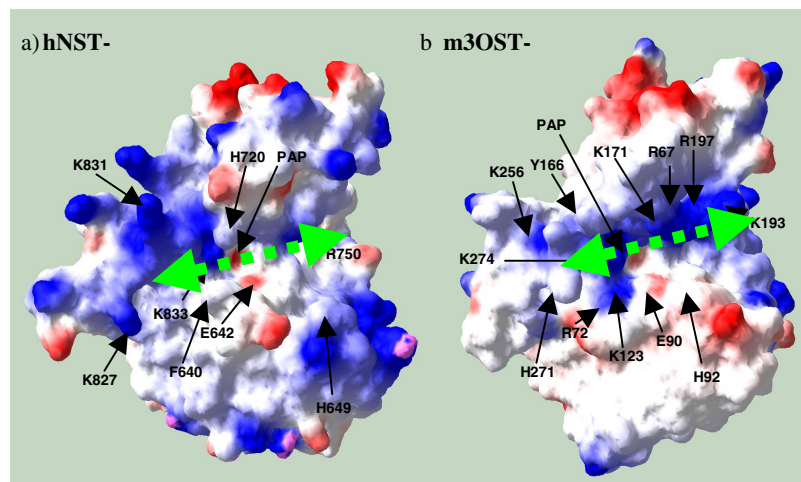


Figure 12. A charged surface diagram of the proposed heparan binding cleft of the sulfotransferase domains of NST-1 (a) and 3-OST-1 (b). The global position of the cleft is marked with a *green dashed line*. Blue surfaces signify positive charge, whereas *red* surfaces signify negative charge. The *double-sided dash arrows* (in *green*) indicate the region where HS likely binds. This figure was created using Swiss PDB viewer.

The crystal structure of the 3OST3 ternary complex showed that the tetrasaccharide unit (shown in Figure 13) was bound in the positively charged cleft. As shown in Figure 14, the U4-G3 units make more contacts with the protein than the I2-G1 disaccharide unit. The U4

unit, which is the uronic acid at the nonreducing end of the acceptor glucosamine unit, makes extensive contacts with 3OST3 and is predicted to play a role in substrate specificity. Of particular interest, the residues Q255 and K368 make contacts with the 2-*O*-sulfo and C5 carboxylate groups of U4 respectively. In Table 3 the 3OST3 point mutants Q255A and K369A show significantly reduced sulfotransferase activity. Notably, these mutations in the 3OST1 isoform do not impact

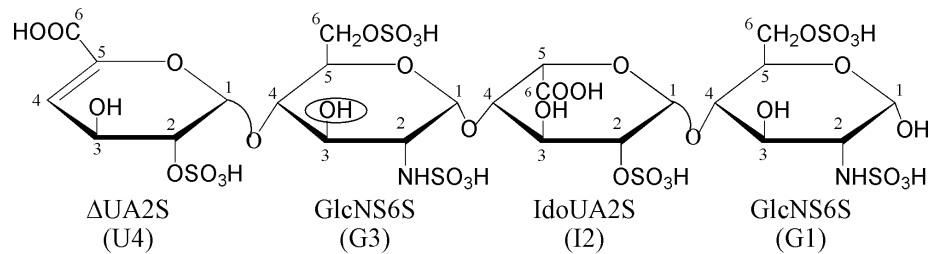


Figure 13. The structure of the tetrasaccharide substrate. The 3-*O*-sulfonation site is circled. For clarity, U4 represents ΔUA2S; G3 represents GlcNS6S linked to ΔUA2S; I2 represents IdoUA2S; and G1 represents GlcNS6S at the reducing end.

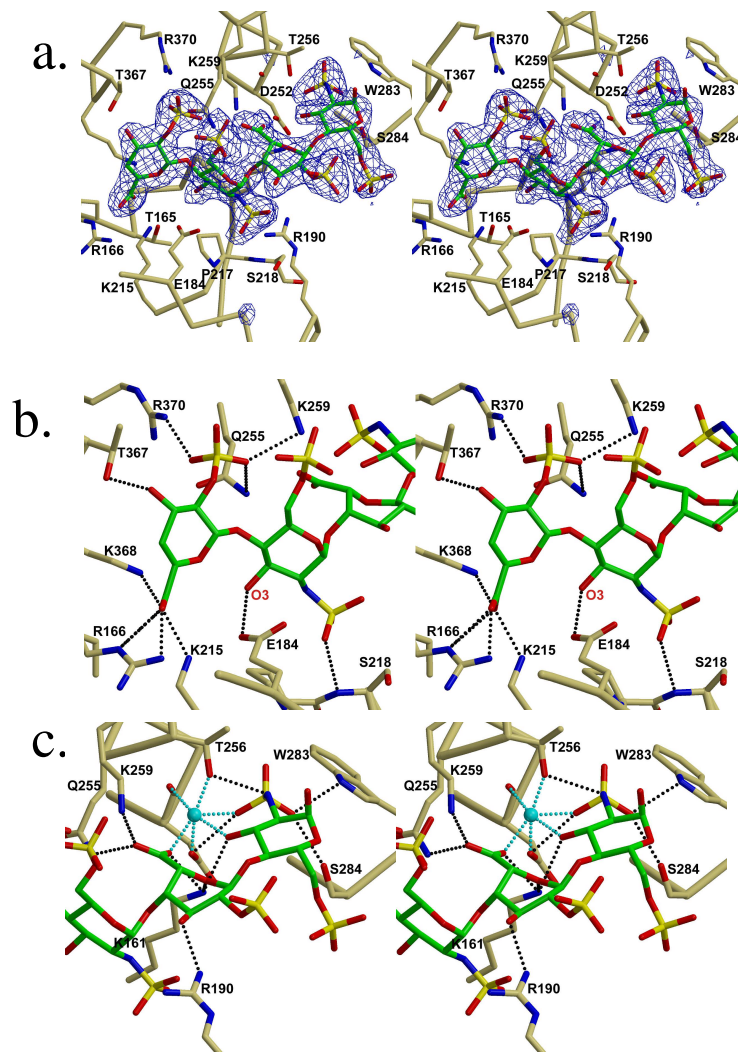


Figure 14. Stereo diagrams of the binding of 3OST3 and tetrasaccharide. a) Stereo diagram of HS acceptor substrate binding cleft with tetrasaccharide (green) bound. Residues that line the cleft are pictured. Displayed in blue is the simulated annealing Fo-Fc omit electron density map contoured at 2σ . b) Stereo diagram displaying the interactions between 3OST3 and U4-G3 units. The O3 oxygen of G3 unit is labeled. c) Stereo diagram of the interactions between 3OST3 and I2-G1 units. A metal ion modeled as a sodium ion is colored cyan, as are interactions between the metal and the coordinating atoms. Possible hydrogen bonds between the protein and tetrasaccharide are displayed as black dashed lines. These figures were created using Molscript and Raster3d (Kraulis, 1991; Merritt and Bacon, 1997).

enzymatic activity as critically, suggesting that these residues may affect HS binding rather than sulfo-transfer (Moon et al., 2004). One potential explanation for these differences is that these residues are not as significant in substrate recognition of 3OST1. It should be noted that the commonly characterized HS disaccharide structure modified by 3OST1 is GlcUA-GlcNS3S6S.

Table 3. Analysis of the sulfotransferase activity of selected 3OST1 and 3OST3 mutants.

3OST1 construct ^a	% Activity ^b	3OST3 construct ^a	% Activity ^b
R67E	1.1	K161A	0.4
R72E	0	R166E	0.2
K123A	0.2	K215A	0.1
Q163	34	Q255A	0.4
K274	17.4	K369A	0.1

- a. The mutants were prepared using a site-directed mutagenesis kit from Invitrogen and purified.
- b. The activity of 3OST3 was assayed by incubating the purified mutant proteins with HS and [³⁵S]PAPS, and the resultant [³⁵S]HS was quantified by DEAE chromatography. 100% activity represents the transfer of 18 pmoles of sulfate/μg of protein under the standard assay condition.

The ternary complex provides a great deal of information about contacts between the enzyme and those HS residues adjacent to the acceptor glucosamine unit. Many questions remain about the interactions that extend beyond this site. In addition, conformational changes observed in the 3OSTs upon heparan binding suggest a potential for allosteric effects that can impact enzyme function.

Physiologic and Pathophysiologic Roles of HS

Cardiovascular biology- HS plays a critical role in controlling the blood coagulation process (Conrad, 1998). Heparin, a HS analogue, is the most commonly used anticoagulant drug due to its functions as a cofactor in the AT-mediated inhibition of factor Xa and thrombin. The 3OST isoform 1 has been shown to make the essential modification of high affinity AT-binding HS (Liu et al., 1996). A recent report of a murine 3OST1 knockout model has raised some questions about the role of this enzyme in hemostasis (HajMohammadi et al., 2003). They observed that levels of AT-binding HS in 3OST1^{-/-} mice were not completely eliminated, nor did these animals possess a procoagulant phenotype. It was suggested that in these models, additional anticoagulant factors compensated for the loss of AT-binding HS generated by 3OST1. As a follow up to this

work they demonstrated that in epithelial cells of the glomerulus of the 3OST1^{-/-} mouse, additional 3OSTs can generate anticoagulant HS from a limiting precursor pool of HS (Girardin et al., 2005). These results suggest that expression of one isoform of the 3OSTs may be insufficient to observe a procoagulant phenotype. In order to completely delineate the role of anticoagulant HS in the blood coagulation cascade it is essential to generate a model organism that is completely devoid of 3-*O*-sulfated HS polysaccharides. The biosynthesis of AT-binding HS is believed to be highly regulated, which is supported by the fact that only 1 to 10% of total HS isolated from the cells bind to AT.

Heparanase in cancer- Heparanase is a heterodimeric endoglycosidase that specifically cleaves the polysaccharide chain of HSPGs. Heparanase is a glycosylated molecule that is secreted into the extracellular matrix by a variety of normal cells including platelets, neutrophils, and activated lymphocytes. Overwhelming genetic and biochemical evidence implicates heparanase in cancer progression (Baraz et al., 2006; Hulett et al., 1999; Joyce et al., 2005; Roderick M. Quiros, 2006; Simizu et al., 2004; Vlodaysky et al., 1999). The heparanase gene is overexpressed in malignant cancer cells including carcinoma (Kim et al., 2002), melanoma (Kelly et al., 2003; Motowo Nakajima, 1988), and breast cancer (Maxhimer et al., 2002). A significant increase in heparanase activity in the serum of cancer patients is often associated with a poor prognosis (Roderick M. Quiros, 2006). A study that utilized a HS mimetic, PI-88⁴, *in vivo* demonstrated that this molecule can decrease tumor cell proliferation, increase apoptosis, and decrease angiogenesis (Joyce et al., 2005). These effects were due in part to a reduction in the association of VEGF, a HS binding protein, with its cognate receptor. The authors suggest that the increased metastatic potential of tumors

⁴ PI-88 is a sulfated phosphomannopentose molecule isolated from yeast and chemically sulfonated.

that express heparanase may, in part, be the result of improved growth factor mobilization within the microenvironment.

Microbial attachment and cellular entry- A variety of microbes including bacteria, viruses, and parasites utilize HSPGs to make initial attachment to host epithelia. After attachment, the microbe can colonize the host or be internalized by a variety of entry mechanisms. The role of cell surface HS has been validated in these processes by the observed loss of colonization through the administration of exogenous HS and heparin, and through the chemical or genetic ablation of cell surface HSPGs (Alvarez-Dominguez et al., 1997; Taraktchoglou et al., 2001; Tonnaer et al., 2006).

Recent studies have also demonstrated that soluble forms of HSPGs and heparin can serve as virulence factors for gram negative bacteria (Park et al., 2004; Park et al., 2001; Park et al., 2000a). *Pseudomonas aeruginosa* has been shown to secrete a soluble factor LasA that can promote the release of the cell surface HSPG syndecan 1 from lung epithelial cells. In the presence of soluble HSPGs, exogenous HS, and heparin, the ability of the microbe to colonize and invade host tissues is substantially enhanced. The mechanism for this enhanced virulence is unclear but studies have suggested that soluble HSPGs can serve to alter the host immune response. For example HS can bind to circulating antimicrobial peptides. Additionally, HSPGs are important in the chemotaxis of leukocytes (Li et al., 2002; Wang et al., 2005). Alterations in the immune response can serve to create an environment that is amenable to microbial infection.

A variety of microbes promote interaction with its host by binding extracellular matrix proteins. Pathogens also use host matrix components to evade the immune response. Studies

have shown that *Neisseria gonorrhoeae* and other pathogenic bacteria can bind vitronectin and fibronectin via heparin and HS (Duensing and Putten, 1998; Duensing et al., 1999; Gómez-Duarte et al., 1997).

Chemoenzymatic Synthesis of Heparin and HS Analogues

With the multitude of biological functions of heparin and HS, it is of great interest to expand current chemical methods to synthesize structurally defined oligosaccharides. Access to a variety of well defined heparin analogues will aid in the development of structure activity relationships for this therapeutically relevant molecule. The monumental synthesis of the AT activating pentasaccharide by Petitou represents the beneficial role of producing specific heparin structures to examine their role in a pathophysiologic context (Petitou et al., 1986). The low yield (~0.4%) coupled with the approximately 80 step synthesis of the pentasaccharide also emphasizes the need to develop strategies to complement the *de novo* synthesis of heparin oligosaccharides. Solid phase methodologies along with the development of advanced protection group chemistry may aid in realization of more feasible routes to heparin production (Noti and Seeberger, 2005). Another more recent advancement in this area is the use of enzymatic and chemoenzymatic methods to generate heparin and HS analogues (Chapman et al., 2004).

Enzymatic and chemoenzymatic synthesis of heparin- For over 70 years, various forms of heparin have been used in the clinic to treat thrombotic episodes and as prophylaxis during invasive surgery (Linhardt, 2003). The HIT side effects associated with heparin treatment have been reduced with the use of low molecular weight heparins (LMWHs) (Sundaram et

al., 2003). However, since heparin is a natural product, there is a potential for the presence of animal-borne pathogens in these preparations. Also, if the therapeutic potential of heparin is to be extended beyond anticoagulation, the heterogeneity of heparin should be reduced (Lever and Page, 2002). Recently it has been demonstrated that challenges associated with the *de novo* chemical synthesis of heparin may be overcome with the use of HS biosynthetic enzymes. These catalysts provide proper regio-selective sulfonation and can be carried out in a combined or stepwise manner. Rosenberg and colleagues have pioneered this approach in three papers published in 2003. In their first effort the group synthesized low microgram quantities of anticoagulant heparin termed “Mitrin” with measured activity against factor Xa (Kuberan et al., 2003a). They reported the expression of NDST2, epimerase, 6OST2, and 3OST1 using a baculovirus expression system. Using the capsular polysaccharide from the K5 strain of *E. coli* a rapid two step synthetic route was carried out. NDST and epimerase reactions were coupled in the first step while 6OST2 and 3OST1 mediated reactions were carried out in the second. Surprisingly, the group reported 70% of the disaccharide units contained IdoA and nearly 50% of the disaccharide units contained 3-*O*-sulfo glucosamine.

Previous reports of epimerization in the absence of 2-*O*-sulfonation suggested that *N*-sulfonated HS could contain 50% IdoA acid since the epimerization is a reversible reaction. Additionally 3-*O*-sulfation is a rare constituent of HS and heparin (between 0.5-10% for HS and approximately 30% for heparin), and the paucity of this modification was believed to be the result of a restricted enzyme substrate specificity. The authors also demonstrated that the Mitrin preparation has 4-5 times the anti-factorXa activity of heparin, when using an *in vitro* spectrometric assay. Importantly, 2-*O*-sulfation was excluded from the preparation because this modification is important in PF4 binding heparin. The absence of 2-*O*-sulfation could

minimize HIT if Mitrin is applied in a clinical setting. One challenge in Mitrin synthesis is the use of PAPS in the reaction. PAPS is an expensive molecule to produce and is not very stable at $\text{pH} \leq 7$. Also the by-product of PAPS is PAP and this molecule can inhibit the sulfotransferase reactions with an IC_{50} of approximately $100 \mu\text{M}$.

In a second report Rosenberg and colleagues utilized a chemoenzymatic strategy to synthesize anticoagulant heparin (Kuberan et al., 2003b). In this effort the authors devised a stepwise synthetic route that involved the base catalyzed deacetylation and regio-selective N-sulfonation with the reagent trimethylamine sulfur trioxide. This first step was followed by subsequent enzymatic reactions outlined in Figure 15. In this approach the degree of epimerization was increased to 85% while that of 3-*O*-sulfation was reduced 5-17 fold based the number of 3-*O*-sulfated disaccharides. The increase in the degree of epimerization could be due to the increase in *N*-sulfo glucosamine which is a prerequisite for the epimerase-mediated conversion of glucuronic acid to iduronic acid. A potential explanation for the reduction in 3-*O*-sulfation is the increased percentage of IdoA acid. The characteristic disaccharide unit in 3OST1 modified heparin is GlcA-GlcNS3S±6S. The increase in epimerization would lead to a decreased availability of the preferred substrate for 3OST1.

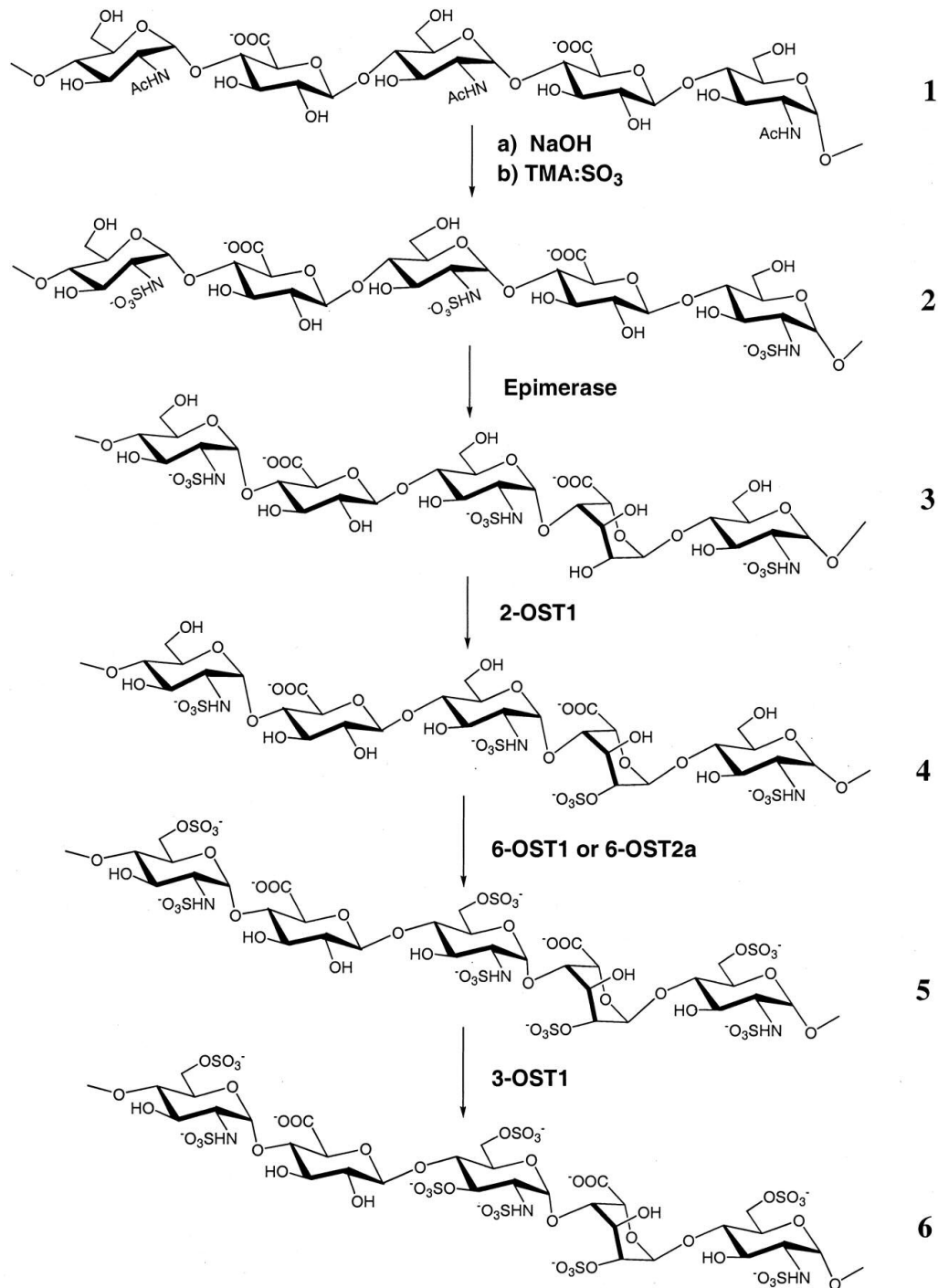


Figure 15. The synthetic route to anticoagulant heparan sulfate. Chemoenzymatic synthesis of heparan sulfate was carried out in six steps. Chemical deacetylation and *N*-sulfonation of K5P resulted in the *N*-sulfo K5 precursor for subsequent enzymatic reactions. Each of the enzymatic reactions were carried out in a stepwise manner.

In their final effort, Rosenberg and colleagues utilized an enzymatic approach to synthesize the AT binding pentasaccharide (Kuberan et al., 2003c) through the synthetic route depicted in Figure 16. In order to generate the polysaccharide they utilized heparitinase I to degrade the non N-sulfonated domain of NDST modified K5 polysaccharide. This enzyme proceeds through an elimination type mechanism to generate $\Delta^{4,5}$ unsaturated uronic acid residues (Hovingh and Linker, 1970; Lohse and Linhardt, 1992). The hexasaccharide was then used as a substrate for the subsequent sulfotransferase and epimerase reactions. In their synthetic route 2OST and epimerase reactions were coupled as well as 6OST1 and 6OST2 reactions. Hexasaccharides containing the unsaturated uronic acid were purified by size exclusion and then cleaved to a pentasaccharide by the hydrolase $\Delta^{4,5}$ glucuronidase. In the final step the pentasaccharide was modified with 3OST1 and radiolabeled PAP³⁴S in order to purify it from nonreacted material and to perform a gel shift assay.

Another unique chemoenzymatic approach for anticoagulant “neoheparin” has recently been published by Lindahl and coworkers (Lindahl et al., 2005). The overall approach to attain anticoagulant heparin was complete sulfonation of K5 polysaccharide, partial epimerization, followed by graded desulfation via solvolysis. The first step in the strategy was to perform regio-selective *N*-sulfonation on capsular K5 polysaccharide, followed by epimerization with epimerase. In the next steps, the author use a per-*O*-sulfonation in which all of the hydroxyl groups on the polysaccharide are sulfonated, followed by graded solvolytic desulfonation to selectively remove some of the *O*-sulfuryl groups. In the final step of the synthesis, controlled cleavage of the polysaccharide was carried out with nitrous acid. Upon structural analysis of the final product, approximately 46% of glucosamine was

3-*O*-sulfated. The authors reported gram scale preparation with activity against factor Xa and

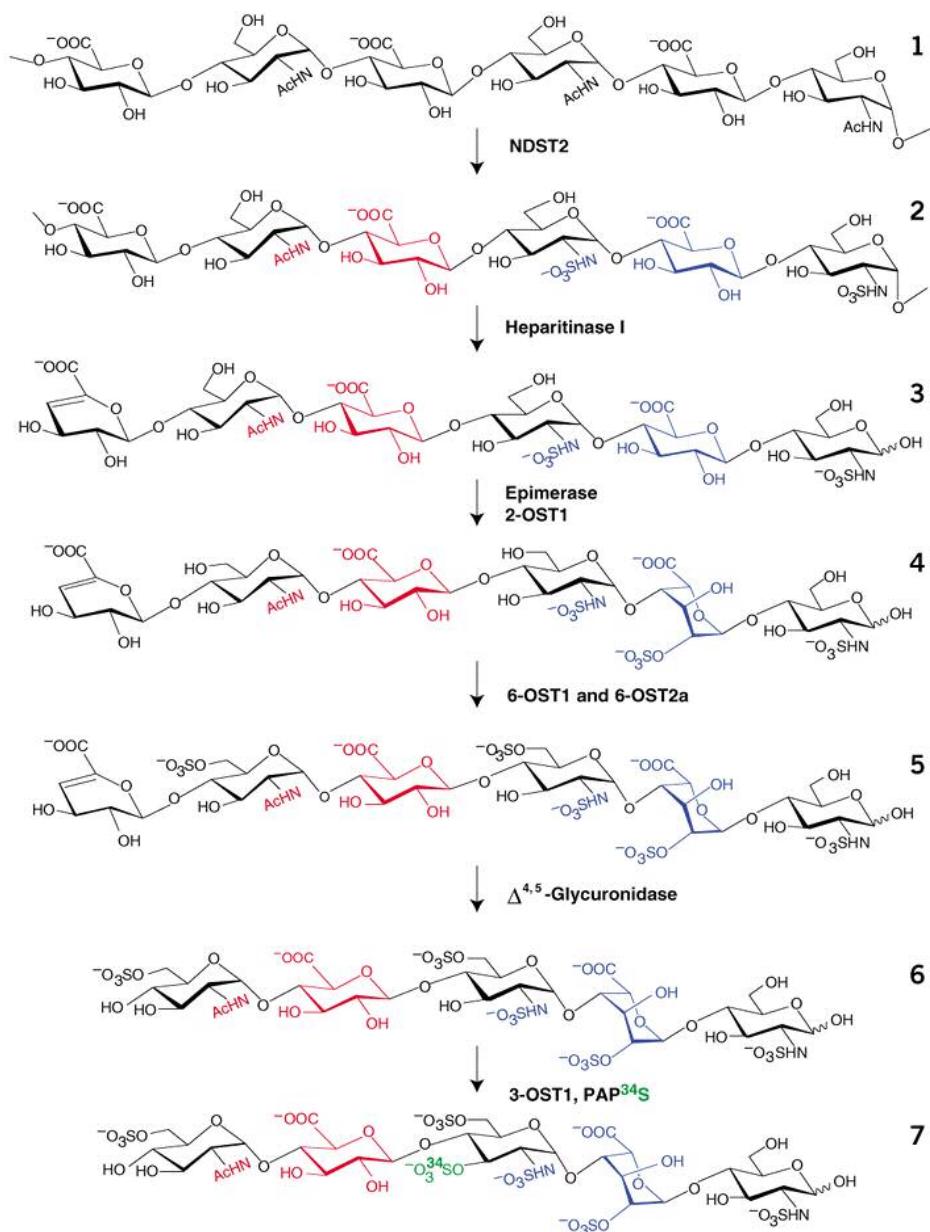


Figure 16. Enzymatic synthesis of the HS derived AT binding pentasaccharide. The K5P polysaccharide was partially N-sulfonated with NDST isoform 2 followed by partial enzymatic degradation by heparitinase I which preferentially cleaves at the glycosidic linkage between glucuronic acid and N-acetyl glucosamine. Hexasaccharide fragments were isolated and subjected to additional modifications. Unlike their previous effort, epimerization and 2-*O*-sulfonation reactions were coupled together. To access the pentasaccharide, the hydrolytic $\Delta^{4,5}$ glycuronidase was used to remove unsaturated uronic acid at the nonreducing end. The synthesis was completed with the 3OST1 modification of the pentasaccharide.

thrombin that is similar to heparin. The major limitation in this work is the presence of unnatural sulfuryl groups in the polysaccharide, specifically at the C3 position of glucuronic and iduronic acid. These moieties can have a negative impact on the anticoagulant activity of the neoheparin and were reported in <5% (IdoA) and 46% (GlcA) abundance.

In 2005 Chen et al. reported an enzymatic approach to the synthesis of heparin with anticoagulant, gD-binding, and FGF binding (Chen et al., 2005) activities. The advances of this effort were the milligram scale preparation that only requires two or three steps. In this approach, heparin was selectively de-*O*-sulfonated, followed by redesign of the polysaccharide with 2-*O*-, 6-*O*-, and/or 3-*O*-sulfotransferases as shown in Figure 17A. A major advantage to this approach is the use of a PAPS regeneration system (Figure 17B) developed by Wong and colleagues. In this system the rat arylsulfotransferase IV (AST IV) and high concentrations (5-10 millimolar) of the small molecule p-nitro phenol sulfate (PNPS) is used to convert PAP to PAPS. The advantages of this system are threefold: 1) Only catalytic amounts of PAP (~40µM) are required, thus allowing reaction scale up while limiting the potential for PAP mediated enzyme inhibition, 2) AST IV can be prepared easily and in large quantities (40-50 milligrams per liter in a bacterial expression system), and 3) PAP and PNPS are substantially less expensive and more stable reagents than PAPS.

A. Modification route

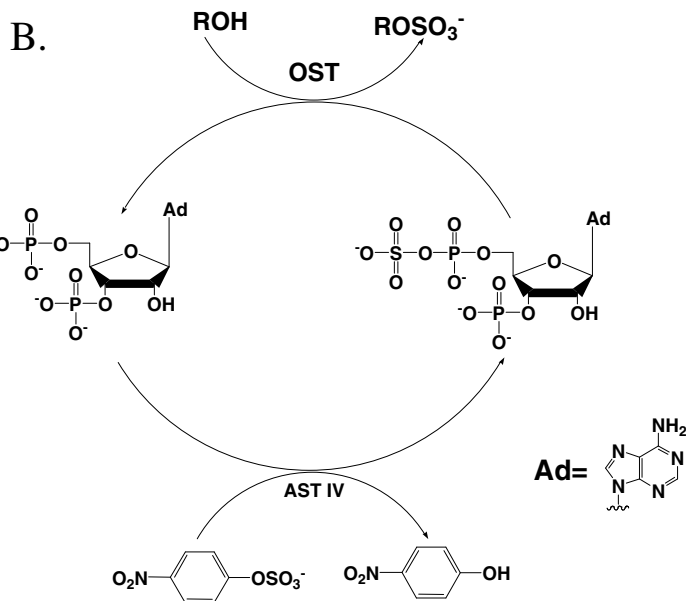
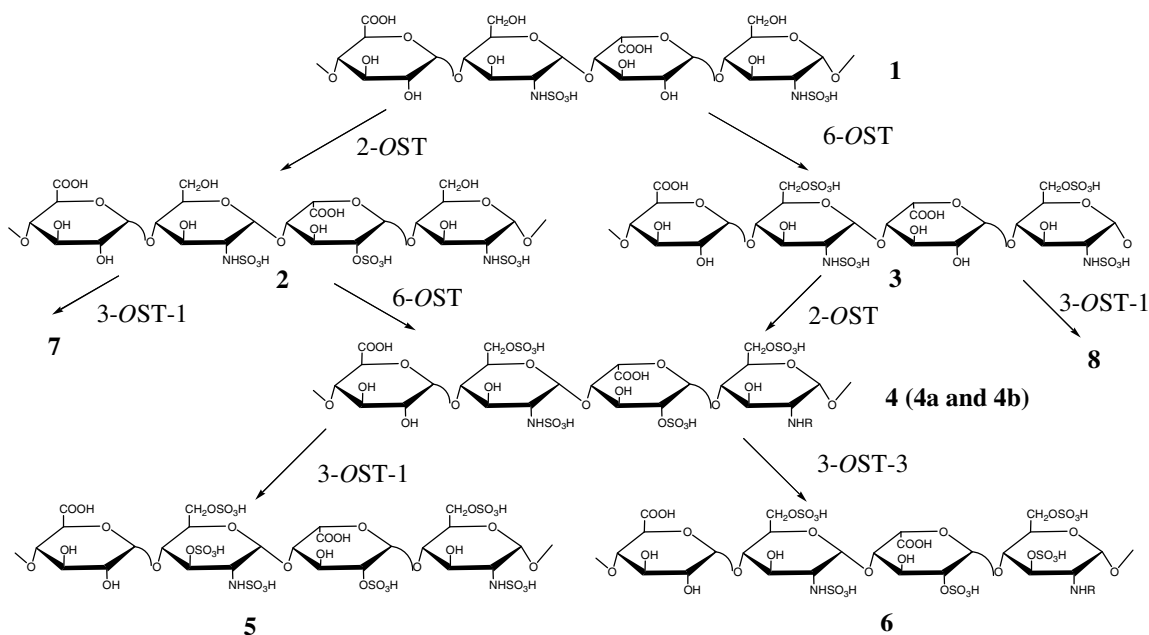


Figure 17. A schematic of the synthesis of sulfated polysaccharides and the PAPS regeneration system. The stepwise enzymatic synthesis of sulfated polysaccharides using HS sulfotransferases is shown in panel A. Compound 1 was prepared by solvolysis using dimethyl sulfoxide/methanol mixture (9:1, v/v) at 80 °C for 24 h. Compounds 4a and 4b were prepared by inverting the order of sulfation steps. 4a was prepared by incubating compound 1 with 2OST followed by 6OST, whereas 4b was prepared by incubating compound 1 with 6OST followed by 2OST. Panel B depicts the reaction cycle catalyzed by arylsulfotransferase IV (AST IV) to generate PAPS. R represents -H or -SO₃H. Figure was adapted from (Chen et al., 2005)

Statement of Problem

From the structural heterogeneity and manifold functions of HS and heparin it is readily evident that the biosynthetic pathway of these biomolecules is complex. In order to understand how this complexity arises, it is essential that the components of this pathway are explored. In addition, expansion of the therapeutic potential of HS and heparin depends on the development of efficient strategies to synthesize well defined oligosaccharides of varying length. The chemoenzymatic synthesis of heparin analogues is a promising method to attain biologically relevant heparin structures in sufficient quantities. This work focuses on two major challenges in the pursuit of heparin synthesis. Specifically, the further elucidation of two isoforms of the essential biosynthetic enzymes NDST and 3OST as well as the development of a chemoenzymatic approach to synthesizing anticoagulant heparin analogues will be addressed.

Heparan sulfate 3OST5 is a unique member of the 3OST family based on its broad substrate specificity *in vitro*. Previous work involved the molecular cloning, expression and purification of this novel family member. Additional work involved the detailed characterization of the HS structures generated by this enzyme. Chapter III of this text describes the functional analysis of 3OST5 involvement in the biosynthetic pathway of anticoagulant HS. A stable cell line that expresses 3OST5 was generated and characterized for its ability to generate AT activating HS. This cell line has proven useful in studying additional functional roles of 3-*O*-sulfated HS and should prove useful for future efforts to delineate the roles of 3OST5 modified HS.

The HS NDST family of sulfotransferases is essential in the production of biologically active HS structures. The *N*-sulfotransferase domain of this enzyme has been studied at

some length. Localization of the dually important *N*-deacetylase activity in this bi-functional enzyme has remained elusive. Chapter IV outlines efforts towards the expression and characterization the *N*-terminal domain of NDST and proves that this domain possess *N*-deacetylase activity. This preliminary work should lead to a more detailed understanding of the mechanisms of NDST action, and initiate efforts to use this enzyme in the synthesis of HS and heparin analogues.

Heparin and HS isolated from natural sources are heterogeneous in nature. Chemical synthesis of heparin is not feasible beyond the oligosaccharide level, yet much of the biological activity is dependent on polysaccharide length. The development of a chemoenzymatic approach to producing heparin should significantly reduces synthetic complexity (no protection/deprotection steps) while affording proper regio-selective sulfonation of the polysaccharide. Chapter V presents a chemoenzymatic synthesis of anticoagulant heparin analogues that will serve as the basis for the milligram scale preparation for additional studies. The relative ease of this method should allow its extension into the development of additional types of HS and heparin based therapeutics.

CHAPTER II. METHODS

General Procedures

Mammalian cell culture- Maintenance of CHO cells was performed according to established protocol. Cells were grown in a T75 flask with F12 media (Gibco) supplemented with 10% Fetal Bovine Serum (FBS, JRH Bioscience) and the appropriate antibiotics Penicillin/Streptomycin or Geneticin 418 (for selection of stable expression cell lines). Once cells reached 85-90% confluence, the cells were passaged using a standard protocol. Briefly, cells were washed three times with 1× Phosphate Buffered Saline (Gibco), and detached from the flask with 2 mL of buffered trypsin, EDTA (Gibco) at 37 °C. Once detached, the cells were diluted to 10 mL with F12 media and the concentration (cells/mL) was determined using a hemocytometer under microscope. Cells were seeded into new flasks at approximately 10^5 cells per flask. Cells were considered metabolically active after at least three rounds of passage.

For long term storage, cells were passaged as described above and then centrifuged at 1000×g for ten minutes. The cells were then resuspended in FBS with 10% dimethyl sulfoxide⁵ and frozen slowly at -80 °C by placing them in a double insulated box.

Preparation of chemically competent origamiB cells expressing groES/EL- The groES/EL

⁵ Cells concentration was typically 10^7 cells/mL

chaperone (Takara Mirus Bio, Japan) system was employed to improve protein expression and solubility. OrigamiB cells (Novagen) were transformed with the pG-KJE8 construct that carries groEL and groES. Briefly, 10ng of plasmid was mixed with 100 μ L of the bacterial cell suspension and incubated on ice in a 1.5 mL eppendorf tube for 30 minutes with intermittent mixing by tapping the tube. The cells were heat shocked at 42 $^{\circ}$ C for 45 seconds and then placed directly back on ice for two minutes. Next, 0.9 mL of pre-warmed SOC media was added to the tube and the shaken at 250 rpm for one hour. Varying amounts (50-500 μ L) of the transformation reaction was plated on agar plates containing 20 μ g/mL chloramphenicol. The plates were incubated at 37 $^{\circ}$ C for 12-15 hours. A single colony was selected and amplified in 2mL of Luria Broth (LB) media overnight by shaking at 250 rpm at 37 $^{\circ}$ C. To prepare chemically competent cells, the next day 100 mL LB media was inoculated with 1 mL of the overnight cell culture and shaken vigorously at 37 $^{\circ}$ C until the OD₆₀₀ reached ~0.25-0.3. The culture was chilled on ice for 15 minutes, and then centrifuged for 10 minutes at 3300 \times g and 4 $^{\circ}$ C. The media was decanted and the cell pellet was resuspended in 30-40 mL of ice cold 0.1 M calcium chloride. The cell suspension was kept on ice for 30 minutes and centrifuged again. The cell pellet was resuspended again in 6 mL of 0.1 M calcium chloride and 15% glycerol. The suspension was aliquoted at 200 μ L and frozen in a dry ice and ethanol bath before storage at -80 $^{\circ}$ C. The cells were designated oriB_{groEL/ES}.

Agarose gel electrophoresis- PCR products and DNA plasmid construct quality were assessed by agarose gel electrophoresis. Briefly, a 1% agarose solution was made by microwaving 0.4 g agarose with 40 mL 10 mM Tris-acetate 1 mM EDTA (TAE) buffer.

Once the solution cooled to ~70 °C, 1 µL of 5 mg/mL solution of ethidium bromide was added and the agarose was poured into a standard gel casting box with a well comb. After the gel set 1x TAE buffer was added to the gel box and samples were diluted 2 fold with loading buffer (50% glycerol, 0.0125% bromophenol blue) and added to separate wells. The gel was run at 120 volts and analyzed under UV light.

Concanavalin A(ConA) sepharose aging- In a column format, ConA Sepharose (Sigma-Aldrich) was washed with 2 column volumes of AT binding buffer that contains 10 mM Tris-HCl (pH 7.5), 150 mM sodium chloride, 1 mM Mn²⁺, 1 mM Mg²⁺, 1 mM Ca²⁺, 10 µM dextran sulfate, 0.02 % sodium azide and 0.0004 % Triton X-100. The ConA Sepharose was then transferred to a 50 mL centrifuge tube and incubated at room temperature in the AT binding buffer for one hour with end over end rocking. The buffer was eluted and replaced with 1% FBS in AT binding buffer and incubated under previously stated conditions. The beads were then eluted and washed with 10 mM Tris-HCl (pH 7.5), 1000 mM sodium chloride, 1 mM Mn²⁺, 1 mM Mg²⁺, 1 mM Ca²⁺, 10 µM dextran sulfate, 0.02 % sodium azide and 0.0004 % Triton X-100. The beads were re-equilibrated with the AT binding buffer and incubated with 1 mg/mL heparin at a final volume of 40 mL as stated above. The beads were again washed with a high salt solution and stored at 4 °C in the AT binding buffer.

Polysaccharide Preparation

Heparosan isolation- K5 *E. coli* strain was grown in LB media at 37°C overnight. If [³H] labeled heparosan was to be prepared, D-[³H]glucose was added at a concentration of 2 µCi/mL once the culture reached an OD₆₀₀ of 0.2. The overnight culture was centrifuged for

10 min at $6000 \times g$. The supernatant was collected and diluted in equal volume of 20 mM sodium acetate buffer, pH 4. The diluent was then filtered through 0.45 μm filter and applied to a 10 mL diethylaminoethyl sephacel (DEAE, Sigma) column that was pre-equilibrated with 100 ml of 20 mM sodium acetate, 50 mM sodium chloride, pH 4. The column was washed with 20 ml of the same buffer and eluted with 100 ml of 20 mM sodium acetate, 1000 mM sodium chloride, pH 4. Three hundred milliliters of absolute ethanol was added to the eluted material and chilled at $-20\text{ }^{\circ}\text{C}$ for at least 4 hours. Next, the mixture was centrifuged at $6000 \times g$ for 30 minutes. The supernatant was decanted and the pellet was re-solubilized in 3 mL of 1M NaCl. The remaining protein was removed by phenol/chloroform extraction. One additional ethanol precipitation was performed and the resultant heparosan was further purified by gel permeation chromatography on a TSK-GEL G2500PWXL column (7.8mm \times 30 cm, TOSOH BIOSEP) with a mobile phase of 100mM ammonium bicarbonate at a flow rate of 0.5 mL/min. The fractions containing [^3H] radioactivity were collected and dried. The pellet was resuspended in water. The amount of heparosan and specific [^3H]activity of ^3H -labeled heparosan were determined using the reverse phase ion-pairing (RPIP)-HPLC disaccharide analysis described below.

Preparation of [^{35}S]HS- Wild-type CHO and 3OST5/CHO (preparation described below) were grown to 90% confluence in F12 media containing 10% FBS and 100 Units/ml Penicillin/Streptomycin or 1 mg/ml G418 respectively. Cells were grown in the growth media containing 1 mCi/ml of sodium [^{35}S]sulfate (ICN) for 10 h. [^{35}S]HSPGs were harvested and purified on a DEAE column and subjected to β -elimination under alkaline conditions followed by phenol extraction to remove polypeptides. [^{35}S]HS was then isolated

by ethanol precipitation. The estimated specific ^{35}S -radioactivity of the [^{35}S]HS was 4×10^7 cpm/ μg . We observed that the yield of [^{35}S]HS from 3OST5/CHO cells was about 50% of that from wild type CHO cells.

Preparation of [^3H , ^{35}S] HS- Cells were grown in low glucose media as described by Invitrogen (www.invitrogen.com), 10% dialyzed FBS, 0.1 mCi/mL sodium [^{35}S] sulfate and 0.12 mCi/mL [^3H]glucosamine hydrochloride (ICN) overnight. The [^3H , ^{35}S]HS was purified as described above.

[^{35}S]PAPS Preparation

[^{35}S]PAPS was prepared using adenosine 5' triphosphate (ATP), [^{35}S]Na₂SO₄, and dialyzed yeast extract. The reaction was assembled in a final volume of 5 ml of 120 mM Tris-HCl (pH = 8.5), 36 mM MgCl₂, 16 mM ATP (Sigma), 5 mg/ml dialyzed yeast extract (Sigma) and 0.4 to 2 mCi/ml [^{35}S]Na₂SO₄ (carrier-free, ICN). This reaction was incubated at 37 °C for 1 hour. After 1 hour, the reaction was terminated by boiling the solution for 2 minutes. The solution was centrifuged at 10,000 g for 10 minutes to remove any insoluble material and the supernatant was reserved.

The [^{35}S]PAPS was purified from the reaction mixture using anion-exchange chromatography. A 2 mL DEAE column was equilibrated with 10 mL of 10 mM triethylammonium bicarbonate buffer (TEA buffer, pH = 8.1), and then the supernatant was applied. The column was washed with 10 mL of 200 mM TEA buffer and then eluted with 4 mL 400 mM TEA buffer. The eluent was dried and stored at -80 °C.

Purity and specific activity were determined using a silica based amino-bound anion exchange HPLC column (0.46 x 24 cm, Waters). The [³⁵S]PAPS was eluted by a gradient of 1 M potassium phosphate monobasic (30% to 100% in 60 min. at 0.5 ml/min.) and detected using an on-line radioactive detector and by UV absorbance. [³⁵S]PAPS absorbs UV light at $\lambda = 266$ nm. The UV and radioactive peaks for [³⁵S]PAPS will overlap (elutes at approximately 38 minutes) and allows for purity determination (the ratio of [³⁵S] found in the [³⁵S]PAPS peak to all other [³⁵S] peaks).

Protein Expression and Purification

Preparation of NDase expression plasmid- The N-terminal domain of human NDST2 (A66-P604) was cloned into a PET21b vector (Novagen) using the BamH1 and Hind III sites to generate NDase-(His)₆ fusion protein. The full length cDNA of human NDST-2 was a gift from Dr. Rosenberg (Massachusetts Institute of Technology). The coding region of the expression plasmid was sequenced to confirm the reading frame and the absence of deleterious mutations (University of North Carolina DNA sequencing facility).

Expression of NDase was achieved in oriB_{groEL/ES}. The bacteria were grown in LB medium supplemented with 12.5 μ g/mL tetracycline, 15 μ g/mL kanamycin, 35 μ g/mL chloramphenicol, and 50 μ g/mL carbenicillin at 37°C. When the OD₆₀₀ reached 0.6–0.8, Isopropyl- β -D-thiogalactopyranoside (IPTG) and L-arabinose⁶ was added to a final concentration of 0.1mM and 1mg/ml, respectively. Cells were pelleted at 7000 \times g for ten minutes and resuspended in buffer containing 25 mM Tris, 500 mM NaCl, 10mM imidazole, pH 7.5. The suspension was sonicated at duty cycle 50% and output control 7. The protein

⁶ L-Arabinose is used to induce expression of the groEL/ES construct.

was purified by NTA-agarose column (Qiagen) following the protocol provided by the manufacturer. Protein yield and concentration were determined by SDS-PAGE and A_{280} nm absorbance. Typically, 5-7 mg of NDase protein was purified from a 1L culture and purity was ~50%.

Expression of N-sulfotransferase (NST)- The NST expression plasmid was obtained from Dr. Negishi (National Institute of Environmental Health Sciences). Glutathione transferase-NST fusion was expressed in BL 21 cells and purified as described by Kakuta and colleagues (Kakuta et al., 1999).

Preparation of C5-epimerase bacterial expression plasmid and protein expression- The catalytic domain of human C₅-epimerase (E53-N609) was cloned into pMAL-c2X vector (New England Biolabs) using the *Bam*H1 and *Hind*III sites to generate a maltose-binding protein (MBP)-epimerase fusion protein. The full length cDNA of C₅-epimerase was a gift from Dr. Rosenberg (Massachusetts Institute of Technology). Expression of C₅-epimerase was achieved in oriB_{groEL/ES}. The bacteria were grown in LB medium supplemented with 2 mg/mL glucose, 12.5 µg/mL tetracycline, 15 µg/mL kanamycin, 35 µg/mL chloramphenicol, and 50 µg/mL carbenicillin at 37 °C. When the OD 600 nm reached 0.6–0.8, IPTG and L-arabinose were added to a final concentration of 0.1 mM and 1 mg/mL, respectively. The protein was purified following the protocol provided by the manufacturer. The purified protein migrated at 97 kDa on SDS-PAGE with the purity greater than 60%.

Preparation of 2OST and 6OST1 bacterial expression plasmid and protein expression-

The catalytic domain of 2OST of Chinese hamster ovary (Arg51–Asn356) was cloned into the pET21 vector (Novagen) using the Nde I and Hind III sites to generate a C-terminal His₆ tagged fusion protein. The full-length cDNA of 2OST was a gift from Dr. Rosenberg (Massachusetts Institute of Technology, Cambridge, MA). The catalytic domain of mouse 6OST1 (His53–Trp401) was cloned into the pMAL-c2X vector (New England BioLabs) using the BamHI and HindIII sites to generate maltose-binding protein fusion protein. The full-length cDNA of 6OST1 was a gift from Dr. Kimata (Aichi University, Japan), respectively. The expression of 2OST and 6OST1 was achieved in oriB_{groEL/ES} and Rosetta-gami B (DE3) cells (Novagen), respectively, using a standard procedure. Briefly, cells containing the plasmid expressing 6OST1 were grown in LB medium supplemented with 2 mg/mL glucose⁷, 15 µg/mL tetracycline, 15 µg/mL kanamycin, 35 µg/mL chloramphenicol, and 50 µg/mL carbenicillin at 37°C. When the OD₆₀₀ reached 0.6-0.8, the temperature was reduced to 22C and IPTG was added at a concentration of 0.1 mM (L-arabinose was added to 2OST at a final concentration of 1 mg/mL). 2OST expressing cells were grown in a similar fashion with the exception of the addition of glucose. The bacteria were harvested, and the proteins were purified by affinity chromatography following a protocol from manufacturer (Qiagen and New England Biolabs). The purified proteins migrated on 12% SDS-PAGE with the purity greater than 90 % (2OSTHis) and 60% (6OST1MBP). The yield for 2OST was approximately 20 mg/liter and 6OST1 was 50 mg/liter

⁷ Glucose is used in the growth media to reduce expression of amylase. Amylase can degrade the amylose affinity column (New England Biolabs) used in the subsequent purification step.

Preparation of 3OST1 bacterial expression plasmid and protein expression- The cDNA fragment encoding the catalytic domain of 3OST1 (Gly48-His311) was amplified from 3OST1 pcDNA3 containing an NdeI site and EcoRI site and inserted into the pET28a vector (Novagen) using the NdeI and EcoRI restriction sites to produce an N-terminal His₆ tagged protein. The resultant plasmid (3OST1) was sequenced to confirm the reading frame and the lack of mutations within the coding region (University of North Carolina, DNA sequencing core facility). The plasmid, 3OST1, was transformed into BL21 (DE3)RIL cells (Stratagene) for the expression of 3OST1. Cells containing the 3OST1 were grown in 1 liter of LB media with 50 µg/ml kanamycin at 37 °C. When the A₆₀₀ reached 0.6-0.8, the temperature was lowered to 22 °C for 30 min. IPTG was then added to a final concentration of 100 µM, and the cells were allowed to shake overnight. Cells were pelleted and resuspended in 120 ml of sonication buffer, 25 mM Tris, pH 7.5, 500 mM NaCl, and 10 mM imidazole. Cells were disrupted by sonication, and 3OST1 was purified as described above. Enzyme yield was approximately 20-25 mg/liter

Preparation of AST IV bacterial expression plasmid and protein expression- N-terminal (His)₆ tagged AST-IV was expressed in *E. coli* and purified as described by Burkat and colleagues (Burkart et al., 2000) at a yield ≈ 50 mg/liter of bacterial culture. The full length cDNA of rabbit AST-IV was a generous gift of Dr. Michael Duffel (University of Iowa) (Sheng et al., 2004).

Enzymatic Activity Assay

N-deacetylation of heparosan by NDase- Purified heparosan was added to buffer containing 50mM MES pH 6.5, 0.5% Triton X 100, and 10 mM MnCl₂. Typically 5-200 µg

of total protein was added to the reaction and allowed to incubate at 37°C. The reaction volume varied from 50-500 µL. The incubation time period varied from 1 to 16 hours. After incubation, the reaction was terminated at 100°C for 2 minutes then centrifuged at 16000 × g for 1 minute. The supernatant was collected for an additional *N*-sulfonation step or dialyzed against 25 mM ammonium bicarbonate and dried by centrifugal evaporation for further analysis.

Radioactive sulfotransferase assay- This protocol was followed for NST2, 2OST, 6OST2, 3OST1, and 3OST5 and their respective substrates shown in Table VI. Approximately 5-10 µg of Sulfotransferase, 0.5 to 1 × 10⁶ cpm 3'-phosphoadenosine 5'-phosphosulfate ([³⁵S]PAPS), and 5-50 nmoles of unlabeled PAPS was added and the reaction was incubated at 37 °C for 1-4 hrs. The reaction was heat deactivated in a 100 °C for two minutes. Heparan polysaccharides were purified by DEAE ion exchange chromatography. Briefly, the reaction mixture was diluted in 0.8 to 1 mL of a buffer containing 20 mM sodium acetate, 150 mM NaCl, 0.001% Triton X, and pH 5 and applied to a 0.2 mL DEAE column. The column was washed four times with 1 mL of UPAS buffer (20 mM sodium acetate, 150 mM NaCl, 3 M urea, 0.02% Triton X, pH 5) and re equilibrated with 2 mL of the dilution buffer. The column was eluted with 1 mL of 20mM sodium acetate, 1 M NaCl. The amount of ³⁵S-labeled polysaccharide was determined by scintillation counting (10% of the total eluent volume). The remainder of the eluent was dialyzed against 20 mM ammonium bicarbonate overnight at 4 °C. The dialyzed polysaccharide solution was dried by centrifugal evaporation and reconstituted in water for further use.

Table 4. Summary of the substrates used in radioactive sulfotransferases reaction

Enzyme	Substrate
NST	HS or DeAcK5P ^a
2OST	CDNSHp ^b
6OST1	CDNSHp ^b
3OST1	HS
3OST5	HS

a. DeAcK5P is completely deacetylated capsular K5 polysaccharide

b. (CDSNS) is completely desulfonated re-N-sulfonated heparin.

Polysaccharide digestion by heparin lyases- Recombinant Heparin Lyase I, II, and III (Hep I-III) was used to depolymerize HS polysaccharides to yield disaccharides. Briefly, purified polysaccharide was dissolved in buffer containing 40 mM ammonium acetate and 3 mM CaCl₂ to a final volume of 48 µL. Two microliters of purified Hep I-III (2 mg/ml in phosphate buffered saline) was added and the reaction was allowed to proceed overnight at 37°C. The reaction was heat deactivated and the supernatant was recovered for the disaccharide analysis.

Preparation of 3OST5 Stable Expression Cells (3OST5/CHO)

The expression plasmid pcDNA3.1-3OST5 was transfected into wild type CHO cells using LipofectAMINE 2000 (Invitrogen, Inc.) following the manufacturer's protocol. Six days after the transfection, the cells were trypsinized and transferred into a 6 x 8 well plate at the concentration of 0.5 cells per well. The cells were grown in F12 medium containing 10% bovine serum (from JRH Biosciences) and 1 mg/ml Geneticin (G418 sulfate, Invitrogen, Inc.) at 37°C under 6 % CO₂ for two to three weeks until confluence was attained.

RT-PCR and Northern blot analysis- mRNA were purified from CHO-K1 and 3OST5/CHO cells using the kits from Qiagen. From two T75 flasks of confluent CHO-K1

and 3OST5/ CHO cells, we obtained 3.0 µg and 3.3 µg of mRNA, respectively. RT-PCR analysis was carried out using Omniscript RT kit (Qiagen) with two 3-OST-5 specific primers: 5'-primer GAGCCCGCACTCAGGCTGAATTCCC, 3'-primer AAATCTAGAGGGCCAGTTCAATGTCCT⁸. For northern blot analysis, mRNAs were resolved on 1.2% formaldehyde-agarose gel and blotted to Hybond-XL membrane (Amersham) using an electrotransfer approach. The coding sequence of 3OST5 was labeled with [γ -³²P]dCTP in a reaction with Klenow enzyme (Roche Molecular Biochemicals) and used as a probe to hybridize the Human Multiple Tissue Northern (MTN®) blot (CLONTECH). The hybridization was carried out in ExpressHyb Hybridization Solution (CLONTECH) at 60 °C for 1 h, and the blot was washed with 0.1× SSC containing 0.5% SDS at 60 °C for 40 min (where 1× SSC contains 150 mM NaCl and 15 mM sodium citrate, pH 7.0). The membrane was exposed to an x-ray film for 4 days.

HS Polysaccharide Structural Analysis

Degradation of N-deacetylated heparosan by nitrous acid- NDase-treated [³H]heparosan was depolymerized by nitrous acid degradation at pH 4.5. Briefly, polysaccharides were dried by centrifugal evaporation and the resultant oligosaccharides were reduced with NaBH₄ in 0.1N NaOH at 50°C and resolved by size exclusion on a Biogel P6 column (0.5 × 200 cm) equilibrated with 500 mM ammonium bicarbonate at a flow rate of 3 mL/hour. Fractions of approximately 0.8 mL were collected and radioactive content was determined by scintillation counting.

⁸ The 3'-primer contains a *Xho*I site, which does not belong to the sequence of 3OST5. The 3OST5 sequence in this primer is AGGGCCAGTTCAATGTCCT.

Determination of the distribution of N-sulfated glucosamine residue in HS- [³H, ³⁵S]HS from 3OST5/CHO and wild-type CHO were depolymerized by HS specific nitrous acid (pH 1.5) cleavage. The resulting oligosaccharides were reduced with 0.5 M sodium borohydride in 0.1 N sodium hydroxide (Shively and Conrad, 1976) and then resolved on a Bio-gel P-6 column (0.5 × 200 cm, from BioRad) equilibrated with 0.5 M ammonium bicarbonate at a flow rate of 3 ml/h. The void volume was measured by co-eluting dextran blue (average mol wt = 2 × 10⁶ Da).

Reverse phase ion pairing HPLC (RPIP-HPLC) of non-sulfated disaccharides- Resultant disaccharides from the Hep III digestion were separated on a C18 column (0.46 × 24 cm, Vydac) using an isocratic mobile phase of 1.5% acetonitrile, 9.5 mM ammonium phosphate, 0.5 mM phosphoric acid, and 1 mM tetrabutylammonium (TBA) dihydrophosphate (Fluka) at a flow rate of 0.5 mL/min. Fractions of 0.5 mL were collected and ³H radioactive material was detected by scintillation counting. A standard curve correlating molar quantity and UV absorbance (at 232nm) of ΔUA-GlcNAc standard (Sigma) was also determined by RPIP-HPLC. An aliquot of prepared cold and ³H-labeled heparosan was digested with HepIII, analyzed by RPIP-HPLC, and its quantity determined using the standard curve.

RPIP-HPLC of sulfated disaccharides- HS was cleaved with nitrous acid (pH 1.5) and reduced with sodium borohydride as described by Shively and Conrad (Shively and Conrad, 1976). The disaccharides were analyzed by reverse phase ion pairing RPIP-HPLC (Liu et al., 1999). Briefly, a C18 reverse phase column (Vydac) was equilibrated with 38 mM ammonium dihydrogen phosphate, 2 mM phosphoric acid and 1 mM TBA dihydrogen

phosphate and eluted with acetonitrile at 8% for 45 minutes, at 15% for 15 minutes, and at 19.5% for 30 minutes in a solution containing 38 mM ammonium dihydrogen phosphate, 2 mM phosphoric acid, 1 mM TBA dihydrogen phosphate at a flow rate of 0.5 ml/min. The identities of the disaccharides were confirmed by co-elution of ^{35}S -labeled and ^3H -labeled disaccharide standards.

HS/Protein Interactions Biochemical Assays

AT affinity fractionation- Approximately 5×10^6 cpm of [^{35}S]HS was incubated with 5 μg AT in 50 μl of reaction buffer containing 10 mM Tris-HCl (pH 7.5), 150 mM sodium chloride, 1 mM Mn^{2+} , 1 mM Mg^{2+} , 1 mM Ca^{2+} , 10 μM dextran sulfate, 0.02 % sodium azide and 0.0004 % Triton X-100 for 30 minutes at room temperature. 100 μl of 1:1 slurry of aged ConA-Sepharose (see General Procedures for the aging process) was added, and the reaction was agitated for one hour at room temperature on an orbital shaker. The beads were washed three times with the reaction buffer and eluted with buffer containing 10 mM Tris-HCl (pH 7.5), 1000 mM sodium chloride, 1 mM Mn^{2+} , 1 mM Mg^{2+} , 1 mM Ca^{2+} , 10 μM dextran sulfate, 0.02% sodium azide, and 0.0004% Triton X-100.

Determination of the binding affinity by affinity co-electrophoresis- The dissociation constant (K_d) of 3OST5/CHO antithrombin-binding HS and AT was determined using affinity co-electrophoresis, with the detailed procedures described elsewhere (Lee and Lander, 1991; Liu et al., 2002). Approximately 7×10^4 cpm of antithrombin-binding [^{35}S]HS isolated from 3OST5/CHO cells was loaded per lane with zones of AT at the following concentrations 0, 1.5, 3.8, 7.5, 15, 31, 75, 125, and 250 nM. The gel was performed at 400

mA for ~ 6 hours, dried, and analyzed on a PhosphoImager (Amersham Biosciences, Storm 860). The retardation coefficient was calculated as $R = (M_0 - M) / M$, where M_0 is the mobility of free [^{35}S]HS through each AT zone, and M is the mobility of bound [^{35}S]HS through each separation zone. The retardation coefficient was then plotted against the retardation coefficient divided by the concentration of AT. The slope of the line represents $-1 / K_d$.

Assay for the AT-mediated deactivation of factor Xa by HS- The procedures were modified from a report by Zhang and colleagues (Zhang et al., 1998). HS was prepared from wild-type CHO-K1 and 3OST5/CHO in a similar fashion as described above, including treatment with 20 mU of chondroitinase ABC prior to ethanol precipitation. The concentration of the HS isolated was determined by using Alcian blue (Bjornsson, 1993). A final concentration of 27 μM AT was prepared with 1 mg/ml BSA in 1 x PBS. Factor Xa (0.1 μM) was prepared with 1 mg/ml BSA in 1 x PBS. Various amounts of HS, 0.5, 1.0, 1.5, and 2.0 μg of the HS from CHO/3OST5 and 1, 2, 3, and 5 μg of the HS from wild-type CHO, were dissolved in 20 μl of buffer containing 50 mM Tris, 7.5 mM Na_2EDTA , 175 mM NaCl, pH 8.4 (buffer containing no HS was used as a control). The mixture (25 μl) of the AT and factor Xa preparations were incubated with HS from CHO-K1 and 3OST5/CHO for 4 minutes at 37°C followed by the addition of 25 μl of 1 mM S-2765 chromogenic substrate (Diapharma) and 1 mg/ml polybrene (Sigma). The absorbance of the reaction mixture was measured at 405 nm continuously for 2 minutes. The initial rate of absorbance was derived from the slope of the fitted curve for each data set. These initial rates at varying HS concentrations were converted to an activity percentage based on the initial rate of the

reaction without HS (activity % = $v_{0,sample} / v_{0,control} \times 100\%$). The ratios were plotted against HS concentrations and a best fit curve was used to determine an IC₅₀ value.

The binding of the cells to fluorescently labeled AT- The procedures for the preparation of fluorescently labeled AT were carried out as described by Zhang and colleagues (Zhang et al., 2001a) with minor modifications. Briefly, AT (1 mg/ml) was incubated with neuraminidase (0.04 mU/μl, Worthington) and galactose oxidase (40 mU/μl, Worthington) in a buffer containing 25 mM sodium phosphate and 0.3 mM calcium chloride (pH 6.5) at room temperature for 1 hr. The sample was then mixed with fluorescein hydrazide (0.8 mg/ml, Molecular Probes) and incubated at 4°C overnight. The fluorescently labeled AT was purified by passing through a 200-μl heparin-Sepharose (Amersham) column, and the labeled AT was eluted with a buffer containing 1.5 M NaCl, 100 mM Na₂HPO₄, 27 mM KCl, and 18 mM KH₂PO₄ (pH 7.3). To stain the cells with fluorescently labeled AT, CHO-K1 and 3OST5/CHO cells were plated on a chamber slide plate at 5×10⁴ cells per well. The cells were incubated in the growth media at 37°C overnight under 6% CO₂. The cells then were incubated in cold F12 media supplemented with 0.1% FBS containing 5 μg/ml of fluorescently labeled AT with or without 1,250 μg/ml unlabelled AT for 1 hr. The cells were washed with cold 1 x PBS and fixed with 3.7% formaldehyde in PBS. Cells were viewed with a microscope (Leica Diaplan, Leitz Weltzar, Germany) equipped for epifluorescence with a 100× objective, and images were captured using an Orca ER camera (Hamamatsu Corp.) controlled by SimplePCI imaging software (Compix Inc.). The data were exported as 8-bit TIFF files and processed using Adobe Photoshop.

Chemoenzymatic Synthesis of Heparin Analogues

Preparation of immobilized HS sulfotransferases- Dialyzed sulfotransferases (4 ml, 4 mg/ml) in PBS buffer (15 mM NaH₂PO₄, 30 mM Na₂HPO₄, 400 mM NaCl, pH 7) was mixed with 2 ml Aminolink[®] plus beads (Pierce, IL) pre-equilibrated in PBS and 40 µL of 5 M sodium cyanoborohydride in 0.1M M sodium hydroxide in a small fritted column (Pierce or Bio-Rad). The mixture was then subjected to end over end rocking for six hours at room temperature. The column was eluted and washed with 3 column volumes of PBS. To quench active functional groups of the agarose beads, the column was washed with two column volumes of a 1 M Tris-HCl, 0.05% sodium azide, pH 7.4 quenching buffer. An additional 2 mL of the quenching buffer along with 40 L of sodium azide solution was added to the column and subjected to an additional 30 minutes of end over end rocking at room temperature. The solution was eluted and the column was washed with 10 column volumes of a wash solution containing 1M NaCl and 0.05% sodium azide. The column was stored in PBS with 0.05% sodium azide. The immobilization efficiency was assessed by comparing protein concentration by UV spectrometry (at 280 nm) of dialyzed flow through with the starting material. Immobilized enzyme was washed with 50 mM MES, 1% Triton X-100, 1 mM MgCl₂, and 1 mM MnCl₂, pH 7.0, and stored at 4°C.

Measurement of enzymatic activities of immobilized proteins- To determine the activity of 6OST and 2OST, completely desulfonated re-N-sulfonated (CDSNS) heparin was used as a substrate (Figure 18). Immobilized proteins (100 µl, ~300 µg immobilized enzyme) with 100 µg substrate (HS for 3OST, and CDSNS heparin for 2OST or 6OST1) and 200 µM [³⁵S]PAPS (1000 cpm/pmole) in 1 ml of 50 mM MES, pH 7.0, 1% Triton X-100, 1 mM MgCl₂, and 1 mM MnCl₂. After rotating at room temperature for 1 h, the supernatant was

collected, and the beads were washed with $3 \times 200 \mu\text{l}$ of 1 M NaCl in 25 mM sodium acetate (pH = 7.4). The supernatant and washes were combined, diluted with 2 ml water and subjected to the DEAE chromatography to determine the amount of [^{35}S]HS product used to determine the activities of the various HS *O*-STs.

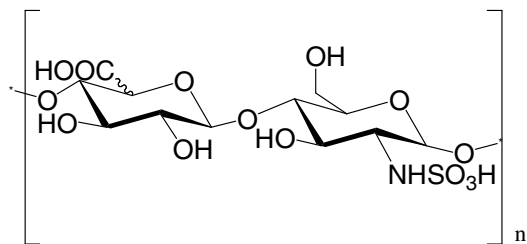


Figure 18. Completely desulfonated re -N-sulfonated heparin (CDSNSHp). This polysaccharide serves as substrate for both 2OST and 6OST.

2OST modification of N-sulfo K5 polysaccharides- Epimerase at 500 $\mu\text{g}/\text{mL}$ was incubated with 200 $\mu\text{g}/\text{mL}$ of K5NS in 50 mM MES, pH 7.0, 1% Triton X-100, 1 mM MgCl_2 , and 1 mM MnCl_2 at 37°C for approximately four hours with end over end rotation. The reaction was then cooled to room temperature and 2-3 mg of purified AST-IV was incubated with 40 μM PAP and 10 mM PNPS at 25°C for 30 min at a final volume of 5 mL. The reaction mixture was mixed with 4 ml of the immobilized sulfotransferase and rotated at 25°C for 24 h. The supernatant was recovered, and the polysaccharide that bound to the beads was eluted by washing two times with 5 mL of 1 M NaCl in 20 mM sodium acetate. Both the supernatant and wash were combined and diluted at least 5 times with 20mM sodium acetate, 50 mM NaCl, 0.001% Triton X, pH 5 and applied to a 1 mL DEAE (fast flow Amersham) column. The column was washed with 20 column volumes of UPAS buffer (20 mM sodium acetate, 150 mM NaCl, 3 M urea, 0.02% Triton X, pH 5) and eluted with 2

mL of 20mM sodium acetate, 1 M NaCl. The eluent was dialyzed against 20 mM ammonium bicarbonate overnight at 4 °C. The dialyzed polysaccharide solution was dried by centrifugal evaporation and reconstituted in water.

Chapter III. BIOSYNTHESIS OF ANTICOAGULANT HEPARAN SULFATE BY 3OST ISOFORM 5

In this study, we utilized Chinese hamster ovary (CHO) cells as a model system to study the biosynthesis of antithrombin-binding HS by 3OST5. We have generated a CHO cell line that stably expresses the human 3OST5 gene (3OST5/CHO). We demonstrate that 3OST5/CHO cells can generate AT-binding HS that has a similar affinity for AT as 3OST1 modified HS. In addition, we demonstrate that HS isolated from 3OST5/CHO cells has the capacity to accelerate the inhibitory effects of AT on factor Xa. These findings suggest that 3OST5 may contribute to hemodynamic processes *in vivo*.

AT- and gD- binding to HS- The AT-binding and gD immunoprecipitation assays are used for measuring the fraction of heparan sulfate that binds to either protein. These experiments are proven indicators of biological function of 3-*O*-sulfated HS (i.e. thrombin and factor Xa deactivation or HSV1 entry). In Figure 19, HS modified by 3OST1 shows a 38.8 fold increase in AT-binding over the control, but only a 5.25 fold increase in gD binding over the control. HS modified by 3OST3 shows only a 1.2 fold increase in AT binding over the control, and a 23.5 fold increase in gD binding over the control. HS modified by 3OST5 shows both a 39.6 fold increase in AT binding over the control, as well as a 20.8 fold

increase in gD binding over the control. The increases in bound modified HSs reflect their capacity to activate AT and/or serve as an entry receptor for HSV1. 3OST5 is unique in its ability to generate both gD and AT binding HS. We sought to generate a CHO cell line that stably expresses 3OST5 in order to assess its contribution in the HS biosynthetic pathway and to more extensively characterize the anticoagulant activity of 3OST5 modified HS.

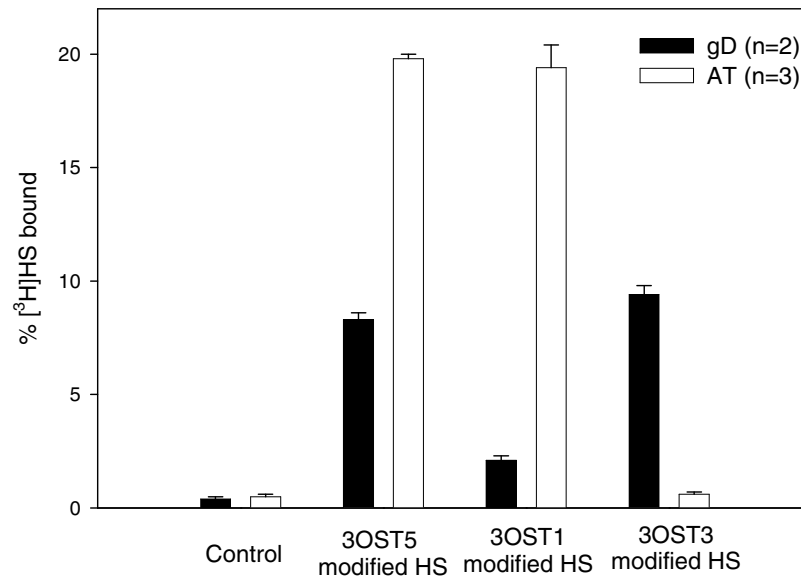


Figure 19. 3OST5 modified HS binds to both AT and gD. The binding of the HS and gD was determined by incubating modified [^3H , 3- O - ^{35}S]HS with gD followed by immunoprecipitation using anti-gD monoclonal antibody (DL6) to precipitate the complex of HS and gD. The percentages binding to gD and AT were calculated based on ^3H -counts. Data are presented as the mean \pm range (or SD); n represents the number of determinations. The binding of the HS and AT was determined by incubating modified HS and AT by using AT/ConA-Sepharose beads. The control was [^3H]HS without enzymatic modifications. 3OST1, 3OST3, and 3OST5 modified HS were prepared by incubating [^3H]HS (from CHO K1 cells), [^{35}S] PAPS, and purified 3OST1 (70 ng), 3OST3 (35 ng), and 3OST5 (70 ng), respectively. 3OST1, 3OST3, and 3OST5 are all recombinant enzymes from insect cells.

Determination of the expression of 3-OST-5 in 3OST5/CHO cells- In order to study the role of 3OST5 in synthesizing anticoagulant HS *in vivo*, we transfected 3OST5 cDNA into wild type CHO cells to obtain a stable expression of 3OST5 (3OST5/CHO). A total of 12 clones were isolated and screened for the expression of 3OST5 by analyzing the structure of the HS from each clone as described under “METHODS”. We chose clone 9 in this study and designated the clone as 3OST5/CHO. The results of the analyses of the level of 3OST5 mRNA in 3OST5/CHO cells are shown in Figure 20. A Northern blot analysis reveals a strong signal at 1.1 Kb, which is very close to the expected size for the 3OST5 coding region of the transfected plasmid (1.06 Kb), whereas the signal was undetectable in the mRNA from wild type CHO (Figure 1A). Using reverse transcriptase-PCR approach, we observed a product at 0.9 Kb, which is identical to the expected size using two 3OST5 specific primers, whereas the PCR product is absent in the mRNA from wild type CHO cells (Figure 1B). These results indicate that the level of 3OST5 mRNA is substantial in the stable expression cells, while it is absent in wild-type cells (CHO-K1). How the production of 3OST5 transcripts in the stable cell lines compares with that of other cell lines was not explored. Empirical evidence suggests that high mRNA levels of the 3OSTs do not translate into high protein expression (Deepak Shukla, correspondence). This may underscore the potential for translational control of 3OST expression [analogous to the NDSTs (Grobe and Esko, 2002)] and the need for cells to regulate the level of 3-*O*-sulfated HS production.

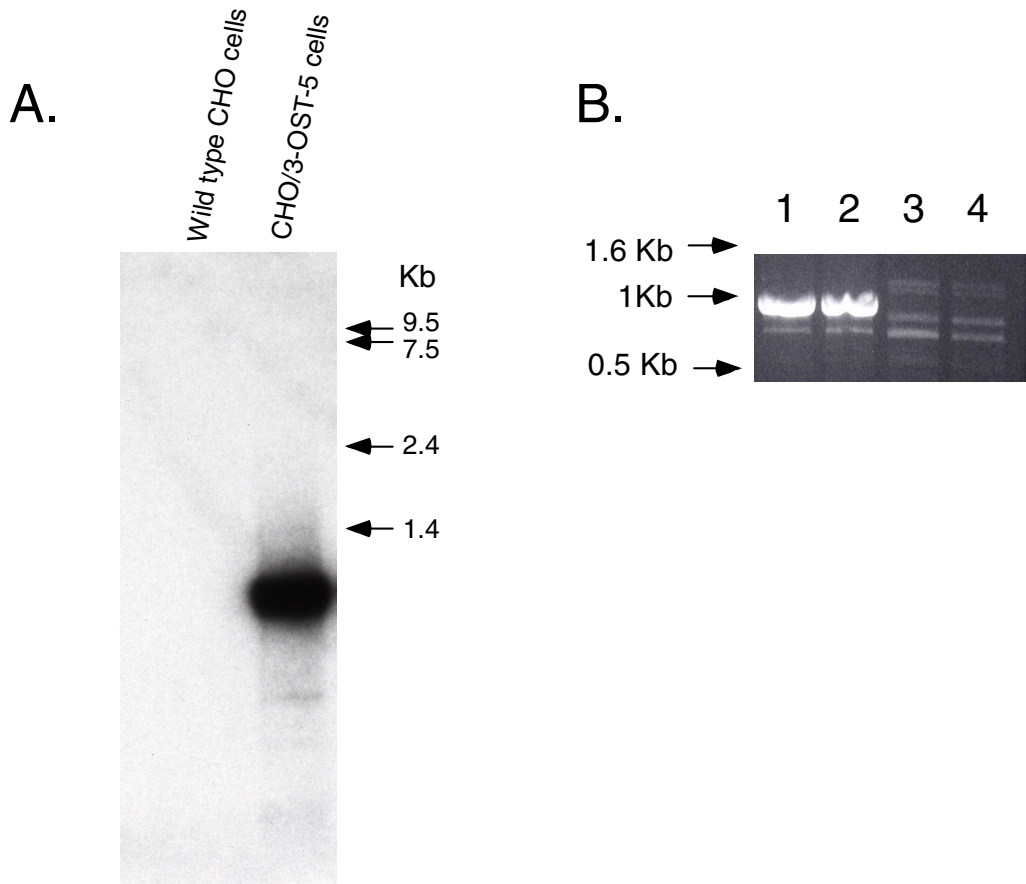


Figure 20. Northern blot and RT-PCR of 3OST5/CHO. (A) Northern blot analysis of wild-type CHO cells and 3OST5/CHO cell line expressing the 3-OST-5 gene. About 2 μ g of mRNA from wild-type CHO and 3OST5/CHO cells was loaded into the agarose gel and blotted. The blot was hybridized with a 32 P-labeled 3OST5 probe as described under Materials and methods. (B) RT-PCR analysis of the mRNA from 3OST5/CHO cells (lanes 1 and 2) and from wild-type CHO (lanes 3 and 4). We used 26 ng (lane 1) and 52 ng (lane 2) of mRNA from 3OST5/CHO cells, and 24 ng (lane 3) and 48 ng (lane 4) of mRNA from wild-type CHO cells for the RT-PCR analysis.

3OST5/CHO generate multiple 3-O-sulfated disaccharides- In order to confirm that 3OST5/CHO cells biosynthesize 3-*O*-sulfated HS, we conducted the disaccharide analysis of metabolically labeled HS isolated from 3OST5/CHO cells and CHO-K1 cells. The [³⁵S]HS were degraded by nitrous acid (pH 1.5) followed by sodium borohydride reduction. The RPIP-HPLC chromatograms of the disaccharide analysis for HS from CHO-K1 and from 3OST5/CHO are shown in Figure 21. As expected, the characteristic disaccharides, IdoUA2S-AnMan3S, GlcUA-AnMan3S6S, and IdoUA2S-AnMan3S6S, of 3OST5 modified HS were observed in HS from 3OST5/CHO (Figure 21B)(Xia et al., 2002) . In addition, we also observed the disaccharide IdoUA-AnMan3S6S, which is another characteristic disaccharide from 3OST5 modified HS (Chen et al., 2003). None of these 3-*O*-sulfated disaccharides were present from nitrous degradation of the HS from wild-type CHO where the major disaccharide was IdoUA2S-AnMan6S (Figure 21A), a common disaccharide in HS.

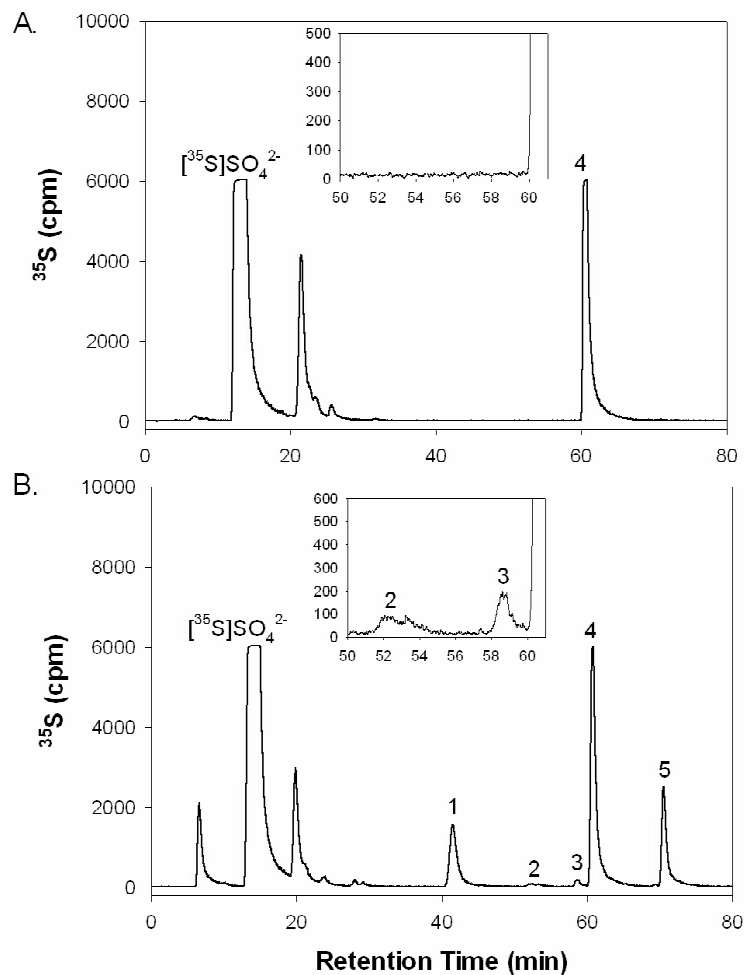


Figure 21. RPIP-HPLC chromatograms of the disaccharide analysis of HS. Metabolically labeled [^{35}S]HS from (A) wild-type CHO and (B) 3OST5/CHO were treated with nitrous acid (pH 1.5) followed by sodium borohydride reduction. The disaccharides were desalted and resolved by RPIP-HPLC. The elution positions of disaccharide standards are indicated by **1**: IdoUA2S-AnMan3S, **2**: IdoUAAAnMan3S6S, **3**: GlcUA-AnMan3S6S, **4**: IdoUA2S-AnMan6S and **5**: IdoUA2S-AnMan3S6S. Insets represent the enlarged region where disaccharides **2** and **3** were eluted. The ^{35}S -peak eluted at ~8 min of panel B is likely to contain both free [^{35}S]sulfate and a small amount of ^{35}S -disaccharide. This additional peak is probably due to high concentration of salt during the sample preparation.

Effects of 3OST5 overexpression on HS structure- To investigate whether expression of 3OST5 gene affected the distribution of *N*-sulfated glucosamine residues within the HS, we compared the oligosaccharide compositions of HS isolated from both CHO-K1 and 3OST5/CHO after nitrous acid degradations at pH 1.5. The BioGel P-6 profiles of nitrous acid degraded (pH 1.5)-[³H, ³⁵S]HS from CHO-K1 and 3OST5/CHO were shown in Figure 22, and the calculated relative percentages of the oligosaccharides with different sizes were shown in Table V. Chondroitin sulfate polysaccharide, which is a contaminant in the preparation of [³H, ³⁵S]HS, was not susceptible to nitrous degradation, and migrated at the void volume of the P-6 column. We observed that the percentages of disaccharides and tetrasaccharides from nitrous acid-degraded HS of 3OST5/CHO was similar, compared to that of wild type CHO cells. The result suggested that the expression of 3OST5 has not significantly altered the distribution of *N*-sulfated glucosamine residues of HS.

Table 5. Relative percentages of oligosaccharides resulted from nitrous acid degraded HS from 3OST5/CHO and from wild-type CHO

HS Oligosaccharides	[³ H] ^a		[³⁵ S] ^a	
	CHO	3-OST-5/CHO	CHO	3-OST-5/CHO
Di-	15 %	13 %	75 %	74 %
Tetra-	18 %	14 %	9 %	9 %
Hexa	7 %	8 %	3 %	3 %
Octa-	11 %	8 %	2 %	3 %

^a Relative amounts of oligosaccharides generated by low pH nitrous degradation were estimated based on the total dpm of [³H] and [³⁵S] for each sample excluding the CS peaks.

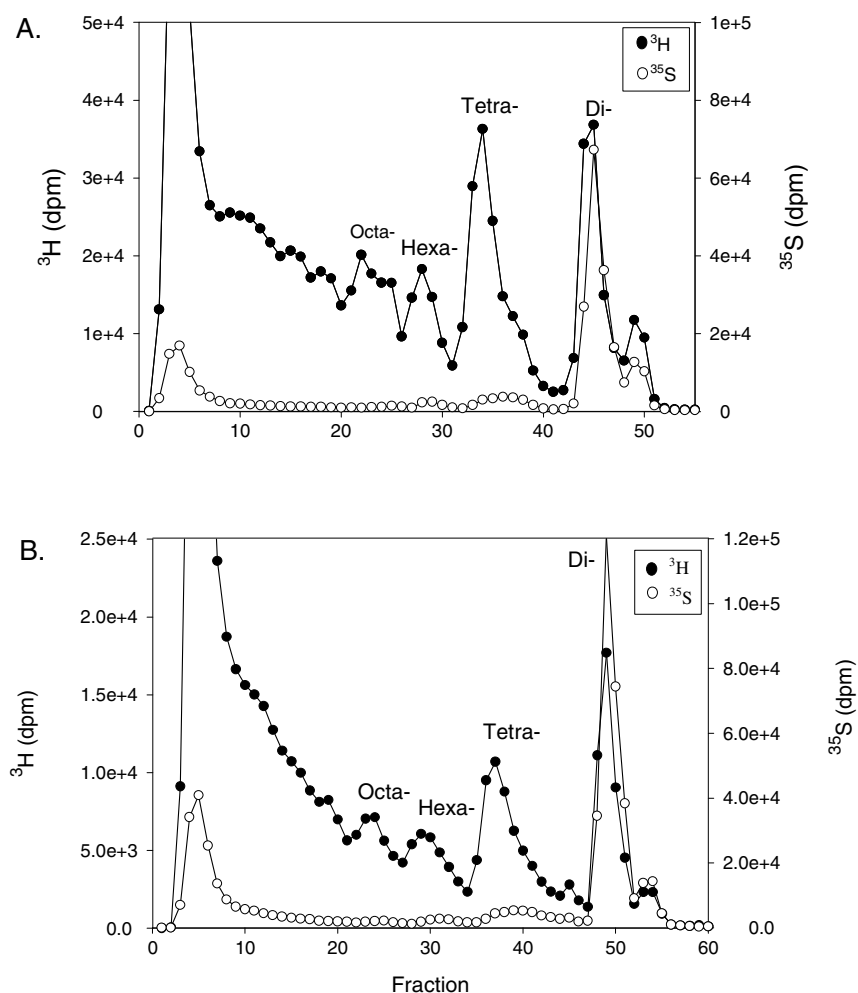


Figure 22. 3OST5/CHO N-sulfo domains do not vary from wild CHO. Profiles of nitrous-degraded [³H, ³⁵S]HS on BioGel P-6. [³H, ³⁵S]HS polysaccharide from wild-type CHO and stable cell line was treated with nitrous acid (pH 1.5) and reduced with sodium borohydride. The resultant oligosaccharides were resolved on a BioGel P-6. Panel A represents ³H profile (—●—) and ³⁵S profile (—○—) from wild-type CHO cells. Panel B represents ³H profile (—●—) and ³⁵S profile (—○—) from 3OST5/CHO cells. The void volume, measured by the elution of dextran blue, was not included in the profiles. The peaks observed in the early fractions of ³⁵S profiles are undigested chondroitin sulfate.

Binding affinity of HS from 3OST5/CHO with AT- The dissociation constant (K_d) of AT-binding HS for AT was determined by affinity co-electrophoresis, a method employed in several studies investigating HS/protein interactions (Lee and Lander, 1991; Liu et al., 2002). The AT-binding HS was isolated from metabolically labeled [35 S]HS of 3OST5/CHO by AT-affinity fractionation. The picture of the gel and Scatchard analysis of the gel were shown in Figure 23. Our analysis revealed that HS from the CHO/3OST5 cell line has a K_d of 10 nM with AT. It is important to note that the binding affinity of 3OST1 modified HS from CHO cells and AT was determined to be 32 nM (Zhang et al., 2001b), and the binding affinity of heparin and AT was determined to be 9 nM (Lee and Lander, 1991). These results suggest that 3OST5 modified HS has a similar binding affinity for AT relative to previously characterized anticoagulant HS.

3OST5 modified HS promotes AT mediated deactivation of factor Xa- The serine protease factor Xa of the blood coagulation cascade plays a key role in regulating the formation of fibrin, a major constituent of blood clots. HS present on the blood vessel wall prevents blood from clotting by inhibiting the activity of factor Xa and other serine proteases via its interaction with AT. We investigated whether the binding of the HS from 3OST5/CHO cells to AT inhibits the activity of factor Xa by using a method described by (Zhang et al., 2001b). Figure 24 shows the inhibition curve of the activity of factor Xa by HS with an IC_{50} value of 10 μ g/ml for the HS from 3OST5/CHO cells, whereas approximately 70% of the factor Xa activity remained in the presence of 50 μ g/ml from wild type CHO cells, suggesting the IC_{50} value for the HS from wild type CHO cells is greater than 50 μ g/ml.

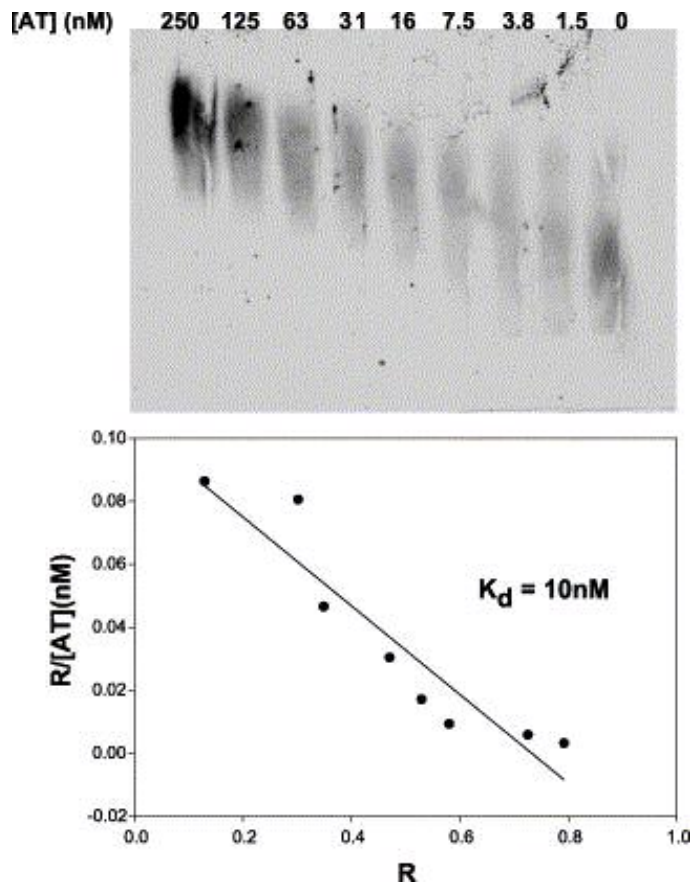


Figure 23. Determination of K_d by affinity co-electrophoresis. The top panel represents an autoradiograph of the agarose gel in which 650,000cpm of AT-binding [^{35}S]HS from 3OST5/CHO was subjected to electrophoresis through zones containing AT at the concentrations indicated. The Scatchard plot of data was obtained from the autoradiograph. A plot of $R/[AT]_{\text{total}}$ versus R , where the retardation coefficient $R = (M_0 - M)/M_0$. M_0 is the migration of free [^{35}S]HS, and M is the observed migration of [^{35}S]HS in the presence of AT. Assuming that [^{35}S]HS and AT forms a 1:1 complex and AT is in great excess, this plot should yield a straight line with a slope of $-1/K_d$ according to the Scatchard equation.

Thus, the HS from 3OST5/CHO is at least five times more potent inhibitor than the HS from wild type CHO cells. We anticipated seeing a greater difference in IC_{50} values for HS from 3OST5/CHO cells and the HS from wild type CHO cells. However since we used total HS (without AT-affinity fractionation) in this experiment, the concentration of anticoagulant HS was diluted by the non-anticoagulant HS in the preparation. Ideally, AT-binding HS should have been purified in order to carry out this study. However, only approximately 7-8% of the HS isolated from 3OST5/CHO are antithrombin-binding HS. We typically obtained 2 to 3 μg of HS from a T75 flask. Based on this yield, it would have been technically difficult to obtain a sufficient amount of antithrombin-binding HS and to determine its concentration by the Alcian blue assay in order to carry out additional experiments.

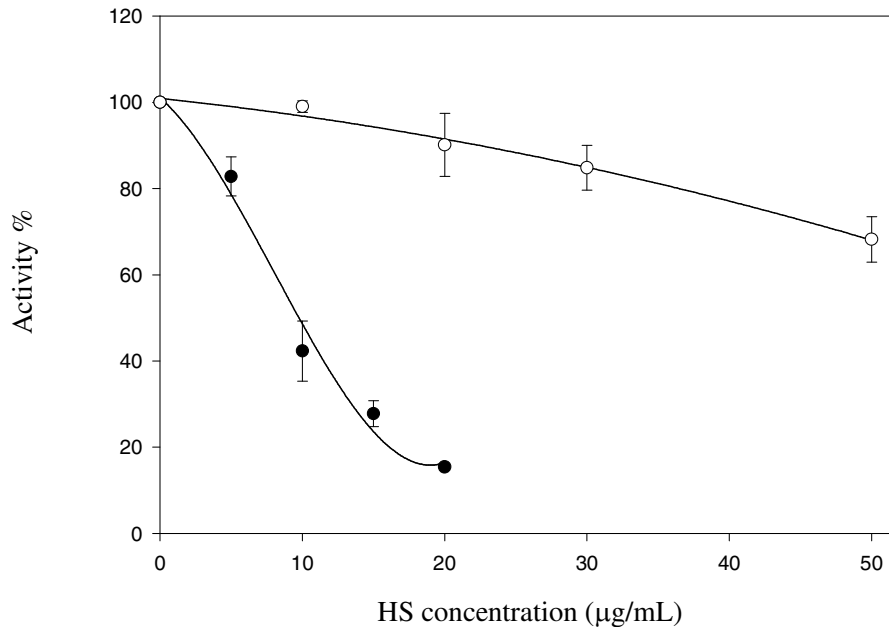


Figure 24. The inhibition of factor Xa activity by HS. HS isolated from 3OST5/CHO (—●—) and isolated from wild-type CHO (—○—) at varying concentrations were incubated with a reaction mixture consisting of 10 μM antithrombin, 40 nM factor Xa, 14 mM Tris-HCl, 2 mM Na_2EDTA , 50 mM NaCl. The reaction was stopped with a 25- μl solution containing 1 mg/ml polybrene and 1 mM S-2765 chromogenic substrate. The activity of factor Xa was then determined by monitoring the increase of the absorbance at 405 nm as described under “METHODS”. Each data point represents the average of two determinations. Error bars indicate the range.

Comparing the cell surface antithrombin-binding sites between 3OST5/CHO cells and CHO-K1 cells- Given the fact that HS is believed to be present on the surface of the cells to serve as a natural anticoagulant, we wanted to confirm that the antithrombin-binding HS that is synthesized by 3OST5 is indeed present on the cell surface. To this end, we compared the binding of fluorescently labeled AT to 3OST5/CHO cells and wild type CHO-K1 cells. Fluorescently labeled AT was incubated with the cells at 4°C, and the cells were washed with PBS to remove unbound fluorescently labeled AT followed by fixing the cells with formaldehyde. The cells were then visualized by fluorescence microscopy as depicted in Figure 25. It is apparent that the fluorescent intensity was substantially higher for 3OST5/CHO cells than that for CHO-K1, suggesting that an increase number of AT-binding sites on the surface of 3OST5/CHO. In addition, the fluorescent intensity was decreased by using 250-fold in molar excess of unlabeled AT, suggesting that the observed fluorescent signals were due to the binding of cell surface HS to AT. Taken together, our results suggested that 3OST5 cDNA is capable of generating cell surface HS that binds to AT.

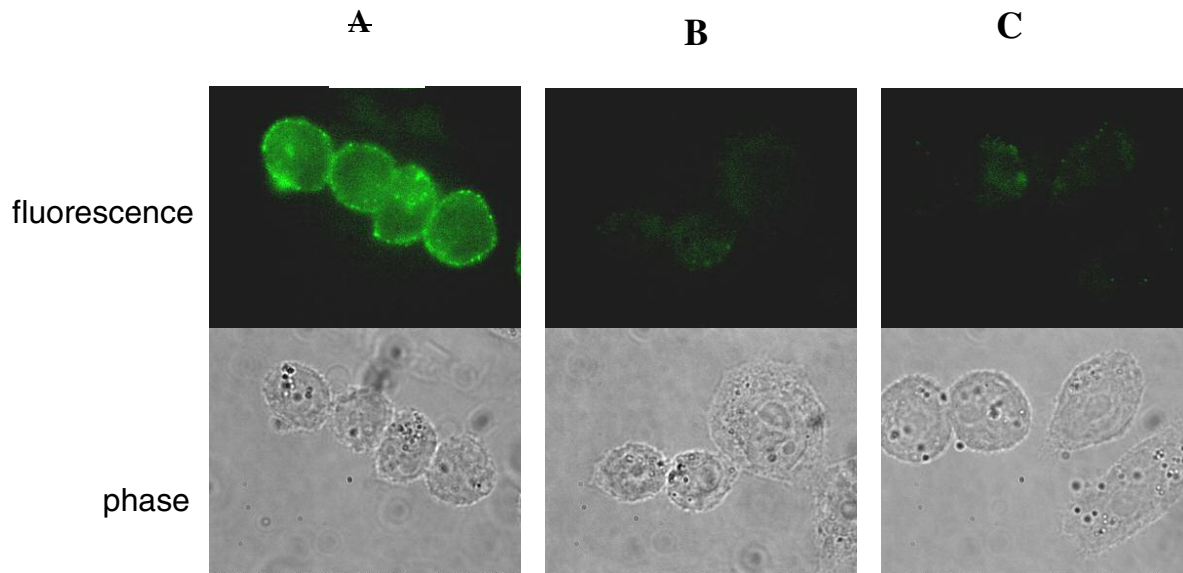


Figure 25. Binding of fluorescently labeled AT to 3OST5/CHO and wild-type CHO cells. Fluorescently labeled AT was incubated with the cells in the presence or absence of 250-fold molar excess of unlabeled AT. Panels A and B are micrographs of 3OST5/CHO cells and wild-type cells, respectively. Upper panels are fluorescent micrographs of cells using identical image intensity settings. Lower panels depict phase-contrast image of cells. Panel C shows 3OST5/CHO cells in the presence of 250-fold molar excess of unlabeled AT.

Conclusions- 3OST5 cDNA was introduced into wild type CHO cells to study the role of 3OST5 in synthesizing anticoagulant HS in cell culture. Results from Northern analysis and RT-PCR revealed high levels of expression of 3OST5 in the stable cell line 3OST5/CHO. The fraction of 3OST5/CHO HS that binds to AT was 24-fold greater than that of wild-type CHO HS. From these results we concluded that a stable expression of 3OST5 in 3OST5/CHO cells was obtained. We found that the expression of 3OST5 was constant for at least five passages (data not shown) as determined by the level of 3-*O*-sulfated disaccharides. The characteristic disaccharides of HS generated by purified enzyme, IdoUA2S-AnMan3S±6S, IdoUA-AnMan3S6S, and GlcUA-AnMan3S6S, are consistent with those observed in the HS from 3OST5/CHO cells. However, it is not known whether the saccharide sequences at the oligosaccharide level from *in vivo* and *in vitro* synthesis around the 3-*O*-sulfated glucosamine residue are identical. Such conclusions would require an in depth structural analyses of the oligosaccharides. It should be noted that 3OST5 modified HS that is generated by purified 3OST5 enzyme *in vitro* also contains two monosulfated disaccharides, GlcUA-AnMan3S and IdoUA-AnMan3S, although those only represent a small portion of 3-*O*-sulfated disaccharides (Chen et al., 2003). We did not investigate whether those monosulfated disaccharides are present in HS from 3OST5/CHO as it was not the focus of the current study.

Antithrombin inhibits the activities of factor Xa and thrombin, which is a major mechanism in regulating the blood coagulation process. The process is primarily dependent on the formation of a complex between AT and cell surface HS (Conrad, 1998). In order to link 3OST5 modified HS and potential anticoagulant activity *in vivo*, the location of 3OST5 modified HS and the binding affinity of 3OST5 modified HS were investigated. Using

fluorescently labeled AT, we established that AT-binding HS is indeed present on the surface of 3OST5/CHO. In addition, we concluded that the binding affinity of 3OST5/CHO HS is very similar to that of the HS modified by 3OST1 and heparin. Furthermore, we demonstrated that 3OST5 modified HS can serve as a potent cofactor in the AT mediated inhibition of factor Xa. Taken together, our results suggest that 3OST5 is capable of generating a natural anticoagulant on the surface of the cells, which is similar to the proposed function of 3OST1 (Shukla et al., 1999). While 3OST1 was reported to be expressed in human umbilical vein endothelial cells (Shukla et al., 1999), we did not detect the expression of 3OST5 in primary human umbilical vein endothelial cells by Northern and RT-PCR (data not shown).

3OST5 has limited expression in human muscle, fetal brain, and adult brain tissues (Xia et al., 2002) (Mochizuki et al., 2003). Northern analyses of the previously discovered 3OSTs have shown them to be expressed at only minute levels in skeletal muscle. It is known that 3OST1 modified HS and 3OST3 modified HS have distinct biological functions (Shworak et al., 1997). The lack of additional 3OSTs in skeletal muscle may be compensated for by the unique substrate specificity of 3OST5, which generates the 3-*O*-sulfated HS with various biological activities. The relationship between the presence of anticoagulant HS and the functions of skeletal muscle is unclear. One strong possibility is that 3-*O*-sulfated HS contributes to a variety of physiological processes besides anticoagulation. The literature suggests that 3-*O*-sulfated HS is involved in binding to growth factor and growth factor receptor (Liu and Rosenbreg, 2002) (McKeehan et al., 1999). However, whether 3OST5 modified HS binds to the growth factors and growth factor receptors is still unknown. Additionally, the study by (HajMohammadi et al., 2003) revealed that a tissue homogenate

from 3OST4⁻ mouse brain maintained both the capacity to generate antithrombin-binding HS and anti-Xa activity. Although both isoforms are shown to be expressed in brain, it is difficult to discern whether these residual levels of AT-binding HS are the result of simultaneous 3OST5 and 3OST1 expression and activity or perhaps the result of the additional 3OSTs compensating for the lost expression of 3OST1.

In summary, this study has provided a biochemical basis for the generation of AT-binding HS by a recently discovered member of the HS 3OST family. Our results indicate that the HS structure generated by 3OST5 has the capacity to bind to AT with high affinity and neutralizes the activity of factor Xa, a key component of the blood coagulation pathway. Further characterization of this enzyme and the HS structures that it generates may provide insight into its roles in cardiovascular physiology/pathology and perhaps the design of novel approaches towards synthesis of relevant HS oligosaccharides.

Chapter IV. LOCALIZATION AND CHARACTERIZATION OF THE *N*- DEACETYLASE DOMAIN OF NDST2

NDST is a type II membrane bound protein consisting of 883 amino acid residues. The expression and characterization of NDST isoforms have been reported in mammalian, insect, and yeast expression systems (Berninsone and Hirschberg, 1998; Kuberan et al., 2003c; Saribas et al., 2004). It has been hypothesized that NDST has two functional domains, responsible for *N*-deacetylase and *N*-sulfotransferase activities, respectively. The *C*-terminal *N*-sulfotransferase domain has been expressed and a crystal structure has been resolved, resulting in a major breakthrough towards defining the catalytic mechanisms and polysaccharide binding site of HS sulfotransferases (Kakuta et al., 1999). Several failed attempts to express NDST in a bacterial system and the putative *N*-terminal *N*-deacetylase domain in a mammalian system have been noted in the literature (Berninsone and Hirschberg, 1998; Kusche Gullberg and Kjellen, 2003; Saribas et al., 2004). Thus, whether the *N*-terminal domain of NDST is a functional domain with *N*-deacetylase activity remains in question. Herein, we report the expression and characterization of the *N*-terminal domain of NDST-2 that retains *N*-deacetylase activity (NDase). The expression of an NDase active construct should prove useful in further analysis of NDST mechanisms of action and potentially in chemoenzymatic synthesis of HS.

Expression and characterization of ND domain fusion protein- Full length human NDST2

contains 883 amino acid residues contains both *N*-deacetylase and *N*-sulfotransferase activities (Eriksson et al., 1994). It has been well documented that *C*-terminal domain of the NDST (599T-883G) maintains the *N*-sulfotransferase activity (Berninsone and Hirschberg, 1998; Kakuta et al., 1999). We hypothesized that *N*-deacetylase and *N*-sulfotransferase activities are located separately at the *N*-terminal and *C*-terminal domains of NDST1 protein. Therefore, expression of *N*-terminal domain of NDST2 should yield a functional protein with *N*-deacetylase activity. We initially prepared a maltose binding protein-NDST2 fusion protein, and the resultant proteins contain both *N*-deacetylase/*N*-sulfotransferase activities (data not shown). The expression was achieved in Origami B cells over-expressing the groES/EL chaperone proteins as described under “METHODS”. We also prepared several truncated *N*-terminal domains of NDST2, including NDase1 (A66-P604), NDase2 (A66 - T614), NDase3 (A66-L625), and NDase4 (A66-W594). While all of these constructs were expressed, and it was determined that NDase1 gave the highest *N*-deacetylase activity. We decided to further characterize the enzymatic activity of NDase1. To simplify the protein purification, we introduced a (His)₆ tag at the *C*-terminal of NDase1. Thus, a *C*-terminal (His)₆-tagged NDase1 construct has been used throughout this study.

The *N*-deacetylase activity of the recombinant protein was determined by coupling with NST, which is outlined in Figure 26A. Bacterial capsular polysaccharide of *E. coli* K5 strain, heparosan, serves as a substrate for *N*-deacetylase as it is structurally similar to the heparin or heparan sulfate precursor (Eriksson et al., 1994). Heparosan was incubated with NDase to generate *N*-unsubstituted glucosamine units (GlcNH₂). After heat deactivation of the NDase reaction, recombinant *N*-sulfotransferase (NST) and [³⁵S]PAPS was added into the reaction mixture to sulfate GlcNH₂ residues. Under our reaction conditions, the rate of sulfo-

transfer shows a linear increase relative to the amount of functional NDase present as shown in Figure 26B, suggesting that the amount of ^{35}S -labeled heparosan correlates with the activity of NDase. To our knowledge this represents the first time that the *N*-deacetylase activity has been detected in which the *C*-terminal *N*-sulfotransferase domain has been truncated from the full length NDST.

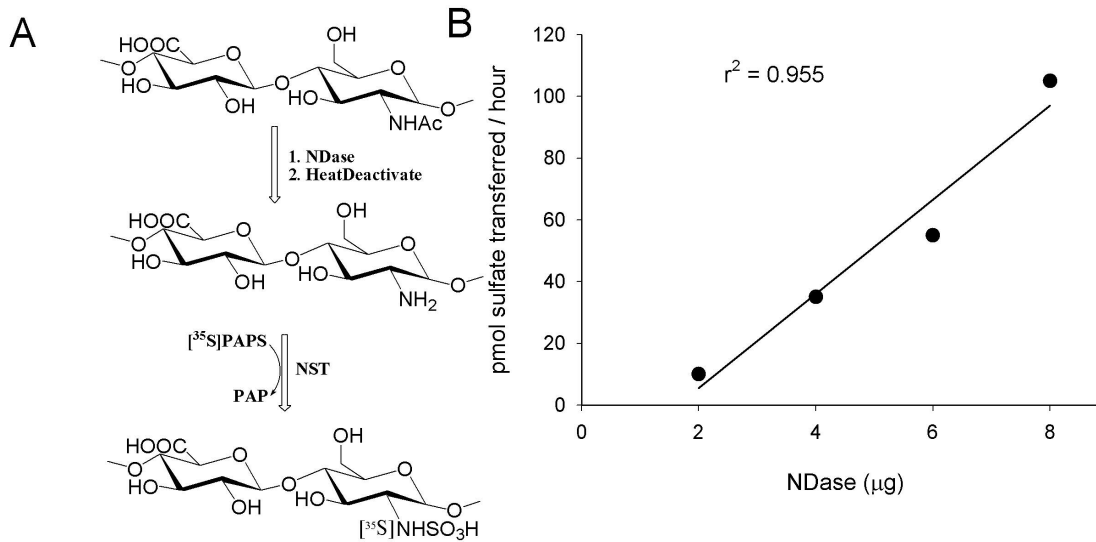


Figure 26. Determination of the activity of *N*-deacetylase activity. The screening method for NDase activity is outlined in (A). The NDase reaction was heat deactivated in a boiling water bath for 2 minutes. The presence of free amino groups was then detected by converting them to *N*-sulfo groups by an exhaustive *N*-sulfotransferase reaction. In (B), a linear dose response is observed with the addition of increasing amount of NDase in a 50 μL reaction.

We also attempted to estimate the K_m of NDase towards the heparosan. We observed that the amount of *N*-unsubstituted glucosamine reached a plateau as determined by the susceptibility to the modification of NST (Figure 27A and 27B). The K_m was estimated at 170 $\mu\text{g}/\text{mL}$. This value is approximately two fold lower than reports using mastocytoma derived NDST constructs expressed in mammalian systems in which the traditional [^3H]acetate release assay was used (Bame et al., 1991; Orellana et al., 1994), suggesting that bacterial expressed NDase has similar binding affinity toward heparosan as that of

mammalian cell expressed NDST. Due to the fact that we indirectly measured the amount of GlcNH₂ generated during the NDase digestion, we could not determine the V_{max} of NDase towards heparosan.

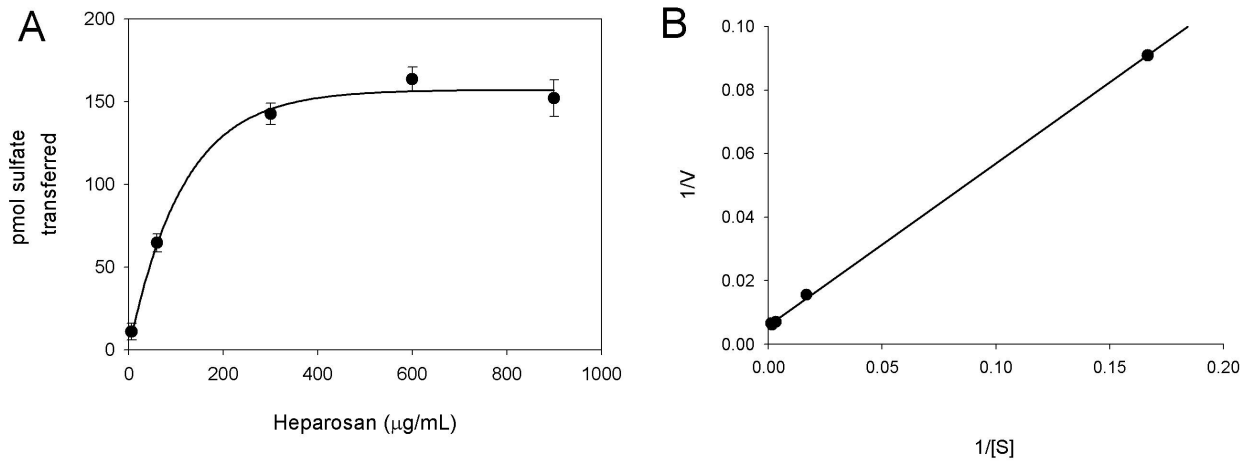


Figure 27. Determination of K_m of NDase towards heparosan. The NDase reaction was allowed to proceed for 45 minutes, followed by heat deactivation and then a NST reaction for 30 minutes. The amount of *N*-unsubstituted glucosamine unit (GlcNH₂) was determined by measuring susceptibility to NST modification, as determined by the amount of [³⁵S]sulfate transferred to the polysaccharide product.

Structural characterization of NDase-treated heparosan- To further confirm that NDase indeed generates the *N*-unsubstituted glucosamine unit in heparosan, a disaccharide and oligosaccharide analyses on the NDase-treated heparosan was performed. To facilitate detection, we prepared metabolically ³H-labeled heparosan as a substrate as described under “Methods”. For the disaccharide analysis, NDase treated [³H]heparosan was enzymatically cleaved with heparin lyase III. We observed that greater than 90% of the ³H-labeled compound migrated as disaccharides on BioGel P-2 (data not shown). The resultant nonsulfated disaccharides were resolved by reverse phase ion pairing HPLC. As shown in Figure 28, approximately 6% of the recovered disaccharides are ΔUA-GlcNH₂, whereas this disaccharide is undetectable in the control (unmodified [³H]heparosan). This result confirmed that NDase has the anticipated enzymatic activity. The degree of deacetylation typically ranged between 5-20% and depended on both reaction time and the amount of NDase used.

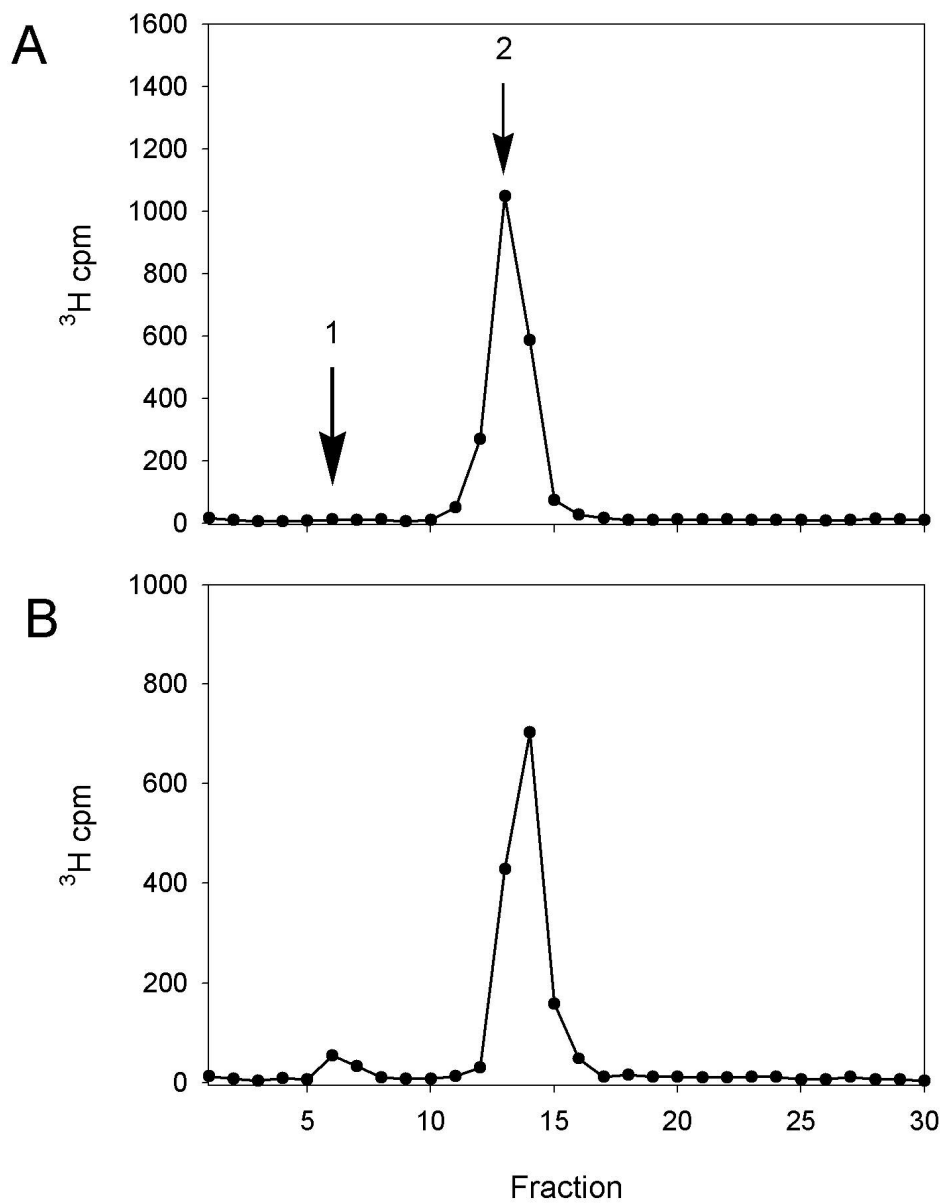


Figure 28. Disaccharide analysis of NDase-treated heparosan. Heparosan (A) and NDase-treated heparosan (B) were digested with heparin lyase III at 37 °C and the reaction was carried out overnight to ensure completeness. The reaction was heat deactivated, centrifuged and the supernatant (25 μL) was diluted in buffer containing 9.5 mM ammonium phosphate, 0.5mM phosphoric acid, and 67 mM tetrabutylammonium phosphate (250 μL final volume). The sample was then analyzed by RPIP-HPLC as described in “Methods”. Arrow 1 indicates $\Delta\text{UA-GlcNH}_2$ and arrow 2 indicates $\Delta\text{UA-GlcNAc}$

Distribution of N-deacetylated glucosamine residues in NDase treated heparosan-

In order to determine the position of GlcNH₂ units within the NDase modified heparosan, an overnight NDase reaction was performed and the resultant [³H]deacetylated heparosan was subjected to nitrous acid deamination at pH 4.5. This reaction specifically cleaves the glycosidic linkage between deacetylated glucosamine and hexuronic acid (Shively and Conrad, 1976). The resulting oligosaccharides were resolved by gel permeation chromatography and the distribution of GlcNH₂ units can be determined (Figure 29). Our results reveal that heparosan (without NDase treatment) is resistant to the nitrous acid degradation (Figure 4A). On the contrary, NDase-treated heparosan was susceptible to nitrous acid degradation, suggesting that *N*-unsubstituted glucosamine residue is present in the NDase-treated heparosan (Figure 4B). We observed that approximately 10% of the oligosaccharides eluted as disaccharides and 30% as ≤ hexasaccharide. These results demonstrate that the disaccharide unit GlcUA-GlcNH₂ generated by NDase can be clustered as evidenced by that fact that about 10% of the total oligosaccharides migrated as a disaccharide. In addition, the disaccharide GlcUA-GlcNH₂ is also separated by different numbers of GlcUA-GlcNAc repeating units. This observation suggests that NDase does not distinguish between GlcUA-GlcNH₂ and GlcUA-GlcNAc around the modification site. The relaxed substrate specificity in the NDase domain of NDST could be one of functional aspects of the holoenzyme that allow for the highly and variably sulfated *N*-sulfo domains observed in naturally occurring HS and heparin structures.

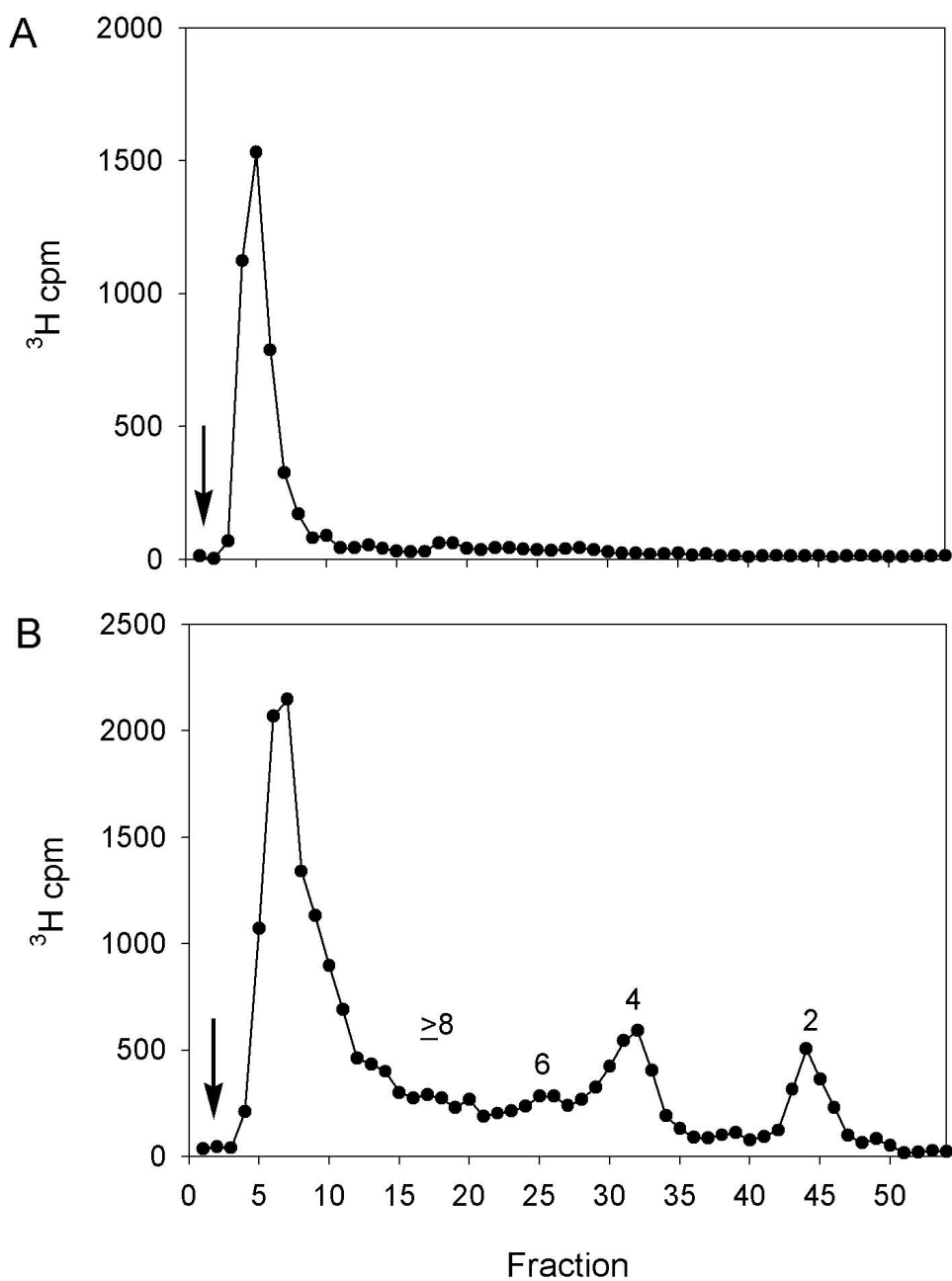


Figure 29. Oligosaccharide profile of high pH nitrous treated NDase-treated heparosan. Heparosan (A) and NDase treated heparosan (B) was deaminated at pH 4.5 which cleaves the glycosidic linkages after *N*-unsubstituted glucosamine residues. The numbers above each peak correspond to size of the eluted oligosaccharides (e.g. 2 for disaccharides, 4 for tetrasaccharide, etc.). The arrow indicates the end of the void volume.

Conclusions- This work demonstrates that the *N*-terminal domain of NDST-2 possesses *N*-deacetylase activity. Although the *C*-terminal domain of NDST-2 contains fully active *N*-sulfotransferase activity, it has been speculated that *N*-deacetylase activity requires the participation of *C*-terminal residues because mutations at the *C*-terminal residues removed both *N*-sulfotransferase and *N*-deacetylase activities(Wei and Swiedler, 1999) . Our results clearly demonstrate that the *N*-terminal domain of NDST-2 (A66-P604) carries fully functional *N*-deacetylase activity as determined by its susceptibility to NST modification and disaccharide analysis of NDase-treated heparosan. Furthermore, the presence of active *N*-deacetylase at the *N*-terminal suggests that NDST-2 contains two substrate binding sites: one site is located at the *N*-terminal for the deacetylase activity, and one is located at the *C*-terminal for the *N*-sulfotransferase activity. Our observed K_m is slightly higher than that of published literature, which leads us believe that two substrate binding sites or one that extends into both domains, provide increased avidity to reduce the effective concentration of polysaccharide. Further analysis of the NDase domain will allow us for a more comprehensive understanding on the mechanism of action of this important enzyme for the biosynthesis of heparan sulfate and heparin.

CHAPTER V. CHEMOENZYMATIC SYNTHESIS OF ANTICOAGULANT HEPARIN ANALOGUES

The synthetic utility of the HS modifying enzymes has been explored in several recent studies. The applicability of the sulfotransferases to remodel de-*O*-sulfonated heparin on the milligram scale suggests that the enzymes can be used to generate heparin analogues with distinct biological activities (Chen et al., 2005). Additional efforts to use cheaper and readily available substrates are desirable. One such substrate is the capsular polysaccharide produced by the K5 strain of *e. coli*. From the wild type strain 20-50 mg can be obtained from a one liter culture (unpublished data). Lindahl and co-workers have reported the expression of the Kfi gene cluster responsible for K5P synthesis in a common laboratory strain of *e. coli* that yielded the polysaccharide at one gram per liter (Lindahl et al., 2005). This chapter outlines a methodology to produce anticoagulant heparin analogues from K5P using a chemoenzymatic approach. The methodology is similar to that of (Kuberan et al., 2003b) with several significant advancements. The preparation of the biosynthetic enzymes is done in a bacterial system as opposed to baculovirus. We report high yields of active enzyme. Additionally, utilization of a PAPS regeneration system should allow for the preparation of milligram quantities of the heparin polysaccharides.

Expression and characterization of the HS biosynthetic enzymes- Epimerase and the HS

sulfotransferases were expressed and purified as outlined in “METHODS”. As illustrated in Figure 30, the purity of MBP fusion proteins was around 60% while that of His tagged proteins was 90-95%. The advantage of utilizing the MBP fusion proteins is that they maintain excellent solubility and could be concentrated at 4 mg/mL which facilitated enzyme immobilization efforts. His tagged sulfotransferases could also be concentrated to 2-3 mg/mL with relative ease.

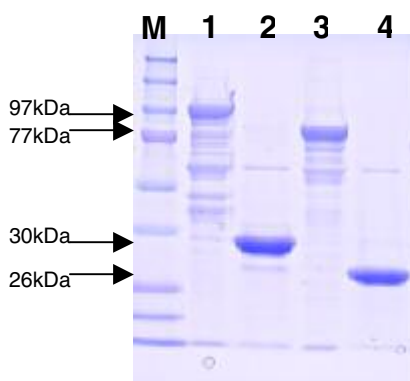


Figure 30. Expression of HS biosynthetic enzymes. The HS biosynthetic enzymes were expressed as maltose binding protein (MBP) or His₆ fusion proteins. The affinity tags do not affect enzyme activity and were retained. Enzyme purity was determined by SDS-PAGE and Comassie Blue staining. The protein bands are labeled for molecular weight marker (MW), Epimerase MBP (1), 2OSTHis (2), 6OSTMBP (3), 3OST1His (4). Purified protein yields are listed in “METHODS”

Chemical deacetylation and N sulfonation- Approximately 200 mg of K5P was prepared as described under in the “METHODS” chapter. The chemical modification of the polysaccharide is a two step procedure that involves base catalyzed deacetylation of the polysaccharide followed by selective N-sulfonation using the reagent trimethylamine sulfur trioxide. This synthesis was carried out in the Linhardt lab as previously described with a 50% recovery yield (Nadkarni et al., 1996) (Munoz et al., 2006). The resultant N-sulfo K5P (K5PNS) was determined to contain a small amount $\leq 5\%$ based on a complete heparin lyase

digestion and disaccharide analysis as well as the radioactive *N*-sulfotransferase assay. From the disaccharide analysis in Figure 31, it appears that the chemical *N*-sulfonation reaction was regio-selective and went to > 95% completion.

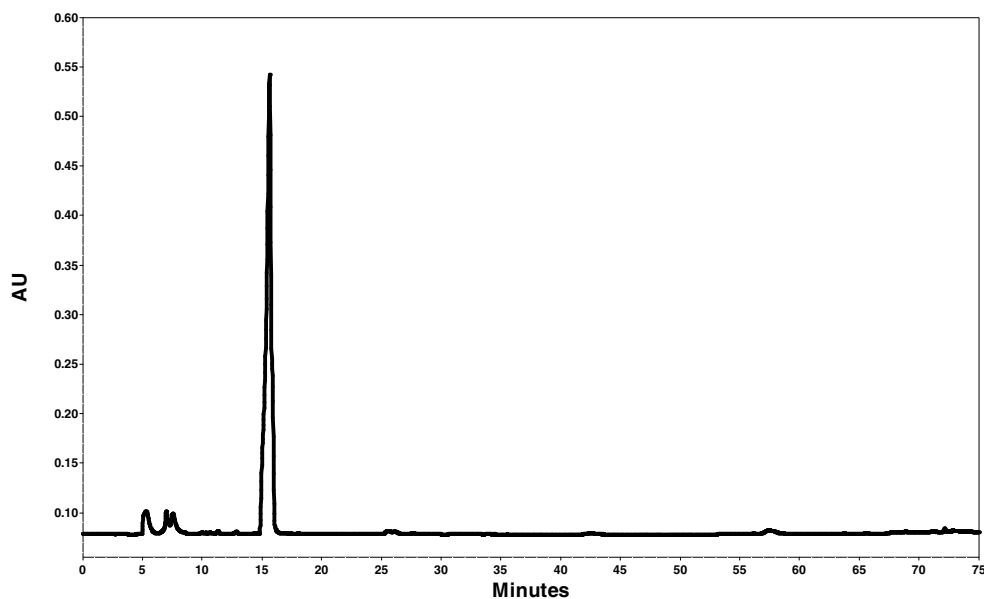


Figure 31. Structural analysis of N-sulfo K5 polysaccharide. Capsular K5 polysaccharide was chemically deacetylated and *N*-sulfonated and designated K5PNS. K5PNS was treated with heparin lyases I, II, and III and subjected to reverse ion pairing HPLC. The predominant peak migrated at 15 minutes and was determined to be the disaccharide 4,5-unsaturated uronic acid linked to *N*-sulfoglucosamine (Δ UA-GlcNS). Minor peaks at 5 and 7 minutes reflect the solvent peak and a small degree of 4,5-unsaturated uronic acid linked to *N*-unsubstituted glucosamine.

Size distribution and chemical degradation of the N-sulfo K5 polysaccharide- To determine the size distribution of the K5PNS, radiolabeled polysaccharide was subjected to size exclusion chromatography. A [35 S] sulfuryl tag was incorporated into the polysaccharide by 2OST modification. The addition of the sulfuryl groups is negligible relative to the molecular weight of the polysaccharide based on the high specific activity donor [35 S]PAPS (10 Ci/mmol). We observed a major shift in the elution profile of the K5PNS2-*O*-[35 S]sulfate (Figure 32A). This suggests that the polysaccharide underwent some

degradation. Efforts to purify the lower molecular weight material proved unsuccessful (Figure 32B).

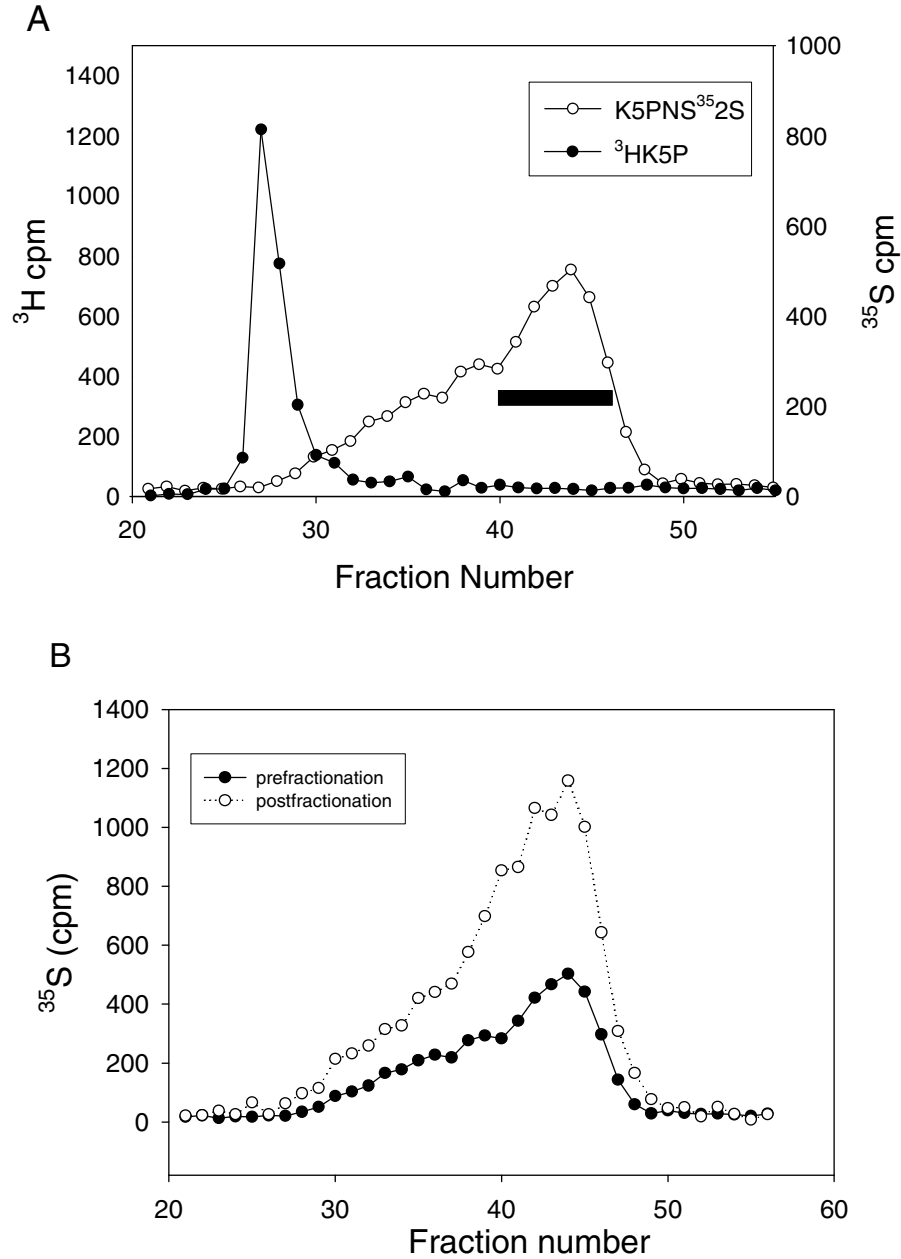


Figure 32. Size distribution of K5PNS. K5PNS Polysaccharide chain length was determined by size exclusion chromatography. K5PNS (—○—) was radiolabeled with high specific activity at the 2-hydroxy position of glucuronic acid using a high specific activity [^{35}S]PAPS. Metabolically labeled K5 Capsular polysaccharide (^3H K5P) was run as a control (—●—). The radioactive material was then eluted on a HiLoad Superdex™ 75 (Amersham) column on a FPLC system with a mobile phase of 25 mM Tris-HCl, 1000 mM NaCl, pH 7. Three milliliter fractions were collected and radioactive content was determined by scintillation counting. Fractions 38-46 of [^{35}S]K5PNS2S from (A) was collected and reapplied to the GPC column as the postfraction (—○—) material depicted in (B).

Epimerization of Capsular K5 Polysaccharide- In the next step of the synthetic route, K5PNS was treated with epimerase that was expressed as a maltose binding protein fusion. To determine the presence of IdoA in the K5PNS we used 2OST to add a radioactive tag [³⁵S] sulfonyl group. The radioactive material was then subjected to a low pH nitrous acid degradation followed by desalting on a P2 gel column and disaccharide analysis. As shown in Figure 33, it is clear that IdoA residues were indeed present in the polysaccharide. For an accurate account of the percentage of IdoA in the polysaccharide, we relied on a previously described NMR method (Chen et al., 2005). From this analysis, ~5% of the hexuronic acid residues were determined to be IdoA⁹. Since IdoA is essential in generating AT-binding heparin, a plan to generate additional IdoA residues was necessary.

Epimerase coupled 2-O-Sulfonation- Epimerase performs a reversible conversion of GlcA to IdoA. In order to drive the reaction towards the formation of IdoA, the 2OST reaction which preferentially generates IdoA2S over GlcA2S was coupled with epimerization in a one pot reaction. Using the sulfotransferase assay to assess the benefit of a one pot strategy, with an excess of K5PNS, 5-6 fold more 2-O-sulfated uronic acid residues were generated with the addition of epimerase as shown in Figure 34.

⁹ NMR experiments were carried out in Bob Linhardt's lab at RPI

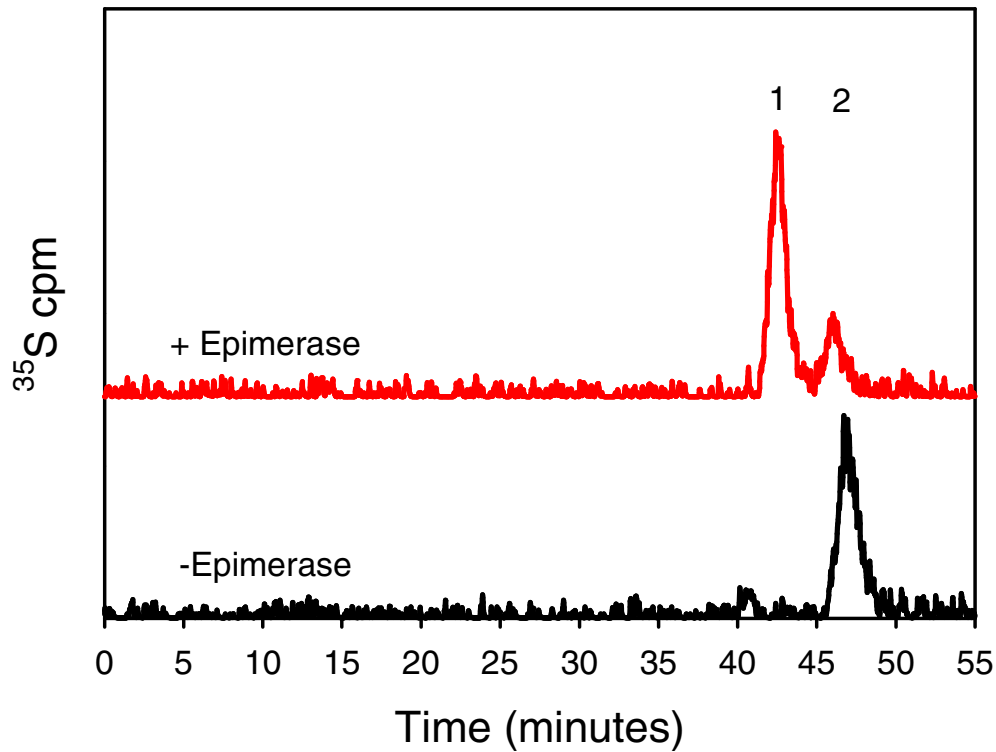


Figure 33. Epimerase generates IdoA residues. A qualitative analysis of epimerization of K5PNS by [^{35}S]sulfo-transfer. K5PNS was incubated with epimerase as indicated in “Methods”. The epimerized polysaccharide was then modified with 2OST and high specific activity [^{35}S]PAPS. The radiolabeled polysaccharide was then subjected to pH 1.5 nitrous degradation, desalted on a P2 gel column and the resultant disaccharides were analyzed by RPIP-HPLC. (1) indicates the disaccharide IdoA2S-anMan and (2) indicates GlcA2S-anMan.

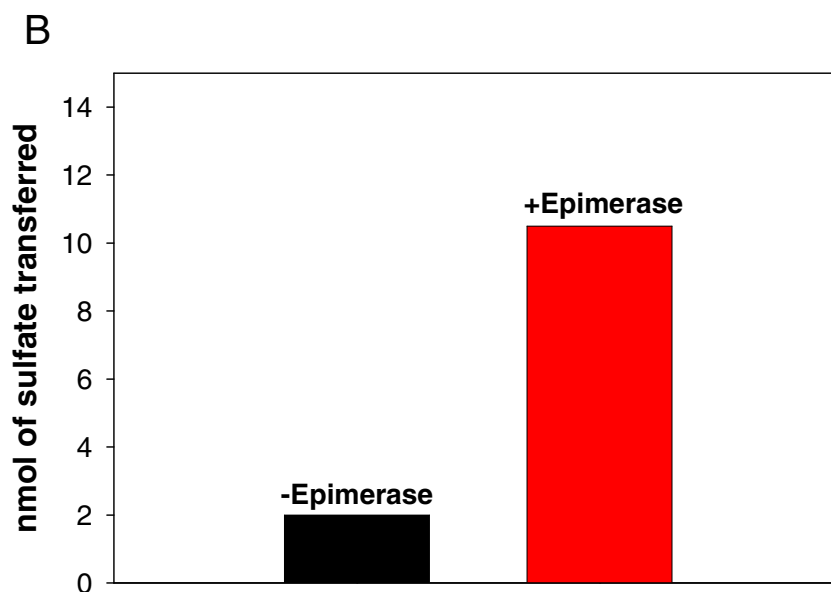
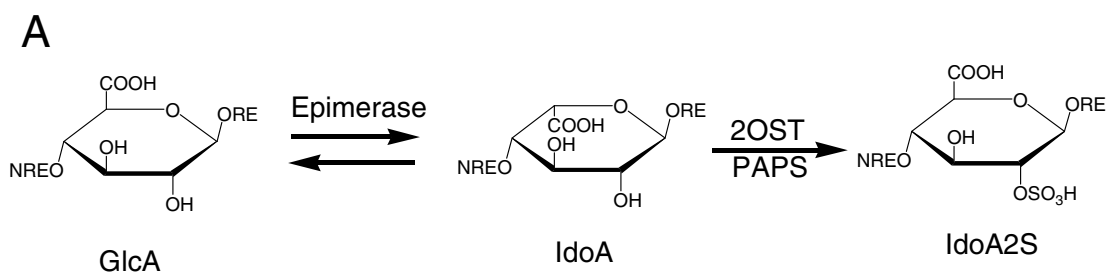


Figure34. Epimerase accelerates 2-O-sulfotransfer. (A) The epimerase reaction is reversible. When coupled with the 2OST reaction the formation of IdoA is favored. (B) K5PNS was incubated with EPI and 2OST and 40 μM PAPS in a 100 μL reaction. The amount of 2-O-sulfonation is increased by greater than five fold with the addition of epimerase.

In order to determine the percentage of IdoA2S to GlcA2S in this preparation we performed a small scale reaction (microgram) using micromolar PAPS in addition to [^{35}S]PAPS. We coupled the EPI and 2OST reaction followed by low pH nitrous treatment and disaccharide analysis. Based on specific activity, an estimated four moles of sulfate was transferred to one mole of K5PNS. Based on the disaccharide analysis shown in Figure 35, >90% of the 2-O-sulfated disaccharides were IdoA2S residues.

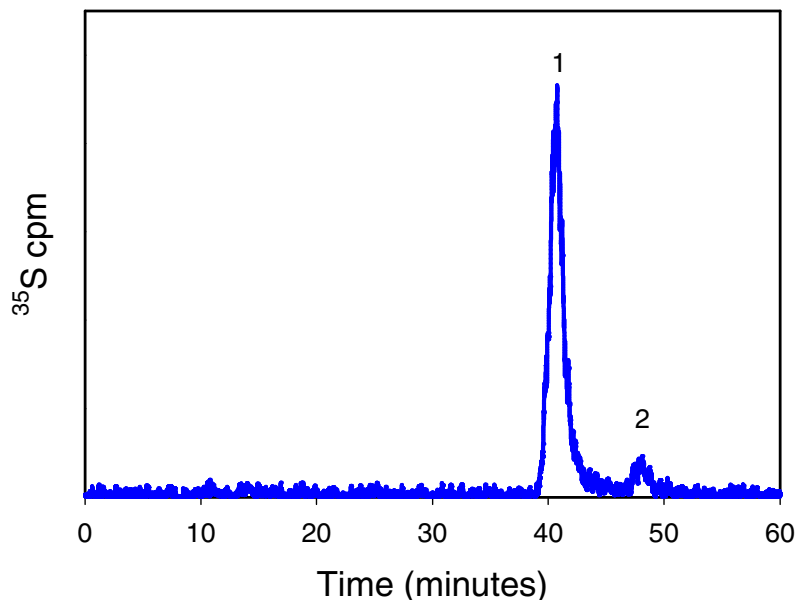


Figure 35. Coupled epimerization and 2-O-sulfonation enhances the IdoA content. The polysaccharide modified with a one pot EPI/2OST was chemically degraded with nitrous acid at pH 1.5. The resultant disaccharides were desalted and a disaccharide analysis was performed. From the chromatogram, approximately 90% of the radiolabeled disaccharide was IdoA2S-anMan (1) and a small quantity of disaccharides was GlcA2S-anMan (2).

A milligram scale preparation of 2-*O*-sulfated K5PNS was initiated to characterize the material by NMR and for additional sulfo-transfer reactions. To achieve a high degree of sulfation, the PAPS regeneration system was employed. In total, the reaction requires three enzymes at a total protein concentration of 1-2 mg/mL. In order to reduce the volume of the reaction as well as the amount of enzyme required for the preparation, 2OST was immobilized using the Aminolink® column. The enzyme is covalently linked to resin that contains activated aldehyde groups via Schiff base formation. The Schiff base is then reduced to the amide with the reducing agent sodium cyanoborohydride. Under these mild conditions, immobilization was achieved at ~3mg protein/mL resin while retaining excellent

enzymatic activity¹⁰. Approximately 2 milligrams of K5PNS2S was generated from 4 milligrams of starting material. A complete heparin lyase digestion resulted in approximately 90% digestion of the polysaccharide to disaccharide units. RPIP-HPLC reveals that the polysaccharide is composed of 46% 2-*O*-sulfated disaccharide units (Figure 36), while NMR data suggests that approximately 90% of the 2-*O*-sulfo residues are iduronic acid (correspondence with Robert Linhardt).

In addition to the 46% 2-*O*-sulfated K5PNS (K5Hp-2), we also generated a 21% 2-*O*-sulfated K5PNS (K5Hp-1), and a 10% 2-*O*-sulfated K5PNS. This reduction in 2-*O*-sulfation was accessed by reducing the amount of 2OST resin and is likely dependent on the catalytic turnover of the enzyme.

6-O-sulfonation of K5PNS2S- The 6OST was also expressed as a MBP fusion protein and immobilized as described above. Based on radioactive the sulfotransferase reaction, 8-10 sulfuryl groups could be transferred to one polysaccharide chain¹¹. Several small scale preparations (~10 µg) were carried out to generate K5Hp-3 (derived from 10% 2-*O*-sulfated K5PNS) and K5Hp-4 (derived from K5Hp-2). The percentages of the four major disaccharides resulting from heparin lyase treatment of the two preparations are listed in Table VI. The additional peaks in the chromatogram could reflect some partially undigested materials. In order to confirm this, the peaks would have to be purified and undergo structural analysis. While it is important to know the complete structure of these synthesized heparin analogues, a detailed structural analysis is beyond the scope of this work.

¹⁰ The immobilized enzyme typically retains 80-90% sulfotransferase activity compared to the soluble form in a radioactive sulfotransfer reaction. Chen et al. demonstrates that the immobilized enzyme retains 80% activity after multiple uses and is stable for approximately one month.

¹¹ Average length of the polysaccharide is 40 monosaccharide units.

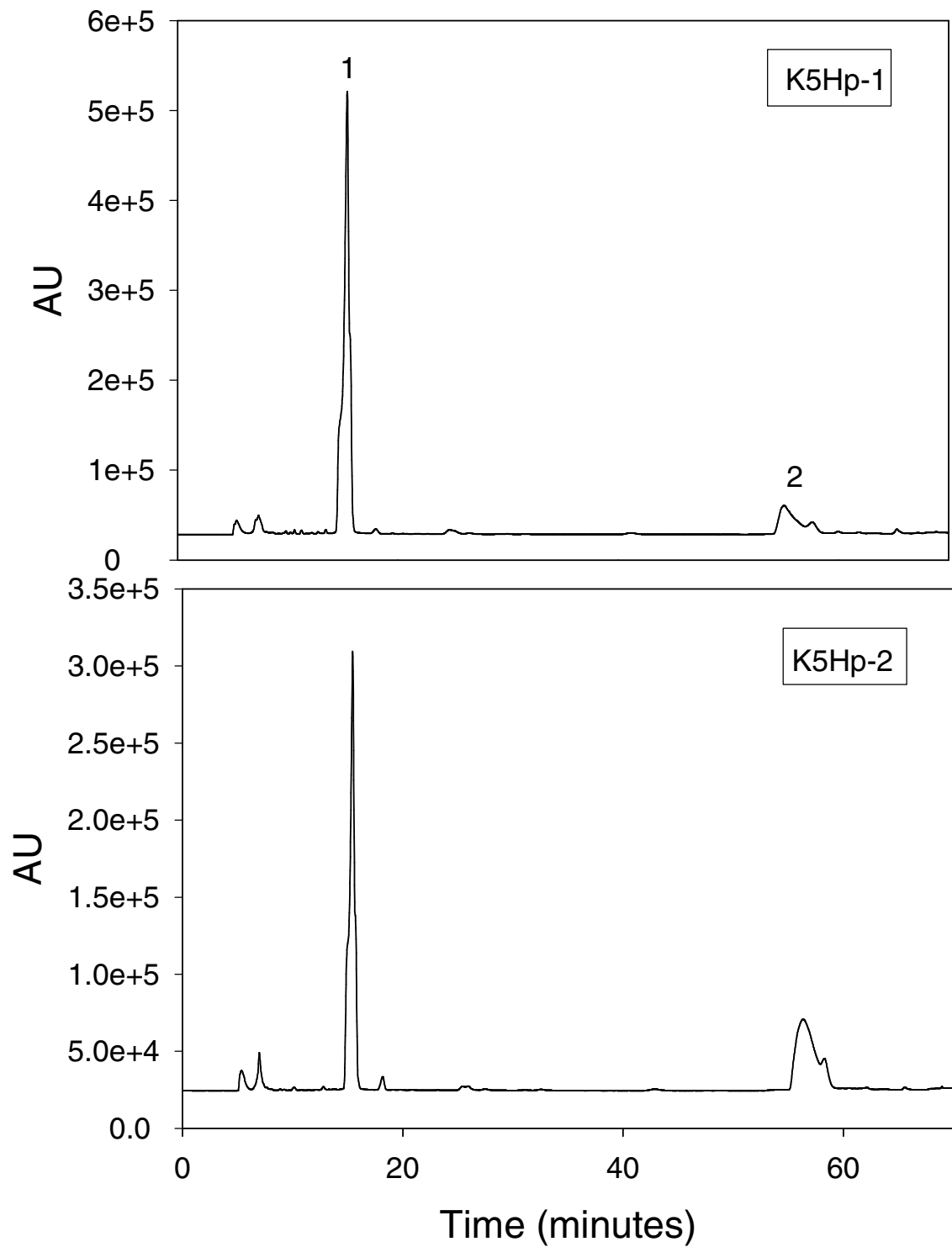


Figure 36. RPIP-HPLC chromatograms of the disaccharide analysis of EPI/2OST modified polysaccharides. The synthesized polysaccharides were digested with a mixture of heparin lyase I, II, and III. The resultant disaccharides were resolved on RPIP-HPLC. The numbers indicate the eluted positions of authentic disaccharide standards, where 1 represents Δ UA-GlcNS and 2 represents UA2S-GlcNS.

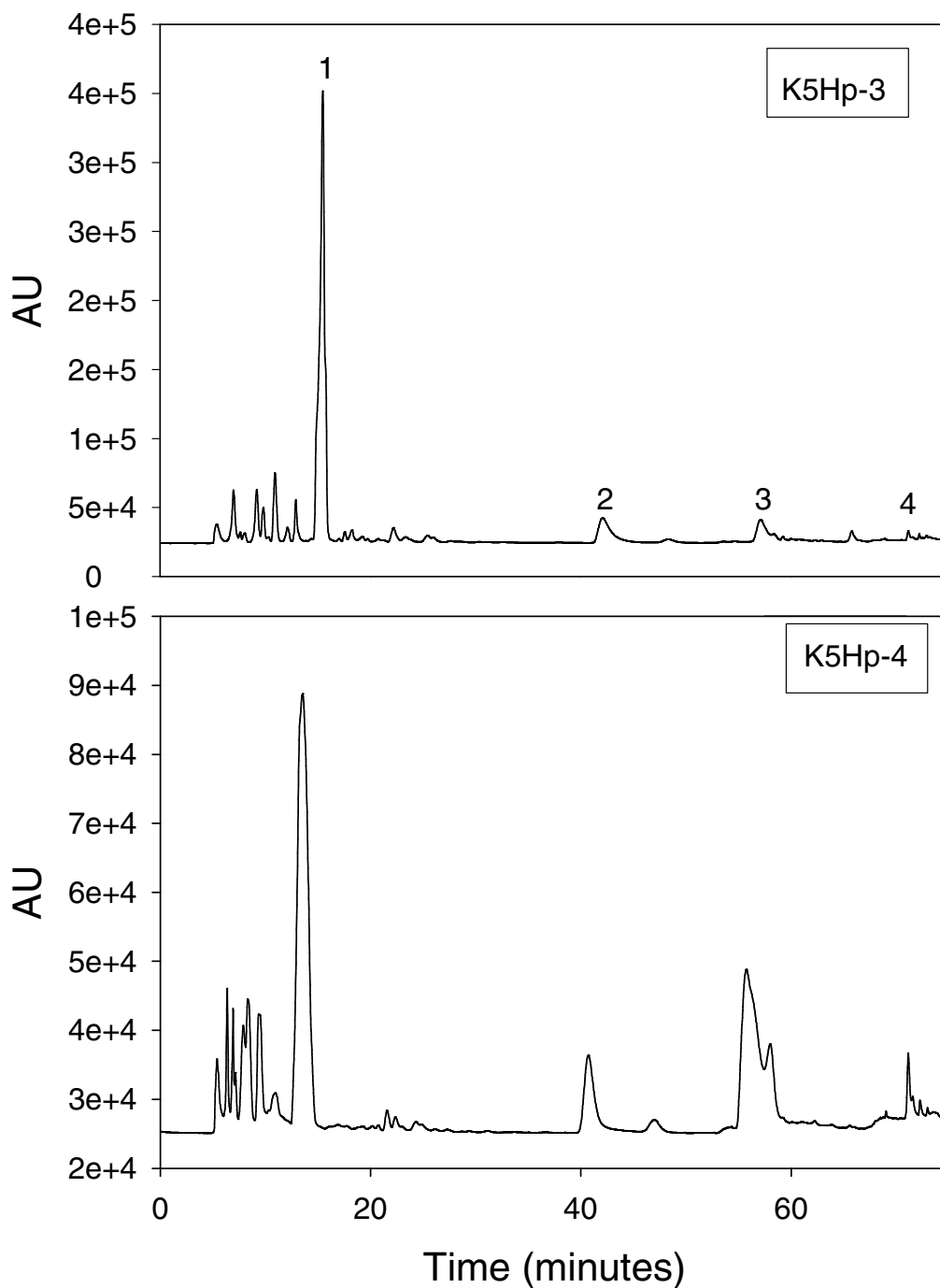


Figure 37. RPIP-HPLC chromatograms of the disaccharide analysis of EPI/2OST and 6OST modified polysaccharides. The synthesized polysaccharides were digested with a mixture of heparinases, including heparin lyase I, II, and III. The resultant disaccharides were resolved on RPIP-HPLC. The numbers indicate the eluted positions of authentic disaccharide standards, where 1 represents Δ UA-GlcNS and 2 represents UA-GlcNS6S, 3 represents Δ UA2S-GlcNS, and 4 represents Δ UA2S-GlcNS6S.

Table 6. Disaccharide composition of Heparin analogues

Heparin analogue	UA-GlcNS	UA2S-GlcNS	UA-GlcNS6S	UA2S-GlcNS6S
K5Hp-1	79 %	21%	—	—
K5Hp-2	54%	46%	—	—
K5Hp-3	73.1%	10.4%	16%	0.5%
K5Hp-4	46%	40%	13%	1%

3-O-sulfonation and anticoagulant activity of K5Hp analogues- The essential 3-*O*-sulfated glucosamine in anticoagulant heparin may be generated by 3OST1. This 3OST isoform was used to radioactively label the K5Hp analogues. These radio-labeled polysaccharides were then assessed for the fraction of 3-*O*-sulfated polysaccharide that binds to antithrombin. This AT-binding assay is an excellent indicator of anticoagulant activity and indicates that the proper AT-binding structure of HS and heparin is present in the polysaccharide. The relative binding of the 3-*O*-sulfated polysaccharides is presented in Figure 38. From the graph it is clear that 6-*O*-sulfation is an important determinate for AT binding of the 3OST1 modified K5Hp. K5HP-4 had the highest fraction of AT binding polysaccharide which is due to its total 6-*O*-sulfo residues and approximately 90% IdoA content (based on NMR). These components coupled with the proper 3-*O*-sulfated glucosamine residues are critical in AT binding.

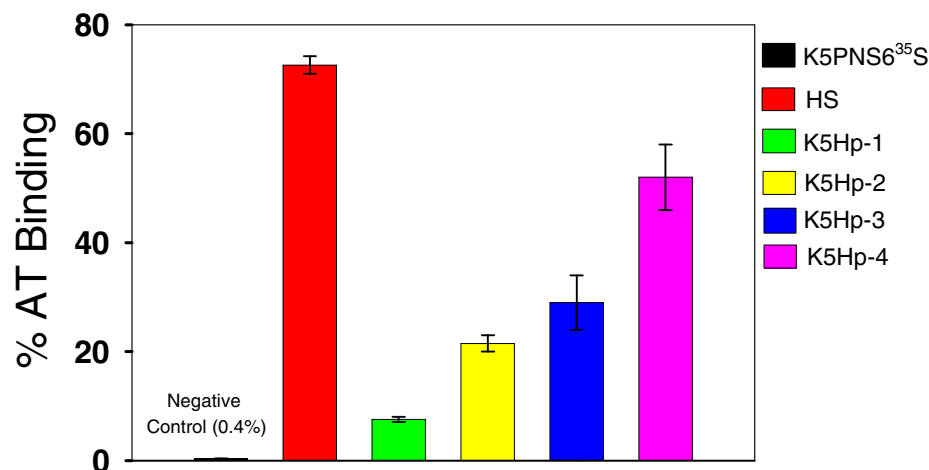


Figure 38. AT binding of heparin analogues. HS and K5Hp analogues were radio-labeled with high specific activity by 3OST1. The polysaccharides were purified by DEAE anion exchange chromatography, dialyzed against 20 mM ammonium bicarbonate, and dried by centrifugal evaporation. 5×10^4 to 1×10^5 cpm of each of the samples was assessed for AT binding as described in “General Procedures”. The negative control was K5NS2S radio-labeled with high specific activity PAP³⁵S and 6OSTMBP.

Conclusions- In this chapter we report the use of a chemoenzymatic approach to generate a panel of heparin analogues with varying degrees of AT binding activity. The major advancements of this work include the use of a PAPS regeneration system and the use of the K5 capsular polysaccharide as the starting material. Enhanced epimerization of the polysaccharide was achieved by coupling the EPI and 2OST reactions together. Based on our results it is clear that in addition to a physical linkage between these two enzymes (Pinhal et al., 2001), it appears that there is also an important link between their activities. The preferred substrate for 2OST is IdoA. Since the epimerase reaction is reversible, the conversion of IdoA to IdoA2S is essential to the formation of additional IdoA residues. A physical linkage between these two enzymes *in vivo* would provide a significant advantage towards the formation of IdoA residues. In addition we were able to demonstrate that the degree of 2-*O*-sulfation of the polysaccharide can be varied based on the amount of enzyme

that is used in the EPI/2OST reaction. The main benefits of immobilization of the enzyme are that it can be recycled and is stable for up to one month at 4 °C. Enzyme immobilization also allows for the reduction of the reaction volume, making the purification of the modified polysaccharides easier. The degradation of the K5P upon chemical deacetylation and N-sulfonation does not appear to impact the AT-binding capacity of the heparin analogue. This degradation may be addressed with the use of the NDST enzyme in this approach or through the development of new chemical methods to modify the *N* position of glucosamine.

This work provides a target structure for which the synthesis of anticoagulant heparin analogues can be based on. The pursuit of multi-milligram quantities of this material is currently underway.

CHAPTER VI. CONCLUSIONS

Heparin, a highly sulfated linear polysaccharide, has successfully been used in the clinic to treat coagulation disorders and as a prophylaxis to reduce aberrant thrombus formation during invasive surgeries. In addition to its use as an anticoagulant drug, a number of heparin and heparan sulfate (HS) analogues are currently being studied in clinical trials as anti-inflammatory, anti-angiogenic, and anti-metastatic agents. Intense research interest in the role of HS in microbial pathogenesis is also emerging. These studies coupled with robust methodologies to synthesize HS will prove useful in extending its therapeutic utility.

The role of heparan sulfate (HS) in regulating blood coagulation has a wide range of clinical implications. We investigated the role of 3-*O*-sulfotransferase isoform 5 (3OST5) in generating anticoagulant HS *in vivo*. A Chinese hamster ovary cell line (3OST5/CHO) stably expressing 3OST5 was generated. The expression of 3OST5 in 3OST5/CHO cells was confirmed by Northern analysis, RT-PCR, and the disaccharide analyses of the HS from the cells. We also determined the effects of the HS from 3OST5/CHO on antithrombin-mediated inhibition of factor Xa. Fluorescently labeled antithrombin bound to the surface of 3OST5/CHO cells, suggesting that the antithrombin-binding HS is indeed present on the cell surface. Our results demonstrate that the 3OST5 gene is capable of synthesizing anticoagulant HS in CHO cells and has the potential to contribute to the biosynthesis of anticoagulant HS in humans.

Heparan sulfate glucosaminyl *N*-deacetylase/*N*-sulfotransferase isoform 2 (NDST-2), key in the biosynthesis of heparin, contains two distinct activities. This bifunctional enzyme removes the acetyl group from *N*-acetylated glucosamine (*N*-deacetylase activity), and transfers a sulfuryl group to the unsubstituted amino position (*N*-sulfotransferase activity). The *N*-sulfotransferases activity of NDST has been unambiguously localized to the C-terminal domain of NDST. Here we report that the *N*-terminal domain of NDST-2 retains *N*-deacetylase activity. The *N*-terminal domain (A66-P604) of human NDST-2, designated as *N*-deacetylase (NDase), was cloned as a (His)₆-fusion protein, and protein expression was carried out in *E. coli*. Heparosan treated with NDase contains *N*-unsubstituted glucosamine and is highly susceptible to *N*-sulfation by *N*-sulfotransferase. Our results conclude that the *N*-terminal domain of NDST-2 contains functional *N*-deacetylase activity. This finding helps further elucidate the mechanism of action of heparan sulfate *N*-deacetylase/*N*-sulfotransferases and the biosynthesis of heparan sulfate in general.

The continued development of chemical and enzymatic methods to synthesize HS and heparin analogues is essential to the future exploration of this biologically important molecule. Herein we have reported the chemoenzymatic synthesis of a variety of heparin analogues that differ in their ability to bind antithrombin. The analogue with the best profile was K5Hp-4, the most highly sulfated molecule, modified by 3OST1. Continued efforts to synthesize unique heparin analogues by the use of the various HS biosynthetic enzymes should aid in the further development of new anticoagulant drugs as well as heparin molecules that can be used to treat a variety of diseases and disorders.

Appendix I.

Curriculum Vitae

Michael Bernard Duncan, II

Division of Medicinal Chemistry
and Natural Products, CB #7360
School of Pharmacy
mbduncan@unc.edu
University of North Carolina at Chapel Hill
Chapel Hill, NC 27599

Work: (919)962-0065

Fax: (919)843-5432

Email:

Hometown: Ridgeland, South Carolina

Education:

University of North Carolina at Chapel Hill, 2001-present
Ph.D. Candidate, Division of Medicinal Chemistry and Natural Products

Hampton University, 1997-2001
B.S. in Chemistry with Honors
Magna cum laude
Hampton University Honors College Graduate, 2001

Current Research Interests:

Molecular and Chemical Biology, Carbohydrate and Protein Biochemistry, Drug design:
Protein/carbohydrate interactions; Chemoenzymatic synthesis of heparin analogs;
Heparin/heparan sulfate biochemistry as it relates to microbial pathogenesis and
cardiovascular biology

Publications:

- 1) M.B. Duncan, M. Liu, C. Fox, J. Liu. Characterization of the *N*-deacetylase domain from the heparan sulfate *N*-deacetylase/*N*-sulfotransferase 2. **Biochem. Biophys. Res. Commun.** (2006) **339**:1232-7.
- 2) Y. Gong, M. Duvvuri, M.B. Duncan, J. Liu, J.P. Krise. Niemann-Pick C1 protein facilitates the efflux of the anticancer drug daunorubicin from cells according to a novel vesicle-mediated pathway. **J. Pharmacol. Exp. Ther.** (2006) **316**:242-7.
- 3) M.B. Duncan, J. Chen, J.P. Krise, J. Liu. The biosynthesis of anticoagulant heparan sulfate by the heparan sulfate 3-*O*-sulfotransferase isoform 5. **Biochim. et Biophys. Acta** (2004) **1671**:34-43.
- 4) V. Tiwari, C. Clement, M.B. Duncan, J. Chen, J. Liu, D. Shukla. A role for 3-*O*-sulfated heparan in cell fusion by herpes simplex virus type 1. **J Gen. Virol.** (2004) **85**:805-9.

5) J. Chen, M.B. Duncan, K. Carrick, R.M. Pope, J. Liu. Biosynthesis of 3-O-sulfated heparan sulfate: unique substrate specificity of heparan sulfate 3-O-sulfotransferase isoform 5. **Glycobiology** (2003) **13**:785-94.

6) J. Liu, Z. Shriver, R.M. Pope, S.C. Thorp, M.B. Duncan, R.J. Copeland, C.S. Raska, K. Yoshida, R.J. Eisenberg, G.H. Cohen, R.J. Linhardt, R. Sasisekharan. Characterization of a heparan sulfate octasaccharide that binds to herpes simplex virus type 1 glycoprotein D. **J Biol. Chem.** (2002) **277**:33456-67.

Patents:

J. Liu, J. Chen, M.B. Duncan, D. Shukla, V. Tiwari. Purified and isolated heparan sulfate 3-O-sulfotransferase isoform 5 nucleic acids and polypeptides and therapeutic and screening methods using the same. International Publication Number WO 2004/005475.

Awards:

Scholar, David and Lucille Packard Foundation, 2001-06

-An award to outstanding students from Historically Black Colleges and Universities engaged in graduate students in the physical and life sciences.

-\$100,000 for graduate studies

Fellow, Minority and Indigenous Fellows Program, Biotechnology Institute, San Francisco CA, 2004

-This program pairs students, post-docs, and faculty from underserved populations at colleges and universities with industry mentors. Fellows are introduced to the biotechnology industry during the Biotechnology Institute Education Conference, where they attend sessions on new and emerging technologies, mentoring, and scientific content updates. Fellows also make field visits to local research facilities and attend the BIO Annual International Convention. The program continues with a year of mentoring.

American Chemical Society Hampton Roads Local Section Award for Outstanding Achievement in Chemistry, Norfolk VA, 2001

Outstanding Oral Presentation in Chemistry, 2nd Place, Beta Kappa Chi Scientific Honor Society National Conference, Atlanta GA, 2001

Scholar, Minority Access to Research Careers (MARC) Program, 1999-2001

Hampton University Presidential Scholar, 1997-2001

Undergraduate Research Experience:

Participant, Research Education Support Program, UNC-CH, Chapel Hill NC, Summer 2001

Advisor: Jian Liu (Medicinal Chemistry and Natural Products)

Project: Characterization of heparan sulfate oligosaccharides by MALDI-TOF mass spectrometry

Participant, Summer Pre-Graduate Research Experience, UNC-CH, Morehead City NC and Chapel Hill NC, Summer 2000

Advisors: Neils Lindquist (Marine Sciences) and Gerhard Meissner (Biochemistry and Biophysics)

Project: Identification of UV absorbing compounds from the Stinker Sponge, *Ircinia felix*, that stimulate Ca²⁺ channels/ryanodine receptors.

Participant, Diversity Graduate Program in Science and Engineering, Rice University, Houston TX, Summer 1999

Advisor: W. Ed Billups (Chemistry)

Project: Synthesis and purification of substituted methylenecyclopropenes at low temperature.

Participant, Summer Life Sciences Training Program, Kennedy Space Center, Cape Canaveral FL, Summer 1998

Advisor: Neil Yorio (Space Life Sciences)

Project: Micronutrient deficiencies of mixed age crops in a hydroponic growth system.

Work Experience:

Graduate Research Assistant, Division of Medicinal Chemistry, School of Pharmacy (SOP), University of North Carolina at Chapel Hill, 2001-current

Thesis advisor: Jian Liu, Assistant Professor

Thesis Title: Biological and Chemoenzymatic Synthesis of Anticoagulant Heparan Sulfate

Rotation/Visiting Student Training-- Over the past year I have trained two rotating graduate students (Spring and Fall 2005) and two high school students (Summer 2005) working in the laboratory.

Instructor, PCAT preparatory course, Chemistry Section; Offered by the UNC-CH SOP Student National Pharmacy Association, October 2-3, 2004

I developed a lecture that served as a review of topics covered in an undergraduate general chemistry course. I presented this lecture to ~100 students during a PCAT review course offered by the School of Pharmacy at UNC.

Graduate Assistant, Summer Pre-Graduate Research Experience (SPGRE) Program, Summer 2002.

This 10 week program offers undergraduates the opportunity to perform research, take a GRE preparatory course, and network with a variety of scientists/scholars on the UNC-Chapel Hill campus. I primarily served as a group leader, directing ten students through their

summer long activities. My duties also included assisting in the organization of weekly seminars and a variety of administrative tasks.

Committee/Organizational Positions Held:

Co-Chair, Invited Lecturer Series, sponsored by the Graduate Student Organization, UNC School of Pharmacy (SOP), 2003

Invited Speaker: Dr. Kim D. Janda, Ely R. Callaway, Jr. Professor of Chemistry, The Scripps Research Institute

President, UNC-SOP Graduate Student Organization, 2004-05

Committee Member, UNC-SOP Graduate Education and Research Committee, 2004-05

Ad Hoc Committee Member, UNC-SOP Graduate Program Governance Policy Committee, 2004-05

Committee Member, UNC-SOP Division of Medicinal Chemistry and Natural Products Chair Search Committee, 2004-05

Skills/Techniques

Molecular Biology

- Agarose gel electrophoresis
- Northern and Western Blotting
- Reverse Transcriptase and Real Time PCR
- Error prone PCR for random mutagenesis studies
- Various aspects of molecular cloning- Primer design, PCR, plasmid amplification/purification, and DNA sequencing data analysis

Biochemical/Bio-Analytical

- Bioassay development--*in vitro* and cell based
- Phage display
- ELISA
- Affinity co-electrophoresis
- Recombinant Protein expression/purification (bacterial systems)
- SDS-PAGE
- HPLC-- Ion exchange, size exclusion, reverse phase ion pairing
- FPLC Ion exchange, size exclusion, affinity
- Capillary electrophoresis--zone electrophoresis in normal and reverse polarity
- Chemical and enzymatic degradation of complex carbohydrates for structural analysis
- Chemical conjugation of complex glycans and glycoproteins
- Covalent Protein Immobilization
- UV Spectrophotometry--Quantitative Analysis of carbohydrates, nucleic acids, and proteins
- Mammalian cell culture--DNA transfection, radioactive metabolic labeling of proteoglycans
- Limited exposure to Mass spectrometry- MALDI-time of flight, ESI-ion trap, MS/MS

REFERENCES

- Aikawa, J., Grobe, K., Tsujimoto, M., and Esko, J. D. (2001). Multiple isozymes of heparan sulfates/heparin GlcNAc N-deacetylase/GlcN N-sulfotransferase: Structure and activity of the fourth member, NDST4. *J Biol Chem* 276, 5876-5882.
- Alvarez-Dominguez, C., Vazquez-Boland, J. A., Carrasco-Marin, E., Lopez-Mato, P., and Leyva-Cobian, F. (1997). Host cell heparan sulfate proteoglycans mediate attachment and entry of *Listeria monocytogenes*, and the listerial surface protein ActA is involved in heparan sulfate receptor recognition. *Infect Immun* 65, 78-88.
- Angulo, J., Hricovini, M., Gairi, M., Guerrini, M., de Paz, J. L., Ojeda, R., Martin-Lomas, M., and Nieto, P. M. (2005). Dynamic properties of biologically active synthetic heparin-like hexasaccharides. *Glycobiology* 15, 1008-1015.
- Arepally, G., and Cines, D. B. (2002). Pathogenesis of heparin-induced thrombocytopenia and thrombosis. *Autoimmun Rev* 1, 125.
- Atha, D. H., Lormeau, J.-C., Petitou, M., Rosenberg, R. D., and Choay, J. (1985). Contribution of monosaccharide residues in heparin binding to antithrombin III. *Biochemistry* 24, 6723-6729.
- Bai, X., Zhou, D., Brown, J. R., Crawford, B. E., Hennet, T., and Esko, J. D. (2001). Biosynthesis of the linkage region of glycosaminoglycans: cloning and activity of galactosyltransferase II, the sixth member of the β 1,3-galactosyltransferase family (β 3GalT6). *J Biol Chem* 276, 48189-48195.
- Bame, K. J., and Esko, J. D. (1989). Undersulfated heparan sulfate in a Chinese hamster ovary cell mutant defective in heparan sulfate N-sulfotransferase. *J Biol Chem* 264, 8059-8065.
- Bame, K. J., Lidholt, K., Lindahl, U., and Esko, J. D. (1991). Biosynthesis of heparan sulfate. Coordination of polymer-modification reactions in a Chinese hamster ovary cell mutant defective in N- sulfotransferase. *J Biol Chem* 266, 10287-10293.
- Baraz, L., Haupt, Y., Elkin, M., Peretz, T., and Vlodaysky, I. (2006). Tumor suppressor p53 regulates heparanase gene expression. *Oncogene*, *in press*.
- Bernfield, M., Gotte, M., Park, P. W., Reizes, O., Fitzgerald, M. L., Lincecum, J., and Zako, M. (1999). Functions of cell surface heparan sulfate proteoglycans. *Ann Rev Biochem* 68, 729-777.
- Berninsone, P., and Hirschberg, C. B. (1998). Heparan sulfate/heparin N-deacetylase/N-sulfotransferase: The N-sulfotransferase activity domain is at the carboxyl half of the holoenzyme. *J Biol Chem* 273, 25556-25559.

Bink, R. J., Habuchi, H., Lele, Z., Dolk, E., Joore, J., Rauch, G.-J., Geisler, R., Wilson, S. W., den Hertog, J., Kimata, K., and Zivkovic, D. (2003). Heparan Sulfate 6-O-Sulfotransferase Is Essential for Muscle Development in Zebrafish. *J Biol Chem* 278, 31118-31127.

Bjornsson, S. (1993). Simultaneous preparation and quantitation of proteoglycans by precipitation with alcian blue. *Anal Biochem* 210, 282-291.

Boyer, C., Wolf, M., Vedrenne, J., Meyer, D., and Larrieu, M. J. (1986). Homozygous variant of antithrombin III: AT III Fontainbleau. *Thromb Haemost* 56, 18-22.
Brinkmann, T., Weilke, C., and Kleesiek, K. (1997). Recognition of Acceptor Proteins by UDP-xylose Proteoglycan Core Protein beta -D-Xylosyltransferase. *J Biol Chem* 272, 11171-11175.

Bullock, S. L., Fletcher, J. M., Beddington, R. S., and Wilson, V. A. (1998). Renal agenesis in mice homozygous for a gene trap mutation in the gene encoding heparan sulfate 2-sulfotransferase. *Genes Dev* 12, 1894-1906.

Burkart, M. D., Izumi, M., Chapman, E., Lin, C., and Wong, C. (2000). Regeneration of PAPS for the enzymatic synthesis of sulfated oligosaccharides. *J Org Chem* 65, 5565-5574.
Capila, I., and Linhardt, R. J. (2002). Heparin-Protein Interactions. *Angew Chem Int Ed* 41, 390-412.

Carfi, A., Willis, S. H., Whitbeck, J. C., Krummenacher, C., Cohen, G. H., Eisenberg, R. J., and Wiley, D. C. (2001). Herpes simplex virus glycoprotein D bound to the human receptor HveA. *Mol Cell* 8, 169-179.

Carter, N. M., Ali, S., and Kirby, J. A. (2003). Endothelial inflammation: the role of differential expression of N-deacetylase/N-sulphotransferase enzymes in alteration of the immunological properties of heparan sulphate. *J Cell Sci* 116, 3591-3600.

Carter, W. J., Cama, E., and Huntington, J. A. (2005). Crystal Structure of Thrombin Bound to Heparin. *J Biol Chem* 280, 2745 -2749.

Chapman, E., M.D., B., Hanson, S. R., and Wong, C. H. (2004). Sulfotransferases: Structure, mechanism, biological activity, inhibition, and synthetic utility. *Angew Chem Int Ed* 43, 3526-3548.

Chen, J., Avci, F. Y., Muñoz, E. M., McDowell, L. M., Chen, M., Pedersen, L. C., Zhang, L., Linhardt, R. J., and Liu, J. (2005). Enzymatically redesigning of biologically active heparan sulfate. *J Biol Chem* 280, 42817-42825.

Chen, J., Duncan, M. B., Carrick, K., Pope, M., and Liu, J. (2003). Biosynthesis of 3-O-sulfated heparan sulfate: unique substrate specificity of heparan sulfate 3-O-sulfotransferase isoform 5. *Glycobiology* 13, 785-794.

- Chen, J., and Liu, J. (2005). Characterization of the structure of antithrombin-binding heparan sulfate generated by heparan sulfate 3-O-sulfotransferase 5. *Biochim Biophys Acta-General Subjects* 1725, 190.
- Conrad, H. E. (1998). *Heparin-binding proteins* (San Diego, CA: Academic Press).
- Corey, L., and Spear, P. G. (1986). Infections with herpes simplex viruses. *N Engl J Med* 314, 686-691 and 749-757.
- Dailey, L., Ambrosetti, D., Mansukhani, A., and Basilico, C. (2005). Mechanisms underlying differential responses to FGF signaling. *Cytokine Growth Factor Rev* 16, 233.
- Desai, U. R., Petitou, M., Bjork, I., and Olson, S. T. (1998). Mechanism of heparin activation of antithrombin. Role of individual residues of the pentasaccharide activating sequences in the recognition of native and active states of antithrombin. *J Biol Chem* 273, 7478-7487.
- Duensing, T. D., and Putten, J. P. (1998). Vitronectin binds to the gonococcal adhesin OpaA through a glycosaminoglycan molecular bridge. *Biochem J* 334, 133-139.
- Duensing, T. D., Wing, J. S., and van Putten, J. P. M. (1999). Sulfated Polysaccharide-Directed Recruitment of Mammalian Host Proteins: a Novel Strategy in Microbial Pathogenesis. *Infect Immun* 67, 4463-4468.
- Edavettal, S. C., Lee, K. A., Negishi, M., Linhardt, R. J., Liu, J., and Pedersen, L. C. (2004). Crystal structure and mutational analysis of heparan sulfate 3-O-sulfotransferase isoform 1. *J Biol Chem* 279, 25789-25797.
- Eriksson, I., Sanback, D., Ek, B., Lindahl, U., and Kjellen, L. (1994). cDNA cloning and sequencing of mouse mastocytoma glucosaminyl *N*-deacetylase/*N*-sulfotransferase, an enzyme involved in the biosynthesis of heparin. *J Biol Chem* 269, 10438-10443.
- Eko, J. D., and Selleck, S. B. (2002). Order out of chaos: Assembly of ligand binding sites in heparan sulfate. *Ann Rev Biochem* 71, 435-471.
- Esko, J. D., Stewart, T. E., and Taylor, W. H. (1985). Animal Cell Mutants Defective in Glycosaminoglycan Biosynthesis. *Proc Natl Acad Sci* 82, 3197-3201.
- Faham, S., Hileman, R. E., Fromm, J. R., Linhardt, R. J., and Rees, D. C. (1996). Heparin structure and interactions with basic fibroblast growth factor. *Science* 271, 1116-1120.
- Fan, G., Xiao, L., Cheng, L., Wang, X., Sun, B., and Hu, G. (2000). Targeted disruption of NDST-1 gene leads to pulmonary hypoplasia and neonatal respiratory distress in mice. *FEBS Lett* 467, 7-11.

Forsberg, E., Pejler, G., Ringvall, M., Lunderius, C., Tomasini-Johansson, B., Kusche-Gullberg, M., Eriksson, I., Ledin, J., Hellman, L., and Kjellen, L. (1999). Abnormal mast cells in mice deficient in a heparin-synthesizing enzyme. *Nature* 400, 773-776.

Frevert, C. W., Kinsella, M. G., Vathanaprida, C., Goodman, R. B., Baskin, D. G., Proudfoot, A., Wells, T. N. C., Wight, T. N., and Martin, T. R. (2003). Binding of Interleukin-8 to Heparan Sulfate and Chondroitin Sulfate in Lung Tissue. *Am J Respir Cell Mol Biol* 28, 464-472.

Gama, C. I., and Hsieh-Wilson, L. C. (2005). Chemical approaches to deciphering the glycosaminoglycan code. *Curr Opin Chem Biol* 9, 609.

Gan, Z. R., Li, Y., Chen, Z., Lewis, S. D., and Shafer, J. A. (1994). Identification of basic amino acid residues in thrombin essential for heparin-catalyzed inactivation by antithrombin III. *J Biol Chem* 269, 1301-1305.

Girardin, E. P., HajMohammadi, S., Birmele, B., Helisch, A., Shworak, N. W., and de Agostini, A. I. (2005). Synthesis of Anticoagulant Active Heparan Sulfate Proteoglycans by Glomerular Epithelial Cells Involves Multiple 3-O-Sulfotransferase Isoforms and a Limiting Precursor Pool. *J Biol Chem* 280, 38059-38070.

Gómez-Duarte, O. G., Dehio, M., Guzmán, C. A., Chhatwal, G. S., Dehio, C., and Meyer, T. F. (1997). Binding of vitronectin to opa-expressing *Neisseria gonorrhoeae* mediates invasion of HeLa cells. *Infect Immun* 65, 3857-3866.

Gotte, M. (2003). Syndecans in inflammation. *FASEB J* 17, 575-591.

Gotting, C., Kuhn, J., Zahn, R., Brinkmann, T., and Kleesiek, K. (2000). Molecular cloning and expression of human UDP-d-Xylose:proteoglycan core protein beta-d-xylosyltransferase and its first isoform XT-II. *J Mol Biol* 304, 517-528.

Gotting, C., Sollberg, S., Kuhn, J., Weilke, C., Huerkamp, C., Brinkmann, T., Krieg, T., and Kleesiek, K. (1999). Serum xylosyltransferase: a new biochemical marker of the sclerotic process in systemic sclerosis. *J Invest Derm* 112, 919.

Grobe, K., and Esko, J. D. (2002). Regulated translation of heparan sulfate GlcNAc N-deacetylase/N-sulfotransferase isozymes by structured 5'-untranslated regions and internal ribosome entry sites. *J Biol Chem* 277, 30699-30706.

Gulberti, S., Lattard, V., Fondeur, M., Jacquinet, J.-C., Mulliert, G., Netter, P., Magdalou, J., Ouzzine, M., and Fournel-Gigleux, S. (2005). Phosphorylation and Sulfation of Oligosaccharide Substrates Critically Influence the Activity of Human {beta}1,4-Galactosyltransferase 7 (GalT-I) and {beta}1,3-Glucuronosyltransferase I (GlcAT-I) Involved in the Biosynthesis of the Glycosaminoglycan-Protein Linkage Region of Proteoglycans. *J Biol Chem* 280, 1417-1425.

Habuchi, H., Miyake, G., Nogami, K., Kuroiwa, A., Matsuda, Y., Kusche-Gullberg, M., Habuchi, O., Tanaka, M., and Kimata, K. (2003). Biosynthesis of heparan sulphate with diverse structures and functions: two alternatively spliced forms of human heparan sulphate 6-O-sulphotransferase-2 having different expression patterns and properties. *Biochem J* 371, 131-142.

Habuchi, H., Tanaka, M., Habuchi, O., Yoshida, K., Suzuki, H., Ban, K., and Kimata, K. (2000). The occurrence of three isoforms of heparan sulfate 6-O-sulphotransferase having different specificities for hexuronic acid adjacent to the targeted N-sulfoglucosamine. *J Biol Chem* 275, 2859-2868.

Hacker, U., Nybakken, K., and Perrimon, N. (2005). HEPARAN SULPHATE PROTEOGLYCANS: THE SWEET SIDE OF DEVELOPMENT. *Nature Rev Mol Cell Biol* 6, 530.

Hagner-McWhirter, A., Li, J., Oscarson, S., and Lindahl, U. (2004). Irreversible glucuronyl C5-epimerization in the biosynthesis of heparan sulfate. *J Biol Chem* 279, 14631-14638.

Hagner-Mcwhirter, A., Lindahl, U., and Li, J. (2000). Biosynthesis of heparin/heparan sulphate: mechanism of epimerization of glucuronyl C-5. *Biochem J* 347, 69-75.

HajMohammadi, S., Enjyoji, K., Princivalle, M., Christi, P., Lech, M., Beeler, D. L., Rayburn, H., Schwartz, J. J., Barzegar, S., de Agostini, A. I., *et al.* (2003). Normal levels of anticoagulant heparan sulfate are not essential for normal hemostasis. *J Clin Invest* 111, 989-999.

Handel, T. M., Johnson, Z., Crown, S. E., Lau, E. K., Sweeney, M., and Proudfoot, A. E. (2005). REGULATION OF PROTEIN FUNCTION BY GLYCOSAMINOGLYCANS AS EXEMPLIFIED BY CHEMOKINES. *Ann Rev of Biochem* 74, 385-410.

Holmborn, K., Ledin, J., Smeds, E., Eriksson, I., Kusche-Gullberg, M., and Kjellen, L. (2004). Heparan sulfate synthesized by mouse embryonic stem cells deficient in NDST1 and NDST2 is 6-O-sulfated but contains no N-sulfate groups. *J Biol Chem* 279, 42355-42358.

Hoogewerf, A. J., Kuschert, G. S. V., Proudfoot, A. E. I., Borlat, F., Clark-Lewis, I., Power, C. A., and Wells, T. N. C. (1997). Glycosaminoglycans Mediate Cell Surface Oligomerization of Chemokines. *Biochemistry* 36, 13570-13578.

Hovingh, P., and Linker, A. (1970). The Enzymatic Degradation of Heparin and Heparitin Sulfate. III. PURIFICATION OF A HEPARITINASE AND A HEPARINASE FROM FLAVOBACTERIA. *J Biol Chem* 245, 6170-6175.

Hricovini, M., Guerrini, M., Bisio, A., Torri, G., Petitou, M., and Casu, B. (2001). Conformation of heparin pentasaccharide bound to antithrombin III. *Biochem J* 359, 265-272.

- Hulett, M. D., Freeman, C., Hamdorf, B. J., Baker, R. T., Harris, M. J., and Parish, C. R. (1999). Cloning of mammalian heparanase, an important enzyme in tumor invasion and metastasis. *Nat Med* 5, 803-809.
- Huntington, J. A. (2005). Molecular recognition mechanisms of thrombin. *J Throm Haemos* 3, 1861-1872.
- Iozzo, R. V. (2005). BASEMENT MEMBRANE PROTEOGLYCANS: FROM CELLAR TO CEILING. *Nature Rev Mol Cell Biol* 6, 646.
- Jin, L., Abrahams, P., Skinner, R., Petitou, M., Pike, R. N., and Carrell, R. W. (1997). The anticoagulant activation of antithrombin by heparin. *Proc Natl Acad Sci* 94, 14683-14688.
- Johnson, D. J., and Huntington, J. A. (2003). Crystal structure of antithrombin in a heparin-bound intermediate state. *Biochemistry* 42, 8712-8719.
- Joyce, J. A., Freeman, C., Meyer-Morse, N., Parish, C. R., and Hanahan, D. (2005). A functional heparan sulfate mimetic implicates both heparanase and heparan sulfate in tumor angiogenesis and invasion in a mouse model of multistage cancer. *Oncogene* 24, 4037-4051.
- Kakuta, Y., Li, L., Pedersen, L. C., Pedersen, L. G., and Negishi, M. (2003). Heparan sulphate N-sulphotransferase activity: reaction mechanism and substrate recognition. *Biochem Soc Trans* 31 (pt2), 331-334.
- Kakuta, Y., Sueyoshi, T., Negishi, M., and Pedersen, L. C. (1999). Crystal structure of the sulfotransferase domain of human heparan sulfate N-deacetylase/N-sulfotransferase 1. *J Biol Chem* 274, 10673-10676.
- Kearns, A. E., Vertel, B. M., and Schwartz, N. B. (1993). Topography of glycosylation and UDP-xylose production. *J Biol Chem* 268, 11097-11104.
- Kelly, T., Miao, H. Q., Yang, Y., Navarro, E., Kussie, P., Huang, Y., MacLeod, V., Casciano, J., Joseph, L., Zhan, F., *et al.* (2003). High heparanase activity in multiple myeloma is associated with elevated microvessel density. *Cancer Res* 63, 8749-8756.
- Kim, A. W., Xu, X., Hollinger, E. F., Gattuso, P., Godellas, C. V., and Prinz, R. A. (2002). Human Heparanase-1 Gene Expression in Pancreatic Adenocarcinoma. *J Gastro Surgery* 6, 167-172.
- Kim, B.-T., Kitagawa, H., Tanaka, J., Tamura, J.-i., and Sugahara, K. (2003). In Vitro Heparan Sulfate Polymerization: CRUCIAL ROLES OF CORE PROTEIN MOIETIES OF PRIMER SUBSTRATES IN ADDITION TO THE EXT1-EXT2 INTERACTION. *J Biol Chem* 278, 41618-41623.
- Kitagawa, H., Tone, Y., Tamura, J.-i., Neumann, K. W., Ogawa, T., Oka, S., Kawasaki, T., and Sugahara, K. (1998). Molecular Cloning and Expression of Glucuronyltransferase I

Involved in the Biosynthesis of the Glycosaminoglycan-Protein Linkage Region of Proteoglycans. *J Biol Chem* 273, 6615-6618.

Kobayashi, M., Habuchi, H., Habuchi, O., Saito, M., and Kimata, K. (1996). Purification and characterization of heparan sulfate 2-sulfotransferase from cultured Chinese hamster ovary cells. *J Biol Chem* 271, 7645-7653.

Kobayashi, S.-i., Morimoto, K.-i., Shimizu, T., Takahashi, M., Kurosawa, H., and Shirasawa, T. (2000). Association of EXT1 and EXT2, Hereditary Multiple Exostoses Gene Products, in Golgi Apparatus. *Biochem Biophys Res Commun* 268, 860.

Koide, T., Odani, S., Takahashi, K., Ono, T., and Sakuragawa, N. (1984). Antithrombin III Toyama: replacement of arginine-47 by cysteine in hereditary abnormal antithrombin III that lacks heparin-binding ability. *Proc Natl Acad Sci USA* 81, 289-293.

Kraulis, P. J. (1991). MOLSCRIPT: a program to produce both detailed and schematic plots of protein structures. *J Appl Crystallogr* 24, 946-950.

Kuberan, B., Beeler, D. L., Lawrence, R., Lech, M., and Rosenberg, R. (2003a). Rapid two-step synthesis of mitrin from heparosan: a replacement for heparin. *J Am Chem Soc* 125, 12424-12425.

Kuberan, B., Beeler, D. L., Lech, M., Wu, Z. L., and Rosenberg, R. D. (2003b). Chemoenzymatic Synthesis of Classical and Non-classical Anticoagulant Heparan Sulfate Polysaccharides. *J Biol Chem* 278, 52613-52621.

Kuberan, B., Lech, M. Z., Beeler, D. L., Wu, Z. L., and Rosenberg, R. D. (2003c). Enzymatic synthesis of antithrombin III-binding heparan sulfate pentasaccharide. *Nat Biotech* 21, 1343.

Kusche-Gullberg, M., and Kjellen, L. (2003). Sulfotransferases in glycosaminoglycan biosynthesis. *Curr Opin Struct Biol* 13, 605.

Kuschert, G. S. V., Coulin, F., Power, C. A., Proudfoot, A. E. I., Hubbard, R. E., Hoogewerf, A. J., and Wells, T. N. C. (1999). Glycosaminoglycans Interact Selectively with Chemokines and Modulate Receptor Binding and Cellular Responses. *Biochemistry* 38, 12959-12968.

Ledin, J., Staatz, W., Li, J.-P., Gotte, M., Selleck, S. B., Kjellen, L., and Spillmann, D. (2004). Heparan sulfate structure in mice with genetically modified heparan sulfate production. *J Biol Chem* 279, 42732-42741.

Lee, M. K., and Lander, A. D. (1991). Analysis affinity and structural selectivity in the binding of proteins to glycosaminoglycans: Development of a sensitive electrophoretic approach. *Proc Natl Acad Sci USA* 88, 2768-2772.

Lever, R., and Page, C. P. (2002). Novel drug development opportunity for heparin. *Nat Rev* 1, 140-148.

- Li, J.-P., Gong, F., Hagner-McWhirter, A., Forsberg, E., Åbrink, M., Kisilevsky, R., Zhang, X., and Lindahl, U. (2003). Targeted disruption of a murine glucuronyl C5 epimerase gene results in heparan sulfate lacking L-iduronic acid and in neonatal lethality. *J Biol Chem* 278, 28363-28366.
- Li, Q., Park, P. W., Wilson, C. L., and Parks, W. C. (2002). Matrilysin shedding of syndecan-1 regulates chemokine mobilization and transepithelial efflux of neutrophils in acute lung injury. *Cell* 111, 635-646.
- Lind, T., Lindahl, U., and Lidholt, K. (1993). Biosynthesis of heparin/heparan sulfate. Identification of a 70-kDa protein catalyzing both the D-glucuronosyl- and the N-acetyl-D-glucosaminyltransferase reactions. *J Biol Chem* 268, 20705.
- Lindahl, U., Li, J., Kusche-Gullberg, M., Salmivirta, M., Alaranta, S., Veromaa, T., Emies, J., Roberts, I., Taylor, C., Oreste, P., *et al.* (2005). Generation of "neoheparin" from *E. Coli* K5 capsular polysaccharide. *J Med Chem* 48, 349-352.
- Linhardt, R. J. (2003). 2003 Claude S. Hudson Award address in carbohydrate chemistry. Heparin: structure and activity. *J Med Chem* 46, 2551-2564.
- Liu, J., and Rosenberg, R. D. (2002). Heparan sulfate D-glucosaminyl 3-O-sulfotransferase, In *Handbook of glycosyltransferases and their related genes*, N. Taniguchi, and M. Fukuda, eds. (Tokyo: Springer-Verlag), pp. 475-483.
- Liu, J., Shriver, Z., Pope, R. M., Thorp, S. C., Duncan, M. B., Copeland, R. J., Raska, C. S., Yoshida, K., Eisenberg, R. J., Cohen, G., *et al.* (2002). Characterization of a heparan sulfate octasaccharide that binds to herpes simplex viral type 1 glycoprotein D. *J Biol Chem* 277, 33456-33467.
- Liu, J., Shworak, N. W., Fritze, L. M. S., Edelberg, J. M., and Rosenberg, R. D. (1996). Purification of heparan sulfate D-glucosaminyl 3-O-sulfotransferase. *J Biol Chem* 271, 27072-27082.
- Liu, J., Shworak, N. W., Sinaÿ, P., Schwartz, J. J., Zhang, L., Fritze, L. M. S., and Rosenberg, R. D. (1999). Expression of heparan sulfate D-glucosaminyl 3-O-sulfotransferase isoforms reveals novel substrate specificities. *J Biol Chem* 274, 5185-5192.
- Liu, J., and Thorp, S. C. (2002). Heparan sulfate and the roles in assisting viral infections. *Med Res Rev* 22, 1-25.
- Lohse, D. L., and Linhardt, R. J. (1992). Purification and characterization of heparin lyases from *Flavobacterium heparinum*. *J Biol Chem* 267, 24347-24355.
- Lyon, M., Rushton, G., Askari, J. A., Humphries, M. J., and Gallagher, J. T. (2000). Elucidation of the structural features of heparan sulfate important for interaction with the Hep-2 domain of fibronectin. *J Biol Chem* 275, 4599-4606.

Maxhimer, J. B., Quiros, R. M., Stewart, R., Dowlatshahi, K., Gattuso, P., Fan, M., Prinz, R. A., and Xu, X. (2002). Heparanase-1 expression is associated with the metastatic potential of breast cancer. *Surgery* 132, 326-333.

McCormick, C., Duncan, G., Goutsos, T., and Tufaro, F. (2000). The putative tumor suppressors EXT1 and EXT2 form a stable complex that accumulates in the Golgi apparatus and catalyzes the synthesis of heparan sulfate. *Proc Natl Acad Sci* 97, 668-673.

McKeehan, W. L., Wu, X., and Kan, M. (1999). Requirement for anticoagulant heparan sulfate in the fibroblast growth factor receptor complex. *J Biol Chem* 274, 21511-21514.
Merritt, E. A., and Bacon, D. J. (1997). Raster3D: Photorealistic molecular graphics. *Meth Enz* 277, 505-524.

Middleton, J., Neil, S., Wintle, J., Clark-Lewis, I., Moore, H., Lam, C., Auer, M., Hub, E., and Rot, A. (1997). Transcytosis and Surface Presentation of IL-8 by Venular Endothelial Cells. *Cell* 91, 385.

Mikhailov, D., Young, H. C., Linhardt, R. J., and Mayo, K. H. (1999). Heparin Dodecasaccharide Binding to Platelet Factor-4 and Growth-related Protein-alpha. *J Biol Chem* 274, 25317-25329.

Mochizuki, H., Yoshida, K., Gotoh, M., Sugioka, S., Kikuchi, N., Kwon, Y.-D., Tawada, A., Maeyama, K., Inaba, N., Hiruma, T., *et al.* (2003). Characterization of a heparan sulfate 3-O-sulfotransferase-5 an enzyme synthesizing a tetrasulfated disaccharide. *J Biol Chem* 278, 26780-26787.

Mohammadi, M., Olsen, S. K., and Goetz, R. (2005a). A protein canyon in the FGF-FGF receptor dimer selects from an a la carte menu of heparan sulfate motifs. *Curr Opin Struct Biol* 15, 506-516.

Mohammadi, M., Olsen, S. K., and Ibrahimi, O. A. (2005b). Structural basis for fibroblast growth factor receptor activation. *Cytokine Growth Factor Rev* 16, 107-137.

Moon, A., Edavettal, S. C., Krahn, J. X., Munoz, E. M., Negishi, M., Linhardt, R. J., Liu, J., and Pedersen, L. C. (2004). Structural analysis of the sulfotransferase (3-OST-3) involved in the biosynthesis of an entry receptor of herpes simplex virus 1. *J Biol Chem* 279, 45185-45193.

Motowo Nakajima, T. I. G. L. N. (1988). Heparanases and tumor metastasis. *J Cell Biochem* 36, 157-167.

Mulloy, B., Forster, M. J., Jones, C., and Davies, D. B. (1993). N.m.r. and molecular-modelling studies of the solution conformation of heparin. *Biochem J* 293, 849-858.

- Munoz, E., Xu, D., Avci, F., Kemp, M., Liu, J., and Linhardt, R. J. (2006). Enzymatic synthesis of heparin related polysaccharides on sensor chips: Rapid screening of heparin-protein interactions. *Biochem Biophys Res Commun* 339, 597.
- Nadkarni, V. D., Toida, T., Van Gorp, C. L., Schubert, R. L., Weiler, J. M., Hansen, K. P., Caldwell, E. E. O., and Linhardt, R. J. (1996). Preparation and biological activity of N-sulfonated chondroitin and dermatan sulfate derivatives. *Carbohydrate Res* 290, 87.
- Noti, C., and Seeberger, P. H. (2005). Chemical Approaches to Define the Structure-Activity Relationship of Heparin-like Glycosaminoglycans. *Chem Biol* 12, 731.
- Okajima, T., Yoshida, K., Kondo, T., and Furukawa, K. (1999). Human Homolog of *Caenorhabditis elegans* sqv-3 Gene Is Galactosyltransferase I Involved in the Biosynthesis of the Glycosaminoglycan-Protein Linkage Region of Proteoglycans. *J Biol Chem* 274, 22915-22918.
- Orellana, A., Hirschberg, C. B., Wei, Z., Swiedler, S. J., and Ishihara, M. (1994). Molecular cloning and expression of a glycosaminoglycan N-acetylglucosaminyl N-deacetylase/N-sulfotransferase from a heparin-producing cell line. *J Biol Chem* 269, 2270-2276.
- Park, P. W., Foster, T. J., Nishi, E., Duncan, S. J., Klagsbrun, M., and Chen, Y. (2004). Activation of Syndecan-1 Ectodomain Shedding by *Staphylococcus aureus* {alpha}-Toxin and {beta}-Toxin. *J Biol Chem* 279, 251-258.
- Park, P. W., Pier, G. B., Hinkes, M. T., and Bernfield, M. (2001). Exploitation of syndecan-1 shedding by *Pseudomonas aeruginosa* enhances virulence. *Nature* 411, 98-102.
- Park, P. W., Pier, G. B., Preston, M. J., Goldberger, O., Fitzgerald, M. L., and Bernfield, M. (2000a). Syndecan-1 shedding is enhanced by LasA, a secreted virulence factor of *pseudomonas aeruginosa*. *J Biol Chem* 275, 3057-3064.
- Park, P. W., Reizes, O., and Bernfield, M. (2000b). Cell surface heparan sulfate proteoglycans: selective regulators of ligand-receptor encounters. *J Biol Chem* 275, 29923-29926.
- Pellegrini, L., Burke, D. F., von Delft, F., Mulloy, B., and Blundell, T. L. (2000). Crystal structure of fibroblast growth factor receptor ectodomain bound to ligand and heparin. *Nature* 407, 1029.
- Petitou, M., Duchaussoy, P., Lederman, I., Choay, J., Sinay, P., Jacquinet, J.-C., and Torri, G. (1986). Synthesis of heparin fragments. A chemical synthesis of the pentasaccharide O-(2-deoxy-2-sulfamido-6-O-sulfo-[alpha]-glucopyranosyl)-(1->4)-O-([beta]-glucopyranosyluronic acid)-(1->4)-O-(2-deoxy-2-sulfamido-3,6-di-O-sulfo-[alpha]-glucopyranosyl)-(1->4)-O-(2-O-sulfo [alpha]-idopyranosyluronic acid)-(1->4)-2-deoxy-2-sulfamido-6-O-sulfo- glucopyranose decasodium salt, a heparin fragment having high affinity for antithrombin III. *Carbohydrate Res* 147, 221-236.

- Pinhal, M. A., Smith, B., Olson, S., Aikawa, J., Kimata, K., and Esko, J. D. (2001). Enzyme interactions in heparan sulfate biosynthesis: uronosyl 5-epimerase and 2-O-sulfotransferase interact in vivo. *Proc Natl Acad Sci* 98, 12984-12989.
- Pye, D. A., Vives, R. R., Turnbull, J. E., Hyde, P., and Gallagher, J. T. (1998). Heparan sulfate oligosaccharides require 6-O-sulfation for promotion of basic fibroblast growth factor mitogenic activity. *J Biol Chem* 273, 22936-22942.
- Rapraeger, A. C., Krufka, A., and Olwin, B. B. (1991). Requirement of heparan sulfate for bFGF-mediated fibroblast growth and myoblast differentiation. *Science* 252, 1705-1708.
- Quiros, R. M., Rao, G., Plate, J., Harris, J. E., Brunn, G. J., Platt, J. L., Gattuso, P., Prinz, R. A., Xu, X. (2006). Elevated serum heparanase-1 levels in patients with pancreatic carcinoma are associated with poor survival. *Cancer* 106, 532-540.
- Rong, J., Habuchi, H., Kimata, K., Lindahl, U., and Kusche-Gullberg, M. (2001). Substrate specificity of the heparan sulfate hexuronic acid 2-O-sulfotransferase. *Biochemistry* 40, 5548-5555.
- Rosenberg, R. D., Oosta, G. M., Jordan, R. E., and Gardner, W. T. (1980). The interaction of heparin with thrombin and antithrombin. *Biochem Biophys Res Commun* 96, 1200-1208.
- Rosenberg, R. D., Showrak, N. W., Liu, J., Schwartz, J. J., and Zhang, L. (1997). Heparan sulfate proteoglycans of the cardiovascular system: specific structures emerge but how is synthesis regulated? *J Clin Invest* 99, 2062-2070.
- Sadir, R., Imberty, A., Baleux, F., and Lortat-Jacob, H. (2004). Heparan Sulfate/Heparin Oligosaccharides Protect Stromal Cell-derived Factor-1 (SDF-1)/CXCL12 against Proteolysis Induced by CD26/Dipeptidyl Peptidase IV. *J Biol Chem* 279, 43854-43860.
- Saribas, A. S., Mobasser, A., Pristatsky, P., Chen, X., Barthelson, R., Hakes, D., and Wang, J. (2004). Production of N-sulfated polysaccharides using yeast expressed N-deacetylase/N-sulfotransferase-1 (NDST-1). *Glycobiology* 14, 1217-1228.
- Sasisekharan, R., Shriver, Z., Venkataraman, G., and Narayanasami, U. (2002). Roles of heparin-sulphate glycosaminoglycans in cancer. *Nat Rev Cancer* 2, 521-528.
- Schlessinger, J., Plotnikov, A. N., Ibrahimi, O. A., Eliseenkova, A. V., Yeh, B. K., Yayon, A., Linhardt, R. J., and Mohammadi, M. (2000). Crystal structure of a ternary FGF-FGFR-heparin complex reveals a dual role for heparin in FGFR binding and dimerization. *Mol Cell* 6, 743-750.
- Sheehan, J. P., and Sadler, J. E. (1994). Molecular Mapping of the Heparin-Binding Exosite of Thrombin. *Proc Natl Acad Sci* 91, 5518-5522.

- Sheng, J. J., Saxena, A., and Duffel, M. W. (2004). Influence of phenylalanines 77 and 138 on the stereospecificity of arylsulfotransferase IV. *Drug Metabol Dispost* 32, 559-565.
- Shively, J. E., and Conrad, H. E. (1976). Formation of anhydrosugars in the chemical depolymerization of heparin. *Biochemistry* 15, 3932-3942.
- Shukla, D., Liu, J., Blaiklock, P., Shworak, N. W., Bai, X., Esko, J. D., Cohen, G. H., Eisenberg, R. J., Rosenberg, R. D., and Spear, P. G. (1999). A novel role for 3-O-sulfated heparan sulfate in herpes simplex virus 1 entry. *Cell* 99, 13-22.
- Shukla, D., and Spear, P. G. (2001). Herpesviruses and heparan sulfate: an intimate relationship in aid of viral entry. *J Clin Invest* 108, 503-510.
- Shworak, N. W., Liu, J., Fritze, L. M. S., Schwartz, J. J., Zhang, L., Logeart, D., and Rosenberg, R. D. (1997). Molecular cloning and expression of mouse and human cDNAs encoding heparan sulfate D-glucosaminyl 3-O-sulfotransferase. *J Biol Chem* 272, 28008-28019.
- Shworak, N. W., Liu, J., Petros, L. M., Zhang, L., Kobayashi, M., Copeland, N. G., Jenkins, N. A., and Rosenberg, R. D. (1999). Diversity of the extensive heparan sulfate D-glucosaminyl 3-O-sulfotransferase (3-OST) multigene family. *J Biol Chem* 274, 5170-5184.
- Simizu, S., Ishida, K., and Osada, H. (2004). Heparanase as a molecular target of cancer chemotherapy. *Cancer Science* 95, 553-558.
- Slungaard, A. (2005). Platelet factor 4: a chemokine enigma. *Inter J Biochem Cell Biol* 37, 1162.
- Smeds, E., Habuchi, H., Do, A.-T., Hjertson, E., Grundberg, H., Kimata, K., Lindahl, U., and Kusche-Gullberg, M. (2003). Substrate specificities of mouse heparan sulphate glucosaminyl 6-O-sulfotransferases. *Biochem J* 372 (pt2), 371-380.
- Spear, P. G. (2004). Herpes simplex virus: receptors and ligands for cell entry. *Cellular Microbiol* 6, 401-410.
- Spear, P. G., Eisenberg, R. J., and Cohen, G. H. (2000). Three classes of cell surface receptors for alphaherpesvirus entry. *Virology* 275, 1-8.
- Spillmann, D., Witt, D., and Lindahl, U. (1998). Defining the Interleukin-8-binding Domain of Heparan Sulfate. *J Biol Chem* 273, 15487-15493.
- Stringer, S. E., Forster, M. J., Mulloy, B., Bishop, C. R., Graham, G. J., and Gallagher, J. T. (2002). Characterization of the binding site on heparan sulfate for macrophage inflammatory protein 1alpha. *Blood* 100, 1543-1550.
- Stringer, S. E., and Gallagher, J. T. (1997). Specific binding of the chemokine platelet factor 4 to heparan sulfate. *J Biol Chem* 272, 20508-20514.

Sugahara, K., and Kitagawa, H. (2002). Heparin and Heparan Sulfate Biosynthesis. *IUBMB Life* 54, 163-175.

Sundaram, M., Qi, Y., Shriver, Z., Liu, D., Zhao, G., Venkataraman, G., Langer, R., and Sasisekharan, R. (2003). Rational design of low-molecular weight heparins with improved in vivo activity. *Proc Natl Acad Sci* 100, 651-656.

Taraktchoglou, M., Pacey, A. A., Turnbull, J. E., and Eley, A. (2001). Infectivity of *Chlamydia trachomatis* Serovar LGV but Not E Is Dependent on Host Cell Heparan Sulfate. *Infect Immun* 69, 968-976.

Tonnaer, E. L. G. M., Hafmans, T. G., Van Kuppevelt, T. H., Sanders, E. A. M., Verweij, P. E., and Curfs, J. H. A. J. (2006). Involvement of glycosaminoglycans in the attachment of pneumococci to nasopharyngeal epithelial cells. *Microbes and Infection* 8, 316.

Ueno, M., Yamada, S., Zako, M., Bernfield, M., and Sugahara, K. (2001). Structural Characterization of Heparan Sulfate and Chondroitin Sulfate of Syndecan-1 Purified from Normal Murine Mammary Gland Epithelial Cells. COMMON PHOSPHORYLATION OF XYLOSE AND DIFFERENTIAL SULFATION OF GALACTOSE IN THE PROTEIN LINKAGE REGION TETRASACCHARIDE SEQUENCE. *J Biol Chem* 276, 29134-29140.

van Boven, H. H., and Lane, D. A. (1997). Antithrombin and its inherited deficiency states. *Semin Hematol* 34, 188-204.

Vlodavsky, I., Friedmann, Y., Elkin, M., Aingorn, H., Atzmon, R., Ishai-Michaeli, R., Bitan, M., Pappo, O., Peretz, T., Michal, I., *et al.* (1999). Mammalian heparanase: Gene cloning, expression and function in tumor progression and metastasis. *Nat Med* 5, 793-802.

Wadstrom, T., and Ljungh, A. (1999). Glycosaminoglycan-binding microbial proteins in tissue adhesion and invasion: key events in microbial pathogenicity. *J Med Microbiol* 48, 223-233.

Wang, L., Fuster, M., Sriramarao, P., and Esko, J. D. (2005). Endothelial heparan sulfate deficiency impairs L-selectin- and chemokine-mediated neutrophil trafficking during inflammatory responses. *Nat Immunol* 6, 902.

Wei, G., Bai, X., Gabb, M. M., Bame, K. J., Koshy, T. I., Spear, P. G., and Esko, J. D. (2000). Location of the glucuronosyltransferase domain in the heparan sulfate copolymerase EXT1 by analysis of Chinese hamster ovary cell mutants. *J Biol Chem* 275, 27733.

Wei, Z., and Swiedler, S. J. (1999). Functional analysis of conserved cysteines in heparan sulfate N-deacetylase-N-sulfotransferases. *J Biol Chem* 274, 1966-1970.

Wu, Z. L., Lech, M., Beeler, D. L., and Rosenberg, R. D. (2004). Determining heparan sulfate structure in the vicinity of specific sulfotransferase recognition sites by mass spectrometry. *J Biol Chem* 279, 1861-1866.

- Xia, G., Chen, J., Tiwari, V., Ju, W., Li, J.-P., Malmström, A., Shukla, D., and Liu, J. (2002). Heparan sulfate 3-O-sulfotransferase isoform 5 generates both an antithrombin-binding site and an entry receptor for herpes simplex virus, type 1. *J Biol Chem* 277, 37912-37919.
- Xu, D., Tiwari, V., Xia, G., Clement, C., Shukla, D., and Liu, J. (2005). Characterization of Heparan Sulfate 3-O-Sulfotransferase Isoform 6 and Its Role in Assisting the Entry of Herpes Simplex Virus, Type 1. *Biochem J* 385, 451-459.
- Yayon, A., Klagsbrun, M., Esko, J. D., Leder, P., and Ornitz, D. M. (1991). Cell surface, heparin-like molecules are required for binding of basic fibroblast growth factor to its high affinity receptor. *Cell* 64, 841-848.
- Ye, J., Rezaie, A. R., and Esmon, C. T. (1994). Glycosaminoglycan contributions to both protein C activation and thrombin inhibition involve a common arginine-rich site in thrombin that includes residues arginine 93, 97, and 101. *J Biol Chem* 269, 17965-17970.
- Yoon, M., and Spear, P. G. (2004). Random mutagenesis of the gene encoding a viral ligand for multiple cell entry receptors to obtain viral mutants altered for receptor usage. *Proc Natl Acad Sci* 101, 17252-17257.
- Yoon, M., Zago, A., Shukla, D., and Spear, P. G. (2003). Mutations in the N-termini of herpes simplex virus type 1 and 2 gDs alter functional interactions with the entry/fusion receptors HVEM, Nectin-2, and 3-O-sulfated heparan sulfate but not with Nectin-1. *J Virol* 77, 9221-9231.
- Zak, B. M., Crawford, B. E., and Esko, J. D. (2002). Hereditary multiple exostoses and heparan sulfate polymerization. *Biochim Biophys Acta- General Subjects* 1573, 346-355.
- Zhang, L., Beeler, D. L., Lawrence, R., Lech, M., Liu, J., Davis, J. C., Shriver, Z., Sasisekharan, R., and Rosenberg, R. D. (2001a). 6-O-sulfotransferase-1 represents a critical enzyme in the anticoagulant heparan sulfate biosynthetic pathway. *J Biol Chem* 276, 42311-42321.
- Zhang, L., Lawrence, R., Schwartz, J. J., Bai, X., Wei, G., Esko, J. D., and Rosenberg, R. D. (2001b). The effect of precursor structures on the action of glucosaminyl 3-O-sulfotransferase-1 and the biosynthesis of anticoagulant heparan sulfate. *J Biol Chem* 276, 28806-28813.
- Zhang, L., Schwartz, J. J., Miller, J., Liu, J., Fritze, L. M. S., Shworak, N. W., and Rosenberg, R. D. (1998). The retinoic acid and cAMP-dependent up-regulation of 3-O-sulfotransferase-1 leads to a dramatic augmentation of anticoagulant active heparan sulfate biosynthesis in F9 embryonal carcinoma cells. *J Biol Chem* 273, 27998-28003.